COURSE 8

TIME-DEPENDENT QUANTUM SYSTEMS

BORIS V. CHIRIKOV

Institute of Nuclear Physics
630090 Novosibirsk, USSR

M.-J. Giannoni, A. Voros and J. Zinn-Justin, eds.
Les Houches, Session LII, 1989
Chaos et Physique Quantique /Chaos and Quantum Physics
© *Elsevier Science Publishers B.V., 1991*

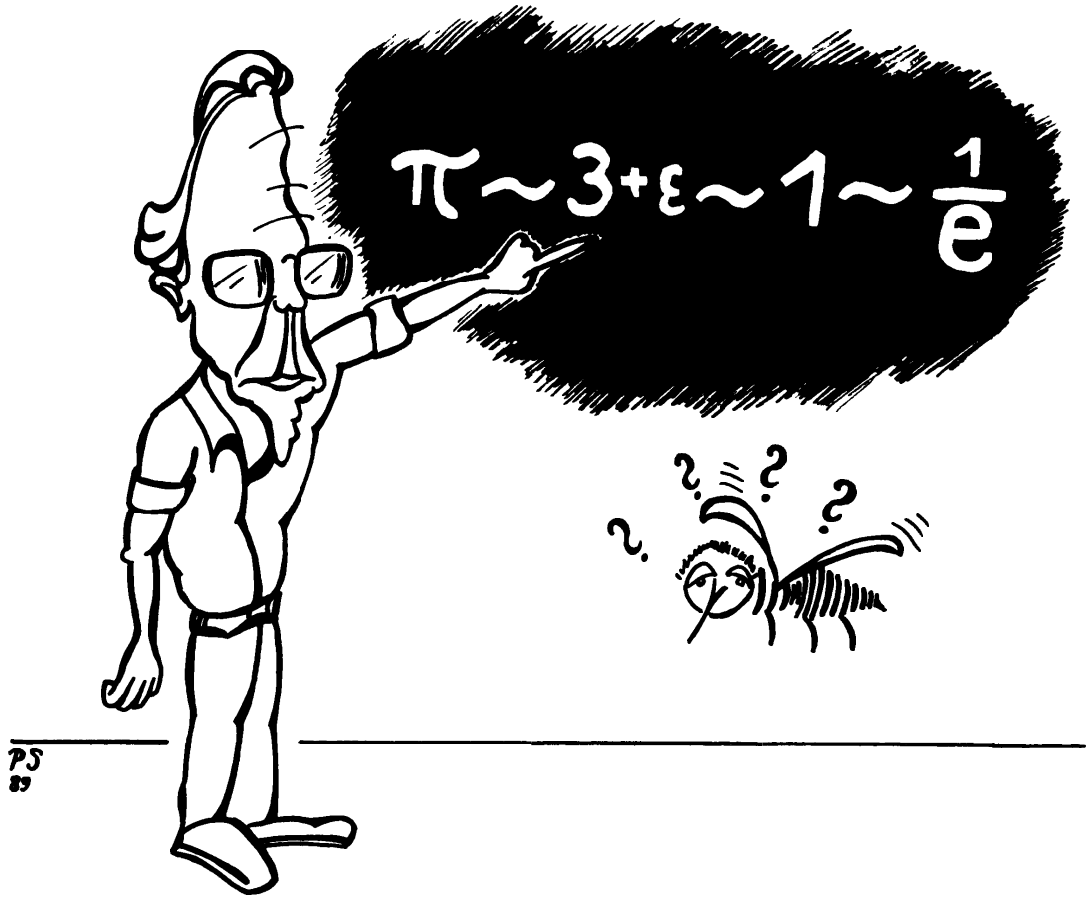
$\pi \sim 3 + \varepsilon \sim 1 \sim \frac{1}{e}$
PS
89

Contents

1. Introduction: a personal view of dynamical chaos

1.1. Philosophy

In this course I am going to discuss in some detail a fascinating topic, *dynamical chaos* as it is often called. I wouldn't say this exciting phenomenon is brand-new (it is a century old already!), yet it is still not widely known. What actually is it? We start with a *purely dynamical system*, specified, say, by an ordinary differential equation, e.g.,

$$\dot{x} = v(x), \tag{1.1}$$

where x and v are generally some vectors. The time evolution of this system is described by a *trajectory* $x(t, x_0)$ where x_0 are the so-called *initial conditions*, i.e., the system's exact position at some fixed time, e.g., $t = 0$. The function $x(t, x_0)$ is sometimes called the *motion law*. Isn't it a surprise that this law is always conditional? That nature never tells us what the motion will be? That instead, it asks first what are the initial conditions? Nevertheless, it has long been assumed that the dynamical evolution is *completely deterministic* (apparently just by those initial conditions). I am afraid some people still believe that it is *always* possible actually to determine the system's future or to reconstruct its past. A great discovery of recent time (or elucidation, if you like) was that this is *not always* the case. And when it is not, we speak of dynamical chaos, or, more formally, of a random solution to the deterministic equation. Random, in which sense? In some, rigorous mathematically, and acceptable physically sense (see refs. [1,2] and some selected comments scattered over this course below). This is an exciting problem as well, but I have to restrict myself to the prescribed topic. The rest is left for late-night discussions!

But this is not yet the whole story. What is even more important, in my opinion, is that the theory of dynamical chaos has solved (in passing!) the great mystery of the statistical laws, the mystery that even affected most of the philosophical systems. Indeed, one of the philosophical beliefs is that the statistical laws are a sort of "superphysics" which would never be completely reduced to (or derived from) dynamical laws. The belief was

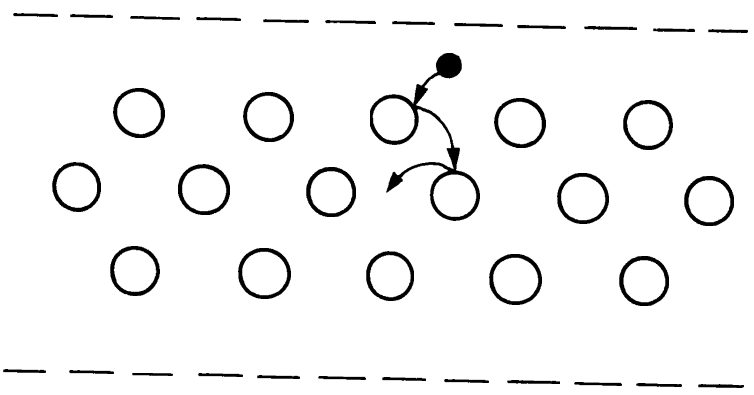

Fig. 1. Galton's Board or Lorentz's gas, the first model of dynamical chaos [3].

(and still is for many) that you always have to add something mysterious (a hypothesis or some conceptions or whatever) to the dynamics to "prepare" the statistics. But we know now that it is no longer true! All physicists should know this.

The statistical laws are a part of the dynamics, very special, unusual, even surprising, I would say, but not at all uncommon. So now, the main problem is not to formulate the additional statistical hypotheses but, on the contrary, to find out the particular conditions that give rise to those *secondary* (with respect to dynamics) laws in Nature as well as to find the particular statistical properties of the dynamical motion under the conditions in question.

1.2. A simple example, and the origin of chaos

Now it's a high time I gave a few examples of dynamical chaos. Of course, it is well known that chaos is all around us. What is apparently less known is that the structure of the dynamical laws, the special role of the initial conditions therein, and their arbitrariness as mentioned above, is also a tricky corollary of the chaos as I hope to discuss at the end of this course.

But now I want to discuss very simple models which exhibit extremely complicated behaviour characteristic of dynamical chaos. Apparently the first of such models was constructed and described by the English psychologist and anthropologist Galton [3], in 1889, a century ago! The model is known as the Galton Board or (the later name for a similar model) as the Lorentz gas. In this "gas", all (classical) "molecules" are at rest and scatter only a single one moving through the system (fig. 1). Ref. [3] is the earliest one in my list, I leave the ancient philosophical (rather than scientific) views also for discussion.

Galton himself did use his model to demonstrate statistical laws as well as statistical methods in studying mass phenomena, the methods he first

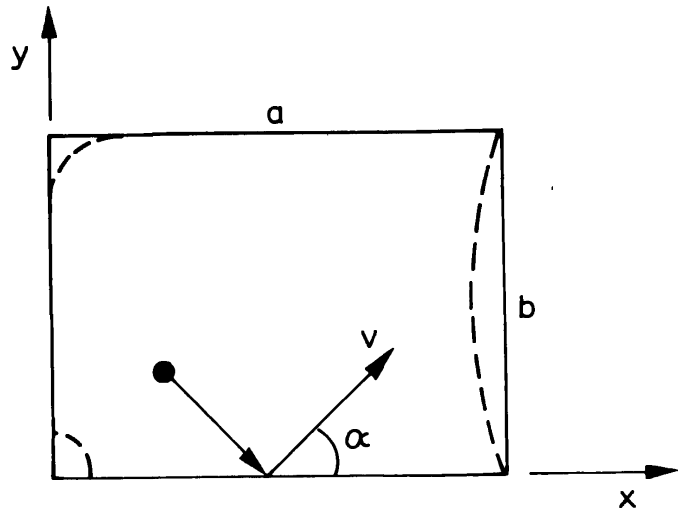

Fig. 2. Sinai's billiards (dashed lines) as slightly deformed ordinary (American) billiards (solid line).

introduced into psychology. Apparently, he had no interest in the model's dynamics which was conjectured 17 years later by Poincaré, who related chaos to a strong local instability (scattering) of trajectories.

Galton's Board is a particular type of the billiard models studied extensively by the Soviet mathematician Sinai and his disciples. In a rectangular billiard table (fig. 2, solid line), the ball's motion is *regular* in the sense that the Fourier spectrum of the motion is discrete with two basic frequencies: $\omega_x = (\pi v/a)\cos\alpha$ and $\omega_y = (\pi v/b)\sin\alpha$. Such motion is called *quasiperiodic*. Note that if the ratio ω_x/ω_y is irrational, the motion is ergodic in the *configurational space* (x, y), but not in the *phase space* (x, v_x, y, v_y), nor on the energy surface $|v| = \text{const.}$, because there are two exact isolating motion integrals in involution: $v_x, v_y = \text{const.}$ (good texts in dynamical systems can be found in refs. [4–6,50]).

Now, if we impose arbitrarily small (but not arbitrary!) deformations of the billiard contour (fig. 2, dashed lines), the ball motion becomes chaotic. What does this really mean?

To begin with, the motion's Fourier spectrum becomes continuous which is, of course, qualitatively different from the discrete spectrum of regular motion. But why is it related to chaos? And how? To answer this, recall that a Fourier amplitude of any stationary (oscillatory) process with continuous spectrum grows like $t^{1/2}$, which is typical of diffusive behaviour, characteristic of a random process. This follows directly from Parseval's equality. Physically, it means that the bouncing ball is a source of random noise. Coupled to another system, for example to a harmonic oscillator, the ball would make it diffuse in energy provided that the oscillator frequency is within the noise frequency band.

But how do we know that the ball motion in Sinai's billiard has a continuous spectrum? To be sure, it is a rigorous mathematical result. A simple explanation relates to the fact that the motion in question is locally unstable, which means the following. In addition to the main equation of motion (1.1), consider an auxiliary linearized equation,

$$\dot{\xi} = \xi \frac{\partial}{\partial x} v\left(x^0(t)\right), \tag{1.2}$$

where $x^0(t)$ is some *reference trajectory*. We call the motion locally unstable if asymptotically, as $t \to \infty$, the vector $\xi \sim \exp(\Lambda t)$ grows exponentially, that is if the limit,

$$\lim_{|t|\to\infty} \frac{1}{|t|} \ln|\xi(t)| = \Lambda > 0, \tag{1.3}$$

i.e., is positive (non-zero). The quantity Λ is called (maximal) Lyapunov's exponent after a Russian mathematician who many years ago studied the stability of motion (but not yet chaos!). Now we only need to solve a "simple" problem.

Problem. Show that the Fourier spectrum of the unstable motion has, at least, a continuous component.

The answer is quite obvious but I am not sure that the rigorous proof is that trivial.

The exponential instability implies that the function $x(t, x_0)$ has a pole at some $t = t_p = t_1 \pm \mathrm{i}\Lambda$ in the complex t plane. There is an interesting connection to the so-called Painlevé property [7], a criterion for integrability of a dynamical system, which can be traced back to work by the Russian mathematician Kowalevskaya (in 1890!). According to her criterion, the system is integrable if all singularities of $x(t, x_0)$ are movable poles, that is if every t_p depends on x_0. As the chaotic motion is nonintegrable by definition, its poles t_p , particularly Λ do not depend on x_0, at least on some set of initial conditions with dimensionality larger than one. This is an additional (to local instability) condition for chaos which is necessary to exclude an isolated unstable periodic trajectory, obviously nonchaotic. Another condition is that the motion must be oscillatory, i.e., bounded in the phase space, to exclude the trivial case of the unstable linear equation. The latter implies in particular that chaotic motion is always described by *nonlinear* equations even though the criterion for chaos relates to a linear

equation (1.2) but with time-dependent coefficients. Moreover, for chaotic motion of the main system (1.1), this time-dependence is also chaotic.

Problem (unsolved). Formulate necessary and sufficient conditions for a motion to be chaotic.

Problem. List all distortion types of the rectangular billiard table that produce chaotic motion.

Notice that whatever the system (1.1) may be, Hamiltonian or dissipative, we can always formally construct a new Hamiltonian system in the combined phase space related to eqs. (1.1) and (1.2). To this end, consider the Hamiltonian

$$H(x,\eta) = \eta v(x), \tag{1.4}$$

which generates the main equation (1.1) if we assume all $x's$ to be "coordinates" while the dynamics of conjugate "momenta" η is that for ξ (eq. (1.2)) in the reversed time ($t \to -t$). If, moreover, the main system (1.1) is time-reversible, the artificial model (1.4) is completely equivalent to the pair (1.1) and (1.2).

You may say that if the motion is unstable it is not surprising that there is statistical behaviour, random properties, etc., as the system is extremely sensitive to any external noise or perturbation. This is certainly true but, logically, the reference to any external effect does not solve the problem of the nature and mechanism of the statistical laws. Instead, this pushes it aside. In contrast to this approach, the modern theory of dynamical chaos has proven:

(i) principally, no external noise is necessary or required to explain chaos, which is a purely dynamical (deterministic) phenomenon;

(ii) a sufficiently weak external perturbation doesn't affect either the statistical properties of the motion or even the trajectories (with suitably modified x_0, of course); this is called the *structural stability*, or *robustness*;

(iii) for the motion of a dynamical system to be truly random, the local instability must be *exponential*, which is the strongest one in a smooth (nonsingular) system; a power-law instability is insufficient for the dynamical chaos.

The latter result is far from trivial, and it corrects an old (and very instructive!) mistake due to Born [8] who thought that quasiperiodic motion with a linear instability, e.g., in rectangular billiards, is unpredictable and, in this sense, indeterministic. Born's idea was certainly correct regarding the prediction of a future trajectory solely from the initial conditions.

Yet, it proved to be wrong if one records a sufficiently long trajectory segment. On the contrary, if the instability is exponential, even observation of the whole past trajectory (back to $t = -\infty$) to any finite accuracy does not allow to predict a finite future segment of the trajectory. This is the strongest chaotic property which many (but not yet all!) researchers mean when speaking of "true dynamical chaos", or of "true randomness". Notice that the continuous spectrum is a much weaker statistical property which only implies some diffusion and a sort of statistical relaxation.

A linguistic remark. Some people understand the terms "stochastic" and "chaotic" as synonyms. I make the distinction that, while the latter term refers to purely dynamical motion, the former is traditionally related to a noise-driven system, e.g., "stochastic differential equations".

Coming back to the effect of external perturbation upon an unstable system, I would say that the physicist's immediate response mentioned above also makes some sense: we really need a stable description. The unstable dynamical theory can only be used as an intermediate step in the evaluation of the statistical properties which prove to be typically (but not always!) stable. If the statistical description is also not stable, a new "secondary" dynamics arises which is sometimes called synergetics. This is also a very exciting problem, but, again, it is not part of the material I have to discuss.

1.3. The basic model

Now let me come closer to my topic "Time-dependent quantum systems". It means in particular an *explicit* time-dependence, e.g., in the Hamiltonian $H(x, p, t)$. Why was I given only this particular part of the chaos? Apparently because the international team that I represent here – at different stages of research it included: G. Casati (Milano); J. Ford (Atlanta); I. Guarneri (Pavia); F. Vivaldi (London), and B. Chirikov, F. Izrailev, D. Shepelyansky, V. Vecheslavov (Novosibirsk) – has indeed studied time-dependent chaos for many years. But why? Certainly, not because we are specially interested in these particular phenomena but simply because it is much simpler. Actually, we have chosen, from the very beginning, to study the models described not by continuous differential but by discrete difference equations, or by *mappings*, or more briefly, *maps*. They are much simpler for analytical treatment, and even simpler for numerical simulations, or *numerical experiments* as we like to say, angering true (laboratory) experimentalists.

At this point I must say that numerical experiments play a very profound role in the studies of dynamical systems in general, and chaotic phenom-

ena in particular. This "third way of cognition" (in addition to laboratory experiments and analytical theory) is justified by definition for all the *secondary* laws (like statistical laws) which are completely contained within a more fundamental theory (like classical or quantum mechanics).

Thus, we are interested not so much in time-dependent dynamical systems but rather in the models represented by maps for their simplicity. The main problem for a physicist here is to choose the model to be as simple as possible but not simpler, that is to choose one which is rich enough, and which, at least, contains the desired phenomenon of dynamical chaos. Also, in what follows we shall restrict ourselves to Hamiltonian systems which are the most fundamental ones, even though less practical (another interesting topic to discuss elsewhere!). Besides, the *invariant measure* of any Hamiltonian system is known beforehand, it is simply the *phase space volume* (in any canonically conjugated variables). This is a great simplification in theoretical analysis. Then, one of the simplest models can be described by a two-dimensional canonical (area-preserving) map, which in turn, it is convenient to specify by the *generating function* of the form,

$$G(x,\bar{p}) = x\bar{p} + \Delta \cdot H(x,\bar{p}). \tag{1.5}$$

The map itself is given by the difference equations $\bar{x} = \partial G/\partial \bar{p}$; $p = \partial G/\partial x$, or,

$$\bar{p} = p - \Delta \cdot \frac{\partial H(x,\bar{p})}{\partial x}, \qquad \bar{x} = x + \Delta \cdot \frac{\partial H(x,\bar{p})}{\partial \bar{p}}. \tag{1.6}$$

Here x,p are old (initial) variables, and $\bar{x},\bar{p}$ are new ones, that is after some period of time Δ. In the limit $\Delta \to 0$ the differences $\bar{p} - p$ and $\bar{x} - x$ vanish, and we have a continuous system with Hamiltonian $H(x,p)$.

For any finite Δ, some time-dependent Hamiltonian can be also introduced. This is especially simple if we assume

$$H(x,\bar{p}) = H_0(\bar{p}) + \frac{k}{\Delta}V(x), \tag{1.7}$$

where H_0 describes the unperturbed system, and V is the perturbation with parameter k. Then, the Hamiltonian we are seeking is,

$$\mathcal{H}(x,p,t) = H_0(p) + \frac{k}{\Delta}V(x)\delta_\Delta(t). \tag{1.8}$$

The explicit time dependence is introduced here via a periodic δ-function,

$$\delta_\Delta(t) \equiv \Delta \cdot \sum_m \delta(t - m\Delta). \tag{1.9}$$

The continuous system (1.8), although singular, is completely equivalent to the map (1.6) with the function H from eq. (1.7). The latter form provides an explicit map which is also a great simplification, especially for computation.

Thus, a map may be viewed as a time-dependent system driven by the external periodic perturbation in the form of short "kicks" represented by the δ-function (1.9) (this is the origin of the topic of my course). Yet, this is not necessarily the case. We may construct a map, the so-called *Poincaré map*, for a conservative system as well. Consider, for example, a billiard in a plane (fig. 2), and let us record the ball's position in 4-dimensional phase space each time when $x = a$ has some prescribed value. Owing to energy conservation, the remaining dynamical space is 2-dimensional and it is called *Poincaré's surface of section*. The equation of motion induces the transformation of this surface onto itself which is described by some map of type (1.5) but, of course, not always of a simpler form (1.7). This is another view of the map. Notice that successive time intervals Δ_i for the map would be generally unequal and sometimes even chaotic. But we may introduce a discrete time, the number of the map's iterations, or change the time variable in such a way to ensure that all $\Delta_i = \text{const.}$, and then construct a continuous "kicked" model like eq. (1.8).

The map (1.6) with Hamiltonian (1.7) will be our *basic model* in discussing the dynamical chaos. But it is a *classical* model, whereas my main topic is *quantum chaos*. Why quantum? Because today quantum mechanics is the most deep, fundamental and universal physical theory which seems to comprise everything in the Universe. Everything but ... true dynamical chaos! This is the most delicate point in the problem of quantum chaos we are going to discuss. But first, in the next section I will briefly review the classical dynamics of the basic model to see (or to revise!) the meaning of dynamical chaos and to see what is absent in quantum mechanics, and why.

2. A brief review of the classical chaos

2.1. The basic model and physical problem

First, we shall specify further the basic model given by eqs. (1.6) and (1.7). If we assume that (p, x) are action–angle variables and let $V(x) = \cos x$, then map (1.6) becomes,

$$\bar{p} = p + k \sin x\,, \qquad \bar{x} = x + \Delta \cdot H_0'(\bar{p})\,, \tag{2.1}$$

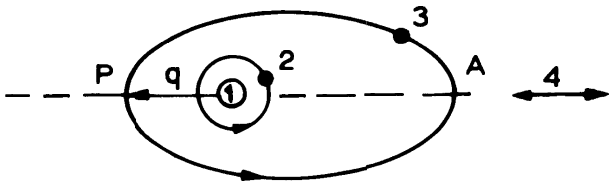

Fig. 3. Chaos in the Coulomb interaction: (1) the central body (Sun or proton); (3) comet or electron; the periodic perturbation is due to Jupiter (2) or to a uniform alternating electric field (4); P is the perihelion and A is the aphelion of the comet's (electron's) orbit.

where $H_0'(p) \equiv \mathrm{d}H_0/\mathrm{d}p$. The phase space of this model is a cylinder, periodic in x (mod 2π) and infinite in both directions of p.

The condition,

$$\Delta \cdot H_0'(p_r) = 2\pi r, \tag{2.2}$$

for any integer r determines the *resonant* values p_r. If their spacing $\delta p_r \approx |2\pi/(\Delta \cdot H_0'')| \ll |H_0''/H_0'''|$ is small enough, we can linearize the second equation (2.1). Introducing the new variable $P = p - p_r$, we arrive at a still simpler map,

$$\bar{P} = P + k \sin x\,, \qquad \bar{x} = x + T\bar{P}, \tag{2.3}$$

where $T = \Delta \cdot H_0''(p_r)$ is a new parameter. The latter model has become very popular in studies of nonlinear dynamics and chaos. It is usually called the *standard map*.

The are two parameters in this map but one of them can be eliminated by another change of variable: $TP = Q$, whence,

$$\bar{Q} = Q + K \sin x; \qquad \bar{x} = x + \bar{Q}. \tag{2.4}$$

Thus, the dynamics of the standard map is completely determined by the only parameter,

$$K = kT, \tag{2.5}$$

together with the initial conditions, of course. However, in quantum mechanics the latter simplification does not work, and we shall have to use version (2.3) of the map (section 3).

The standard map appears so simple that it may seem to be a mathematical exercise rather than a real physical model. To avoid such a misconception let us consider straight away two particular physical examples which can be described by, or, rather, reduced finally to, the standard map.

The first example is from celestial mechanics, namely, the motion of a comet (around the sun) driven by Jupiter. We assume a plane-restricted circular three-body problem as outlined in fig. 3. The comet's orbit is extended (eccentricity $e \approx 1$) and lies outside Jupiter's circular orbit and in the same plane. We may construct a map over either Jupiter's period of motion or that of the comet. Choosing the second (simpler) option, we arrive at the basic model [9],

$$\bar{E} = E + k \sin\varphi\,, \qquad \bar{\varphi} = \varphi + 2\pi\omega \left(-2\bar{E}\right)^{-3/2}. \tag{2.6}$$

Here $E < 0$ is the comet's total energy (per unit mass), and ω and φ are Jupiter's orbital frequency and its phase at the moment when the comet is at perihelion, respectively. We assume the sun's mass, Jupiter's orbit radius and frequency ω to be unity but keep ω in eq. (2.6) to use this equation in the second example.

The perturbation parameter [9],

$$k \approx 8.5\mu q^{-1/4}\, \mathrm{e}^{-q^{3/2}} \tag{2.7}$$

(q is the comet's perihelion distance and $\mu \approx 10^{-3}$ is Jupiter's mass), does not depend on the energy E. This is one reason to use the energy instead of the action. Another reason will be given later on in this section.

Notice that the energy value $\bar{E}$ determining the Kepler period of the comet is actually achieved at the aphelion, further from Jupiter, while its strongest perturbation is concentrated near the comet's perihelion. Thus, the quantities φ and E correspond to different instants of time, and to different positions of the comet. Hence, eq. (2.6) is not the usual Poincaré map.

Problem. Change map (2.6) to the form in which φ and E are both taken at perihelion (aphelion).

The second parameter of the corresponding standard map,

$$T = 6\pi\omega\,(-2E)^{-5/2} \tag{2.8}$$

(as well as K in map (2.4)) is energy dependent.

Map (2.6) is, of course, an approximation if only because the changes in e and q are completely neglected but this can be justified [9]. Thus, the map describes the essential dynamics of this three-body problem which, in particular, may be chaotic. For example, the Halley comet with a somewhat more complicated perturbation term turns out to be chaotic (see ref. [10]).

This example is especially interesting because it belongs to celestial mechanics, the citadel of classical deterministic physics, which falls with the onset of chaos.

Unlike the previous purely classical example, the next one is quantal: the photoelectric effect in hydrogen, i.e., the ionization of a hydrogen atom by a uniform monochromatic electric field. Here we consider the quasiclassical region of large quantum numbers including the initial ones. Such states are called *Rydberg atoms*.

In some approximation, to be discussed in detail in forthcoming sections, we may use the classical model of the atom. Then, the picture of electron motion is essentially the same as for the comet (fig. 3), the only difference being that there is now an alternative uniform field of frequency $\omega \neq 1$, instead of a rotating point mass (Jupiter). Moreover, the map (2.6) as well as the standard map can be used with the same parameter T (eq. (2.8)) but different

$$k \approx 2.6 \frac{\varepsilon}{\omega^{2/3}}. \tag{2.9}$$

Here ε is the field strength [11] (the atomic units $e = m = \hbar = 1$ are used in this example).

Now ω is the field frequency, and φ is the field's phase at the moment when the electron passes the perihelion where the interaction with the field is maximal. The latter is not obvious, perhaps, because the perturbation is uniform, unlike the first example. The cause of the maximal effect of the field near the perihelion is explained by the maximal electron's acceleration at that point.

2.2. Nonlinear resonances and their interaction

First, we shall consider the dynamics of the standard map (2.3), which is quite simple in comparison with the basic model (2.1). Without the perturbation ($k = 0$), the action P is the motion integral while the phase x is uniformly rotating with frequency $\omega = (\bar{x} - x)/T = P =$ const. Such an oscillation is called *nonlinear* because its frequency depends on the action. Notice that nonlinearity is related here to a linear second equation, eq. (2.3). This is because we interpret x as a phase variable, and interpret the motion as an oscillation.

Even if x is a standard Cartesian coordinate, the notion of nonlinear motion sometimes makes sense, depending on the perturbation to be included. Suppose, for example, that the perturbation $\sin x$ is a spatially periodic field. Then, uniform motion in a straight line with constant velocity P would be also termed as a "nonlinear oscillation" in the modern

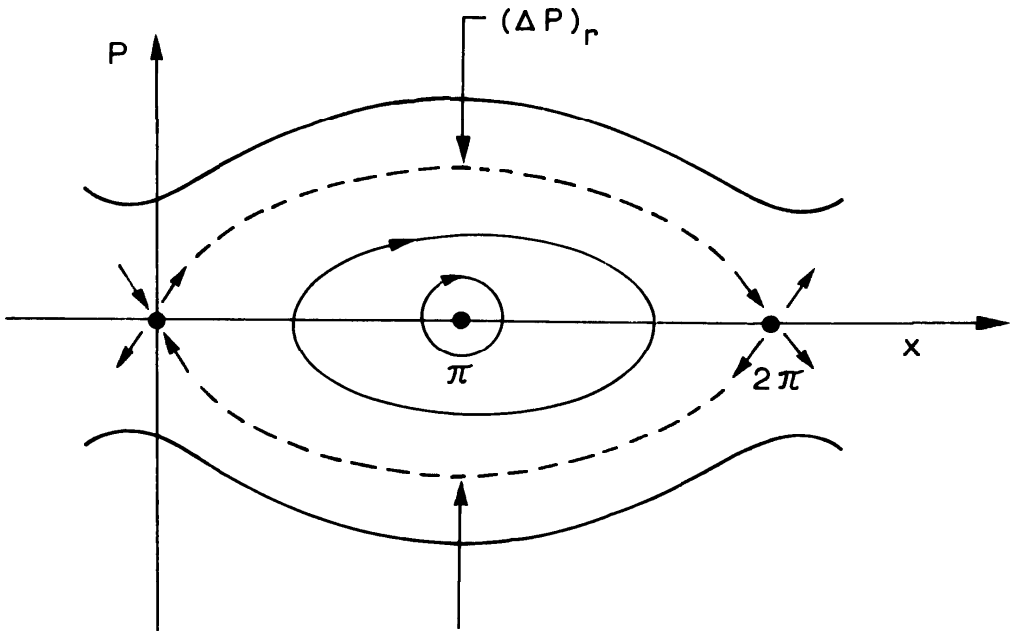

Fig. 4. Phase plane of a nonlinear resonance: the full circles indicate periodic orbits; the dashed line is the separatrix.

theory of dynamical systems. The reason for this somewhat strange terminology is related to the fact that just such a nonlinearity is responsible for chaos as we shall now see.

The unperturbed motion is called *resonant* if the frequency ratio $\omega/(2\pi/T) = TP/2\pi = m/l$ is rational. For a sufficiently small perturbation, only resonances are essential for the dynamics. The principal slogan in Hamiltonian dynamics is,

Look for the resonances!

The resonances form a set that is everywhere dense, yet only part of them are really important.

One resonance ($l = 1$; $m = 0$) can be analyzed in the following simple way. Assume $k \to 0$, and $\Delta P = |\bar{P} - P| \ll 1$; $\Delta x = |\bar{x} - x| \ll 1$. Then we can replace the difference equation (2.3) by the differential one with the Hamiltonian,

$$H_r^0 = \frac{P^2}{2} + \frac{k}{T}\cos x. \tag{2.10}$$

However, this is simply a *pendulum* which, thus, models a nonlinear resonance. Notice that the unperturbed system in this model ($k = 0$) is a *rotator* whose frequency P is equal to the action (in our units).

The phase portrait of a single nonlinear resonance is outlined in fig. 4. There are two periodic trajectories (fixed points), stable ($x = \pi$; $P = 0$) in

the resonance center, and unstable ($x = P = 0$). The latter is asymptotic to a peculiar trajectory – the separatrix (denoted by the dashed line) – which bounds the resonance domain of x-phase oscillation. Outside the domain, x is rotating. The resonance width in P at $x = \pi$ is equal to

$$(\Delta P)_{\mathrm{r}} = 4\sqrt{k/T}, \tag{2.11}$$

and it is much bigger for small k than a non-resonant perturbation $\Delta P \sim k$.

The single nonlinear resonance (2.10) is a completely integrable system with regular motion and no chaos whatsoever. How can we get other resonances in the standard map? One way is to construct the corresponding continuous system as was explained in section 1 (see eqs. (1.8) and (1.9)). For the standard map (2.3), $H_0 = P^2/2$, and $\Delta = T$. Using the formal expansion,

$$\delta_T(t) = T\sum_m \delta(t - mT) = 1 + 2\sum_{m=1}^{\infty} \cos\frac{2\pi mt}{T}\ , \tag{2.12}$$

we arrive at the continuous time-dependent Hamiltonian

$$\mathcal{H}(x, P, t) = \frac{P^2}{2} + \frac{k}{T}\sum_{m=-\infty}^{\infty} \cos\left(x - \frac{2\pi mt}{T}\right), \tag{2.13}$$

which describes the same model (2.3).

A term in eq. (2.13) with $m = 0$ represents the pendulum (2.10), that is, a single nonlinear resonance. But any other term $m \neq 0$ differs from the former only by a shift in P by $(\delta P)_m = 2\pi m/T$. The change of variables $x \to y = x - (\delta P)_m t$, $P \to p = P - (\delta P)_m$ with the generating function $F(y, P) = -[y + (\delta P)_m t]\,[P - (\delta P)_m]$ brings the Hamiltonian (2.13) with a single term $m \neq 0$ into the form (2.10). Hence, the Hamiltonian (2.13) explicitly describes an infinite set of resonances $P_m = 2\pi m/T$ which all are alike. The latter is immediately seen from the map itself because it is periodic not only in x (mod 2π), but also in P (mod $2\pi/T$). This is a peculiarity of the standard map which one should bear in mind.

The standard map describes the local structure of a more complicated basic model, the former being presented as a uniform structure. The periodicity of the standard map in P implies that the structure of motion on the infinite cylinder phase space is essentially equivalent to that on a finite torus (x (mod 2π); P (mod $2\pi/T$)), which is required for unstable motion to be chaotic.

The single resonance approximation (2.10) holds for any of the *primary resonances* $P_m = 2\pi m/T$ in model (2.13) provided the perturbation k is sufficiently small. The question is, how small?

The natural measure is the overlap parameter,

$$s = \frac{(\Delta P)_m}{(\delta P)_1} = \frac{2}{\pi} K^{1/2}, \tag{2.14}$$

which is the ratio of the resonance width (2.11) to the spacing of the primary resonances $(\delta P)_1 = 2\pi/T$. Obviously, s depends on $K = kT$ only.

If $s \ll 1$, or $K \ll 1$, all the resonances but one (depending on the initial conditions) can be neglected. In other words, we may say that resonances do not interact. In the opposite limiting case ($s \gg 1$; $K \gg 1$), they do interact because the system is nonlinear.

When $K \ll 1$, the nonlinearity suppresses, or stabilizes, the resonant perturbation unlike the case of a linear oscillation. However, if $K \gg 1$, a trajectory may pass from one resonance domain to another, thus wandering in P. This is quite comprehensible. What is less expected, and was actually a big surprise, is that the motion becomes of a qualitatively different type, namely, chaotic. How do we know that the motion is chaotic when $K \gg 1$? From the local instability of the motion. Before turning to the latter point, let us briefly discuss the critical value of $K = K_c$, which separates the bounded and unbounded motion in P. Notice that the existence of such a critical value is directly inferred from periodicity in P. A plausible conjecture would be that $s_c \approx 1$, and $K_c = \pi^2/4 \approx 2.5$ (see eq. (2.14)). This is true, but only in order of magnitude. Thorough analytical and numerical studies yield [6,12,13],

$$K_c \approx 1, \qquad s_c \approx 2/\pi. \tag{2.15}$$

The main cause of the discrepancy is related to high-order resonances $P_{ml} = (2\pi/T)(m/l)$ $(l > 1)$, which are not explicitly present in the Hamiltonian (2.13), and which arise in higher approximations of the perturbation theory.

2.3. Local instability and chaos

Local instability is studied most conveniently by using the linearized standard map (2.3). We have,

$$\bar{\eta} = \eta + \xi k \cos x^0, \qquad \bar{\xi} = \xi + \bar{\eta} T, \tag{2.16}$$

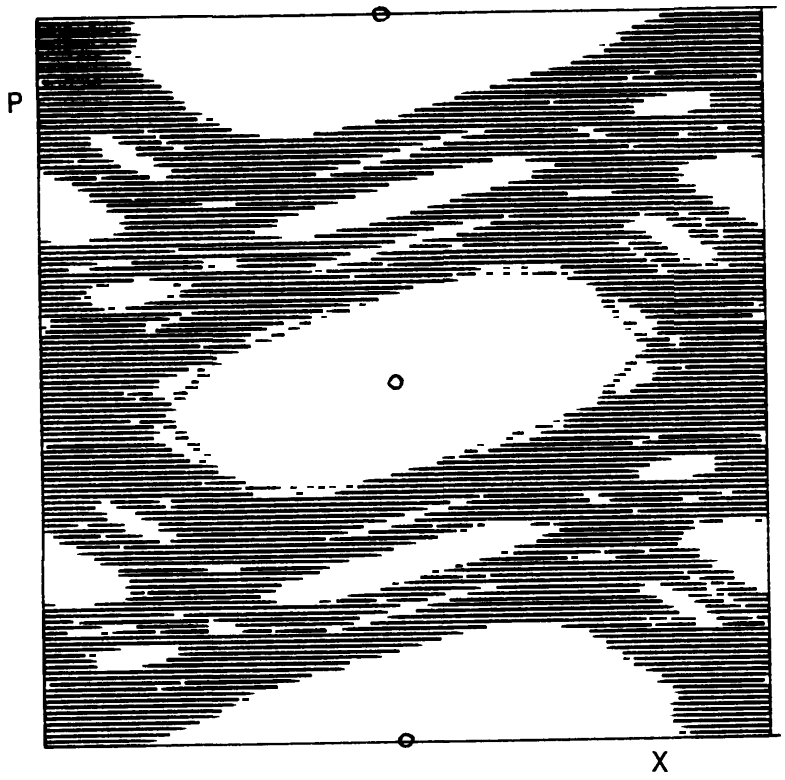

Fig. 5. Two periods of the standard map [13]: $K = 1.13 > K_c$; the connected chaotic component is hatched; the circles are stable fixed points of period one in the centers of three successive resonances $P_n = 2\pi n$.

where x^0 is the reference trajectory, and $\xi = \mathrm{d}x$ and $\eta = \mathrm{d}P$ are infinitesimal. The *local eigenvalues* of the map,

$$\lambda\left(x^0\right) = 1 + \frac{K\cos x^0}{2} \pm \sqrt{K\cos x^0\left(1 + \frac{K\cos x^0}{4}\right)}, \tag{2.17}$$

depend, again, on K but also on x^0. The latter implies fluctuations in the motion's instability.

If the instability were uniform, the Lyapunov exponent (for a bigger $|\lambda|$) would be $T\Lambda = |\ln|\lambda|| > 0$, the latter inequality being the condition for chaos. Consider, for example, a "linear" perturbation kx in the standard model. We use quotation marks because x is a phase variable taken (mod 2π), and the motion is confined to a torus but not to a plane. In this example, the motion is unstable and chaotic for all K outside the interval $(-4, 0)$.

What should we do in the case of eq. (2.17), when $\lambda\left(x^0\right)$ varies along a trajectory? Now we need to average $\ln|\lambda|$,

$$T\Lambda = \overline{\ln|\lambda|} = \langle \ln|\lambda| \rangle, \tag{2.18}$$

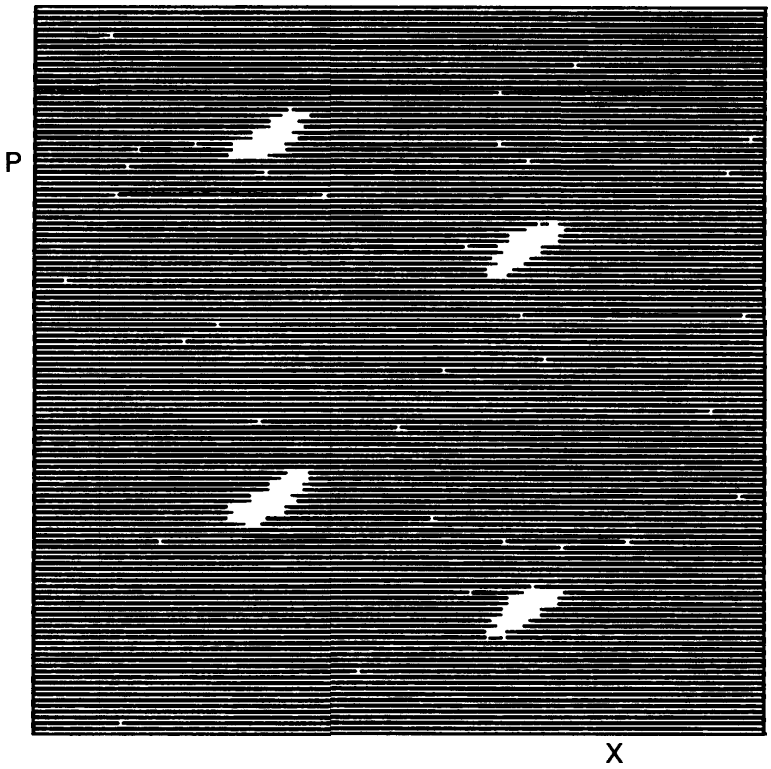

Fig. 6. Same as in fig. 5 but for $K = 5$; the motion time is $\tau = 10^5$ iterations; the resolution is 128 × 128 bins [13].

where the horizontal bar denotes the time-averaging along a trajectory, and the brackets do so for the phase-averaging over the invariant measure of a motion component to which the trajectory belongs. The latter is the principal difficulty because the motion component may happen to have a very complicated structure which is sometimes called a fat fractal [14]. This is certainly the case for $K \sim 1$ (fig. 5).

A plausible conjecture is that for $K \gg 1$, the trajectory will fill up the whole torus as $|\lambda| > 1$ for most x^0 values. Numerical experiments do confirm this conjecture (fig. 6). Then, we can average eq. (2.18) over x^0 to obtain,

$$T\Lambda = \langle \ln |\lambda| \rangle_{x^0} \approx \ln(K/2), \tag{2.19}$$

which proves to be a good approximation for $K > 4$.

Problem. Estimate the number of empty bins (small white spots in fig. 6) missed by a chaotic trajectory because of random fluctuations.

In fig. 7, a few chaotic trajectories of the standard map are shown for illustration. The dashed lines indicate the root-mean-square fluctuations: $\langle (\Delta P)^2 \rangle^{1/2} = k\,(t/2)^{1/2}$ ($T = 1$, see below), while vertical

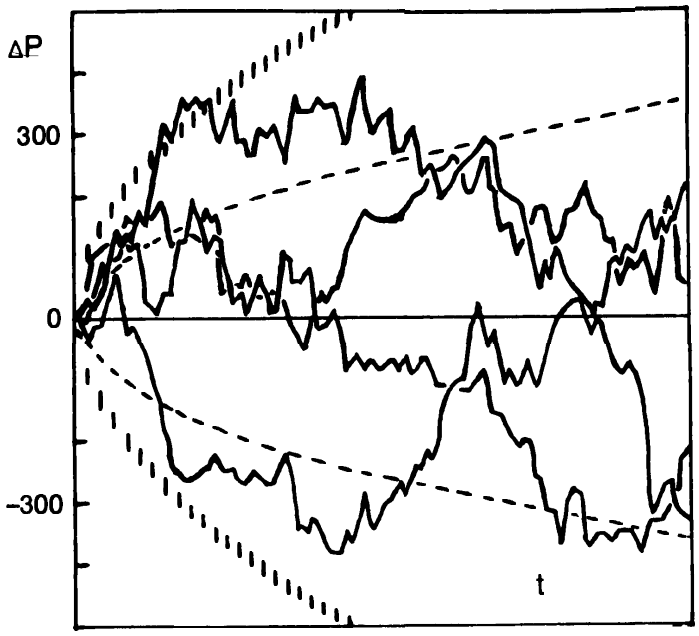

Fig. 7. Four chaotic trajectories of the standard map: $T = 1$; $K = 5$; $t = 10^4$; average (dashed lines) and maximal (vertical hatching) fluctuations are shown.

hatching is the strict upper bound for the diffusion fluctuations: $|\Delta P| < \langle(\Delta P)^2\rangle^{1/2} (2 \ln \ln t)^{1/2}$, the so-called law of the iterated logarithm.

For $K \gtrsim K_c \approx 1$ the connected (global) component occupies about a half of the phase space. If $K \ll 1$ the chaotic motion remains in exponentially narrow isolated layers around resonance separatrices only. It's interesting to note that the motion in these layers can be approximately described, again, by the basic model [13].

The local instability, as described by the linearized equation, characterizes the behaviour of infinitely close trajectories. What would be the evolution of two real trajectories initially at a small but finite distance?

In the standard map, for a sufficiently strong local instability ($K \gg 1$) and a small perturbation ($k \ll T$), the exponential separation of close trajectories proceeds mainly along the x direction. This is easily verified by the linearized eq. (2.16), from which the ratio of eigenvector components is

$$\frac{\xi}{\eta} = \frac{\lambda - 1}{k} \approx T \gg 1. \tag{2.20}$$

As soon as the separation in phase $\xi \sim 1$ reaches the maximal value, the exponential instability in both x and P terminates (for these two particular trajectories only!) and turns into a mixing in x, and into a diffusion in P. The latter separation grows only as $t^{1/2}$ only.

2.4. Regular, or familiar, chaos

The term "regular chaos" should not be confused with the notion of "regular trajectory". The latter is understood to be quasiperiodic motion of discrete spectrum in a completely integrable system – something opposite to chaos. The term "regular chaos" means chaos with commonly expected statistical properties conjectured and described via additional statistical hypotheses long before the contemporary era of dynamical chaos.

One of such routine statistical processes is diffusion (in P for the standard map). The diffusion rate is by definition

$$D_P \equiv \frac{\langle (\Delta P)^2 \rangle}{t} = \frac{k^2}{2T}\, C(K), \tag{2.21}$$

where the latter expression takes account of the dynamics via the correlation factor $C(K)$ that we are going to discuss.

In the old days, a reasonable statistical hypothesis would have been the *random phase approximation*: successive x values are random and statistically independent. Then, obviously, $C = 1$. In the theory of dynamical chaos, we don't need any hypotheses but, instead, we must calculate the correlation $C(K)$ (and the diffusion rate) from the dynamics, eq. (2.3) for the problem under consideration.

If $K \gg 1$, the principal contribution comes from the correlation of the phases $\bar{x}$ and $\underline{x}$, the latter being the backward iterate of x. This was first done in ref. [15] (for a simple calculation see ref. [16]),

$$\begin{aligned} C(K) &\approx 1 + 4\,\langle \sin \bar{x} \sin \underline{x} \rangle \\ &= 1 - 2\,\langle \cos(2x + K \sin x) \rangle \;\; = 1 - 2J_2(K)\;. \end{aligned} \tag{2.22}$$

Here $J_2(K)$ is a Bessel function. The comparison of theoretical and numerical results is shown in fig. 8 and it is fairly good except for a few points to be discussed later on. Occasionally, $C(5) \approx 1$ which we shall use in some numerical illustrations.

This is a good example with which to understand the relation of dynamical chaos to the old traditional statistical mechanics. In case of a strong instability of motion, the trajectory no longer has any direct physical meaning, and we have to turn to a stable statistical description, if there is one. Yet, the dynamical equations, e.g., the standard map, may and can be used to derive the statistical laws.

The diffusion equation for the distribution function, or density,

$$\frac{\partial f(P,t)}{\partial t} = \frac{1}{2}\frac{\partial}{\partial P} D_P \frac{\partial f(P,t)}{\partial P}\,, \tag{2.23}$$

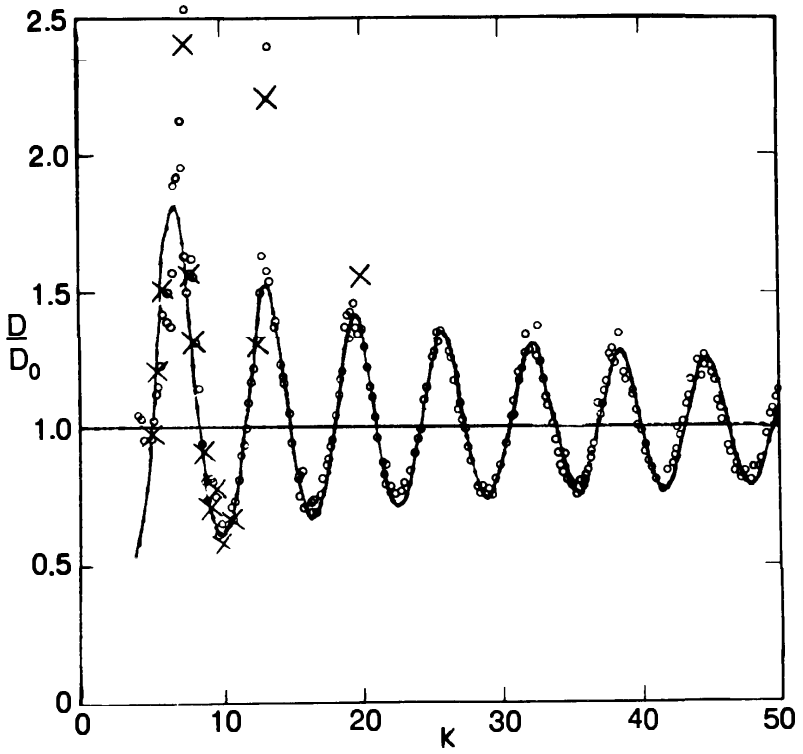

Fig. 8. The diffusion rate in the standard map: $D_0 = k^2/2$; the solid line is the prediction of a simple theory [15]; circles are numerical data [15], and the crosses are the same for the quantized map [17].

has a formal solution for any initial $f(P,0)$. Yet, dynamical chaos imposes on this process some temporal and spatial scales related to the initial exponential spreading of the distribution function prior to the diffusion. The spatial dynamical scale is (cf. eq. (2.20))

$$(\Delta x)_s \sim 1; \qquad (\Delta P)_s \sim 1/T, \tag{2.24}$$

while the spreading time is

$$\frac{(\Delta t)_s}{T} \sim \frac{|\ln (T(\Delta P)_0)|}{T\Lambda}, \tag{2.25}$$

where $(\Delta P)_0 \lesssim 1/T$ is the initial width of the distribution function. Because $(\Delta x)_s \sim 1$, only the motion in P is diffusive.

In an infinite phase space on a cylinder, the uniform diffusion leads eventually to a Gaussian distribution,

$$f(P,t) \to \frac{\exp\left(\dfrac{P^2}{2tD_P}\right)}{\sqrt{2\pi t D_P}}, \tag{2.26}$$

which is spreading out indefinitely (fig. 9).

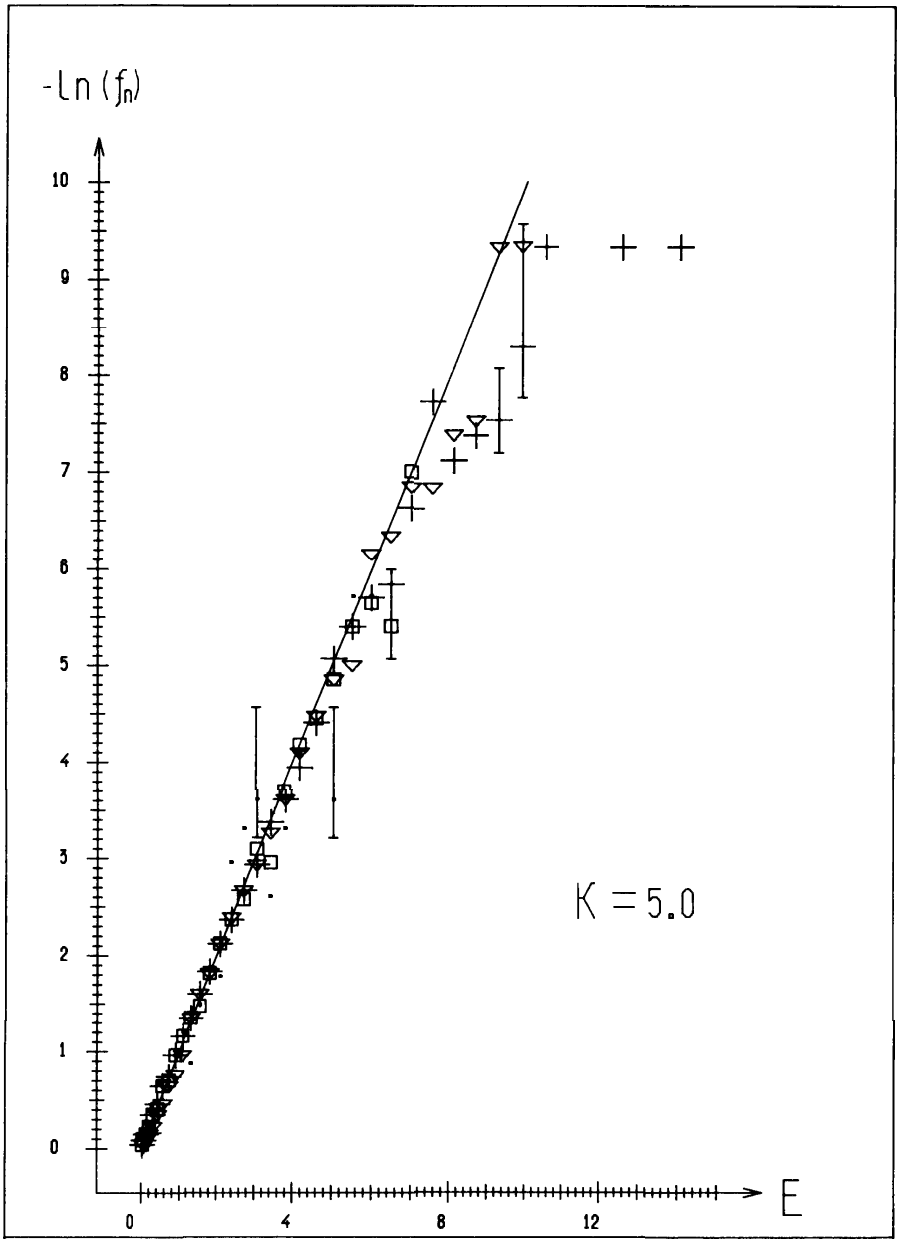

Fig. 9. Gaussian fluctuations in the standard map [13]: $f_n = f\sqrt{2\pi t D_P}$ (see eq. (2.26)); $E = P^2/2tD_P$; the straight line is the prediction corresponding to a normalized Gaussian distribution: $-\ln f_n = E$.

Instead, we may consider a finite P interval of total length L. For example, we may "roll up" the cylinder into a torus, the model we are going to use in future sections. Then, instead of an infinite diffusion, there would be a *relaxation* to the *steady state* $f_s = 1/L$ in accordance with the Hamiltonian invariant measure. The relaxation law is asymptotically determined by the first eigenfunction of the diffusion equation, and has the form,

$$f(P,t) - \frac{1}{L} \approx \mathrm{e}^{-2\pi^2 t D_P/L^2} \cos\frac{2\pi P}{L}. \tag{2.27}$$

Notice that unlike the formal diffusion equation, the maximal number n of

eigenfunctions $f_n \sim \cos(2\pi nP/L)$ under dynamical chaos is restricted by $n \lesssim LT/2\pi = l$, the number of the map's periods in P over the torus (cf. eq. (2.24)).

So far we have interpreted the standard map as a "kicked rotator", hence, x was the angle variable defined (mod 2π). Instead, we may also view this map as describing a particle motion in an infinite periodic field. Then x-motion is also diffusive for $\Delta x \gg 2\pi$. Since $\bar{x} - x = T\bar{p}$ and $p \sim (D_p t)^{1/2}$, the spreading of the distribution function in x grows as $\Delta x \sim TD_p^{1/2} t^{3/2} \sim Kt^{3/2}$ (see eq. (2.21)).

Problem. Derive an exact expression for $\langle (\Delta x)^2 \rangle$.

The maps under consideration are canonical, which corresponds to the Hamiltonian nature of the physical systems modeled by these maps. The models are approximate, of course, and a crucial question is how large are the deviations? Is the simulation quantitative or only qualitative? One origin of the large deviations is related to a somewhat surprising fact that the steady-state distribution depends in general on the time variable chosen.

Consider, for example, our basic model (2.6). Here, the physical time $t_{\rm ph}$ and map's time t (proportional to the number of map's iterations) are related by

$$\frac{\mathrm{d}t_{\rm ph}}{\mathrm{d}t} = \frac{2\pi}{(-2E)^{3/2}} = \frac{2\pi}{\Omega(E)},$$

where Ω is the frequency of the motion in physical time. From the ergodicity of motion, the invariant measure (= steady-state distribution) is proportional to the corresponding time and, hence, is different in the two models provided that the derivative $\mathrm{d}t_{\rm ph}/\mathrm{d}t$ depends on dynamical variables. For the physical time $t_{\rm ph}$, the measure $\mathrm{d}\mu \sim \mathrm{d}J \sim \mathrm{d}t_{\rm ph}$ is related to the action J. Hence, for the corresponding Poincaré map $\mathrm{d}\tilde{\mu} \sim \mathrm{d}t \sim \Omega\,\mathrm{d}J = \mathrm{d}E$, the true measure is determined by the *energy*, not by the action. This is the main reason why one should use energy, rather than action or any other variable, to construct the map for a time-dependent Hamiltonian system.

The chaos so far considered is simple in the sense that it is well known in traditional statistical mechanics. What is not so simple is the dynamical nature of this chaos. Particularly, it resolves an old mystery, how to reconcile dynamical time reversibility with statistical irreversibility, or, in other words, how to explain the nature of the so-called "time arrow"?

The answer given by dynamical chaos theory may surprise you: there is no time arrow whatsoever! The statistical relaxation as well as the diffusion

proceeds in both directions of time. Both of these processes are symmetric with respect to time reversal as well as the dynamical motion of which the former are particular cases.

To be sure, the diffusion equation (2.23) is not symmetric, of course, but this is only because it describes an averaged (over phase x) evolution of the system. In other words, the distribution function $f(P,t)$ is a *coarse-grained density*. The *fine-grained (exact) density* $\tilde{f}(P,x,t)$ would not tend to a constant like $f(P,t)$. Instead, it becomes more and more "scarred" as the relaxation proceeds. These "scars" remember the initial state $\tilde{f}(P,x,0)$ and provide the time-reversal behaviour. Yet, the exact distribution $\tilde{f}(P,x,t)$, as well as the coarse-grained $f(P,t)$ for a chaotic motion would never come back to the initial distribution, unlike an individual trajectory which does so infinitely many times according to Poincaré's recurrence theorem. Moreover, even if the distribution function is related to a single recurrent trajectory, the former would not recur.

In my opinion, much of this confusion is due to ambiguous terminology. One should distinguish two completely different properties: (i) *time-reversibility* as a result of very strong external intervention into the system, the reversal of its velocities, and (ii) *the recurrence* of a free evolution of the autonomous system when it is left alone. The chaotic motion is time-reversible relaxation which is non-recurrent.

The illusion of time arrow in Nature stems from the confusion of the two above conceptions: in a chaotic system there is always some relaxation whatever direction of time you follow (see also section 5).

2.5. Critical phenomena in dynamics: beyond any order

As the statistical properties of a dynamical system are completely determined by the equations of motion and do not depend on our simplified assumptions, it is no surprise that the former are not always as simple as we should expect. Moreover, it is common that neither dynamical nor statistical description reveals any order or simplicity. Reality is highly intricate!

Consider now the basic model in the form (2.6), for example. Its local dynamics is described by a standard map with the principal parameter (2.5)

$$K = 6\pi k\omega(-2E)^{-5/2}, \tag{2.28}$$

which now depends on a dynamical variable E, the energy. The connected chaotic component of the motion is determined by the condition $K > K_c \approx$

1, or,

$$|E| < \tfrac{1}{2}(6\pi k\omega)^{2/5} \equiv |E_b| . \tag{2.29}$$

This condition determines the *chaos border* in the phase space. The structure of the motion near the border is very complicated as is immediately obvious from fig. 5. Particularly, this leads to a high correlation in the phase x which suppresses the diffusion rate as $K \to K_c$, or $E \to E_b$. For the correlation factor near the border [17], we have,

$$C(K) \approx 0.6K\,(1 - K_c/K)^3 . \tag{2.30}$$

This is another example of the particular statistical properties inferred from the dynamics which would be difficult to guess hypothetically. The power-law dependence was obtained first from numerical experiments [13] which are represented in fig. 10. The mean number of iterations N required for the transition between two neighbouring resonances $P_m = 2\pi m$ is related to the correlation factor by

$$C = \frac{8\pi^2}{NK^2} \to \frac{0.8}{K^2}(K - 0.989)^{2.55} . \tag{2.31}$$

The latter expression corresponds to the data in fig. 10. The accuracy of the exponent had not been very high, and subsequently it was changed [18] (see eq. (2.30)).

A low diffusion rate near the chaos border, albeit in a very narrow layer, drastically changes the statistical properties of the whole chaotic component. The most important effect is a slow correlation decay which is described by a power law [19,20]. For example,

$$C_E(\tau) \equiv \overline{E(t)E(t+\tau)} \sim \tau^{-p}, \tag{2.32}$$

instead of the exponential decay usually assumed in traditional statistical mechanics. Moreover, in the case of analytical perturbation, $p \approx 0.5 < 1$ (for peculiarities of a singular perturbation see ref. [24] and the example (2.35) below). The latter inequality implies, first, that the spectrum of the motion, the Fourier transform of $C(\tau)$, becomes singular at $\omega \to 0$, namely,

$$S(\omega) \sim \omega^{p-1} \approx \omega^{-1/2} . \tag{2.33}$$

This results in very large fluctuations so that the statistical description, always incomplete, also loses its attractive simplicity and reliability. Those fluctuations are clearly seen in fig. 10.

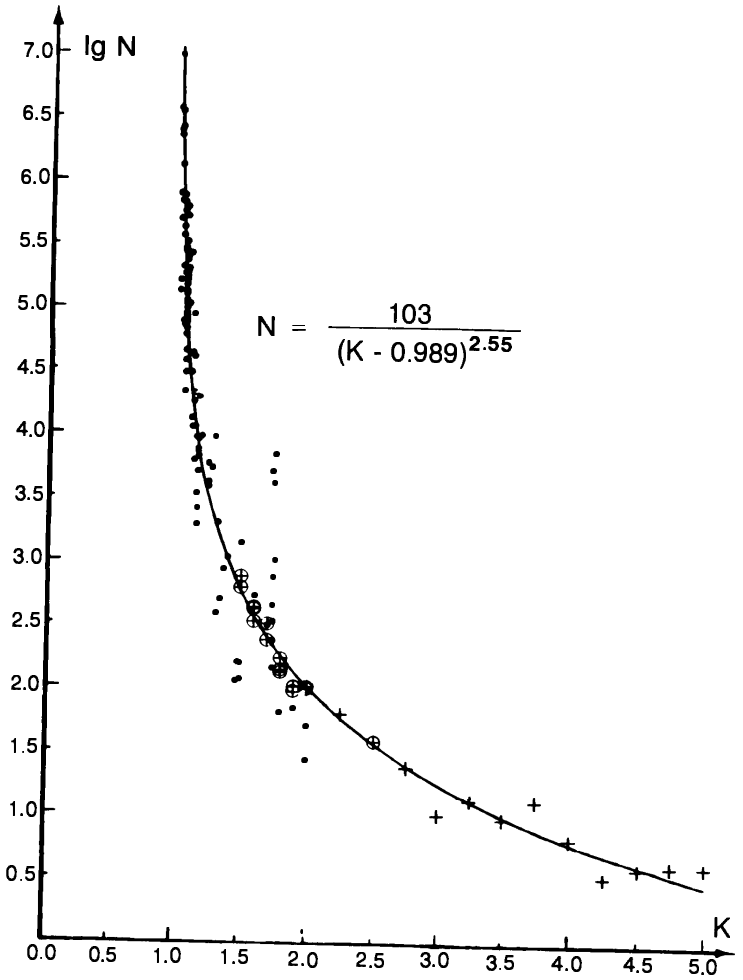

Fig. 10. Critical behaviour in the standard map [13]: $D_P = 4\pi^2/N$; $T = 1.0$.

If critical chaotic motion, with the power-law correlation, is coupled to another freedom, the diffusion in the latter would also be very unusual, namely, "abnormally" fast. The formal diffusion rate, which is proportional to the integral of the correlation function, diverges. Actually, this implies that the dispersion of the distribution function

$$\sigma^2 \sim t^{2-p} \approx t^{3/2}, \tag{2.34}$$

grows faster than time. In addition, the fluctuations of diffusion also diverge in time which, again, restricts the description of such a process, essentially, to order-of-magnitude estimates.

An example of such complicated statistics can be seen in fig. 8 at $K \approx 6.5$. The measured diffusion rate grows as $t^{1/2}$ by orders of magnitude [21] due to a few small islands of stability surrounded by chaos borders (cf. fig. 6).

In conclusion, I would like to mention another very " simple" map

$$\bar{p} = p + kx, \qquad \bar{x} = x + \bar{p} \pmod 1, \tag{2.35}$$

with parameter k in the interval $(-4, 0)$. Formally, the motion is locally stable. Yet, for non-integer k values, the map is discontinuous, and this results in an extremely complicated behaviour, both dynamical and statistical. It is not at all clear what could be a meaningful description, if any, of this apparently trivial model. You might like to play with this map on computer.

3. Quantum dynamics and the classical limit

3.1. The correspondence principle

Now we turn to the central topic of my course, quantum dynamics. Formally, it is described by the Schrödinger equation (or a similar equation) for a very specific physical object, the *wave function*. However, for a physicist, this is not the whole story. Unlike in classical mechanics, you cannot simply presuppose the measurement in quantum mechanics as some routine procedure of a technical significance only. On the contrary, in spite of the tremendous success of quantum mechanics, which has conquered the whole physics and beyond, we still don't know how to describe dynamically the quantum measurement, and even to specify its physical nature. To be sure, there is an unambiguous convention concerning how to relate the results of measurements to the ψ function. It goes back to the work of Born and has been subsequently developed into a beautiful theory (and philosophy) by Bohr and his school. This theory is known as the *Copenhagen interpretation* of quantum mechanics. Yet the physical mechanism of quantum measurement remains a highly controversial topic (see, e.g., a very interesting discussion of the mysteries of quantum physics in ref. [22]; one of the latest suggestions is due to Percival [23]).

As is well known, the Copenhagen convention is probabilistic, and moreover, it is believed that the quantal probability is of some (unknown) fundamental nature beyond the conventional physics. This is very confusing since we intend to discuss the nature of dynamical chaos, particularly, in quantum mechanics.

To avoid this difficulty we restrict ourselves to the dynamics of the ψ function, and its time evolution $\psi(t)$. We understand ψ as a specific dynamical variable of a quantum system. In other words, we divide the whole problem of quantum dynamics into two unequal parts: (i) the proper, or intrinsic, dynamics of a quantum system "itself", that is independent of any measurement, and (ii) the quantum measurement which, although "foreign" to the quantum world, is nevertheless the only way to study the

latter experimentally.

The first part is, of course, much simpler because it is described by well-established quantum equations of motion such as Schrödinger's, for example. This part comprises the essence of quantum dynamics, and it is simply and unambiguously related to experiment, if necessary, via the Copenhagen convention. In the latter case, we assume two and only two measurements in the quantum system under consideration: (i) the first complete measurement which determines the initial $\psi(0)$, and (ii) the final measurement, complete or incomplete, which records the result of the intrinsic quantum evolution. Notice that unlike classical mechanics, any intermediate measurement would drastically change the quantum evolution. In other words, the intrinsic motion of a quantum system, which we are going to discuss, is a sort of "black box". We don't know what is going on "inside" it, yet we can predict the result. In this respect, numerical experiments in quantum mechanics have a key advantage over laboratory experiments: in the former, you can follow the quantum system without changing its dynamics. Of course, you are actually following the model, no matter how universal it might be, and not the real system. But it is pretty-well perfect for a theoretician! Notice that in classical mechanics there is no such difficulty with the process of measurement, nor is there the corresponding advantage of numerical experiments.

The importance of the second part of the general problem of quantum dynamics, the problem of understanding the measurement, arises because the latter results in the so-called *collapse* of the ψ function. This collapse is not described, as yet, by any dynamical equations. Instead, in the Copenhagen interpretation, the collapse is related to the observer rather than to the quantum system itself. However, some researchers, including myself, argue that the collapse must occur somehow independently of the observer. In other words, the controversial question concerns whether the collapse is an intrinsic or extrinsic phenomenon with respect to the quantum system. I plan to briefly discuss this topic, among others, in the concluding section.

As the measurement device in quantum mechanics is by definition a classical system, the mystery of quantum measurement is intimately related to a very difficult physical problem, the *quasiclassical transition* which is still quite far from being completely understood. Quantum chaos, which we are going to discuss, is also an essentially quasiclassical phenomenon as true dynamical chaos occurs only in the classical limit, i.e., in classical mechanics.

A linguistic remark. Some people use the term *semiclassical* instead of (or as a synonym for) *quasiclassical*, but I reserve the former for a different conception related to a system which has both classical and quantum in-

teracting parts. In such a system, true dynamical chaos can occur. An important example is quantum measurement.

Thus, we are going to discuss the so-called *quasiclassical region.* In this region, the fundamental *correspondence principle* is of primary importance. In a narrow sense, this principle had been formulated by Niels Bohr at the dawn of quantum mechanics as a practical method for solving quantum problems before the complete theory was built. However, in a broader sense, the correspondence principle must hold in any new fundamental theory, which simply implies that all firmly established previously scientific laws must be immutable. The future development of the science may only restrict, as a rule, or sometimes even broaden, the domain of their validity but would never refute them altogether. This implies in particular that, whatever quantum dynamics is like, it has to approach somehow dynamical chaos in the quasiclassical region. This is a very important guiding principle, which we are going to exploit.

3.2. Quantization of maps

Consider first the standard map (2.3) in which we change the notation to

$$\bar{n} = n + k\sin x, \qquad \bar{x} = x + T\bar{n}, \tag{3.1}$$

for the reason that I shall now explain. Quantization of this map depends on the interpretation of the x-variable. Suppose the map represents the kicked rotator, so that x is the angle variable defined (mod 2π). Then, in quantum mechanics, the wave function $\psi(x)$ must be periodic (mod 2π),

$$\psi(x) = \sum_n \psi(n)\frac{\mathrm{e}^{\mathrm{i}nx}}{\sqrt{2\pi}}, \tag{3.2}$$

where $\psi(n)$ are Fourier amplitudes of the function $\psi(x)$, and the integer n is (angular) momentum. Here and later we assume Planck's constant $\hbar = 1$ unless otherwise is explicitly stated. Without the perturbation ($k = 0$), the momentum $n = \text{const.}$, hence, $\exp(\mathrm{i}nx)$ are the eigenfunctions, whence the momentum operator

$$\hat{n} = -\mathrm{i}\frac{\partial}{\partial x}\ . \tag{3.3}$$

Notice that because of quantization, it is impossible to get rid of the parameter T as in classical mechanics. Indeed, introducing a new variable $Q = Tn$ (cf. eq. (2.4)) does not help because n is an integer anyway.

Hence, the operator $\widehat{Q} = -\mathrm{i}T\partial/\partial x$, and $T = \hbar_{\mathrm{eff}}$ remains as an effective Planck's constant [25]. For the same reason, one cannot set $T = 1$ because that would contradict the previous condition $\hbar = 1$.

The quantum motion can be described [26] either by the continuous Schrödinger equation $\mathrm{i}\partial\psi/\partial t = \hat{H}\psi$ related to the Hamiltonian (cf. eq. (1.8))

$$\hat{H} = \frac{\hat{n}^2}{2} + \frac{k}{T}\cos x \cdot \delta_T(t), \tag{3.4}$$

or by a quantum map

$$\psi(t+T) \equiv \bar{\psi} = \hat{U}_{Tk}\psi(t), \tag{3.5}$$

where the unitary evolution operator over time period T is

$$\hat{U}_{Tk} = \exp\left(-\mathrm{i}\int \mathrm{d}t\,\hat{H}\right) = \hat{R}_T\hat{W}_k. \tag{3.6}$$

In the last expression we introduced the operators of a free rotation

$$\hat{R}_T = \mathrm{e}^{-\mathrm{i}T\hat{n}^2/2} = \begin{cases} \exp\left(\mathrm{i}\dfrac{T}{2}\dfrac{\partial^2}{\partial x^2}\right), & \psi(x), \\ \exp\left(-\mathrm{i}\dfrac{T}{2}n^2\right), & \psi(n), \end{cases} \tag{3.7}$$

and of a kick

$$\hat{W}_k = \begin{cases} \exp(-\mathrm{i}k\cos x), & \psi(x) \\ \displaystyle\sum_m (-\mathrm{i})^{n-m} J_{n-m}(k), & \psi(m) \end{cases} \tag{3.8}$$

where $J_l(k)$ are the Bessel functions. The operators are given in two forms, for the coordinate $\psi(x)$ and momentum $\psi(n)$ representations of the wave function. In the latter case, the evolution operator is an infinite matrix

$$\bar{\psi}(n) = \sum_m U_{nm}\psi(m), \quad U_{nm} = (-\mathrm{i})^{n-m}\exp\left(-\mathrm{i}Tn^2/2\right)J_{n-m}(k). \tag{3.9}$$

Notice that even though the operators $\hat{R}_T$ and $\hat{W}_k$ do not commute, either order can be used in the map (3.5), the difference being simply a shift in time. Sometimes it is convenient to use a symmetric representation,

$$\hat{U}_{Tk} = \hat{R}_{T/2}\hat{W}_k\hat{R}_{T/2}. \tag{3.10}$$

The explicit time dependence in this case is symmetric with respect to time reversal. This will be used later, in section 5.

In the quantum standard map (3.9), both parameters, k and T, are indispensable as the two corresponding operations are qualitatively different. In the n-representation, the rotation shifts only quantum phases, while the kick causes transitions between unperturbed n-states. Formally, all the states are coupled but actually only transitions within a band of width $\sim 2k$ are significant owing to a fast drop of $J_l(k)$ for $|l| \gtrsim k$ (see eq. (3.9)). This allows us to use efficiently a single n-representation in numerical experiments as was done, e.g., in ref. [26]. Yet, later we found that using both x- and n-representations,

$$\bar{\psi}(x) = \hat{F} \sum_n \mathrm{e}^{-\mathrm{i}Tn^2/2}\, \hat{F}\, \mathrm{e}^{-\mathrm{i}k\cos x}\, \psi(x), \tag{3.11}$$

provides a faster computation in spite of two fast Fourier transforms per iteration ($\hat{F}$ operator).

Now, consider another interpretation of the standard map, namely, let it describe the motion in a spatially periodic potential $\cos x$. Then, the ψ-function does not to have to be periodic in x. Instead, it acquires a phase shift over a period of the potential

$$\psi(x + 2\pi) = \psi(x)\, \mathrm{e}^{2\pi\mathrm{i}\nu} \ . \tag{3.12}$$

The new quantity ν is called *quasimomentum*, and the function satisfying condition (3.12) is a *quasimomentum eigenfunction*. Due to the periodicity of the potential, $\nu = \text{const.}$ is a motion integral according to the Floquet theorem. In other words, the momentum $P = n + \nu$ is no longer an integer but its fractional part $\nu = \{P\}$ is conserved. In particular, $\nu = 0$ corresponds to a periodic $\psi(x)$ as for the rotator considered above, and with the same evolution $\psi(x,t)$. The evolution depends on ν but different quasimomentum eigenfunctions evolve independently of each other as there are no transitions in ν.

The general relation (3.6) between the Hamiltonian and evolution operator holds for any quantum system, in particular, for our basic model (1.6), (1.7). Consider, for example, the map (2.6). First of all, the variable E here is not the action but the energy (of the Rydberg atom for the second example, the photoelectric effect, in section 2). The quantization here is related to an integer number of field quanta $n = (E - E_0)/\omega$ and the "quasimomentum" (integer part included) $\nu = E_0/\omega$ where E_0 is the initial energy. Since $\psi(\varphi)$ is periodic (mod 2π) the operator $\hat{n} = -\mathrm{i}\partial/\partial\varphi$

remains the same (cf. eq. (3.3)), and so does $\hat{W}$ with $k \to k/\omega$. Yet, the rotation operator is now different, namely,

$$\hat{R} = \exp\left[\mathrm{i}\pi\sqrt{2/\omega}\,(-\nu - \hat{n})^{-1/2}\right]. \tag{3.13}$$

Another interesting peculiarity of this example is that the map's time t is related to physical time $t_{\rm ph}$ via n as was discussed in section 2. Hence, the wave function $\psi(n,t)$ at a given t describes the atom's state at different instants of $t_{\rm ph}$! This is a very unusual picture, and it is not clear at all how to relate $\psi(n,t)$ and $\psi\,(n,t_{\rm ph})$ in any simple way, since the relation $t\,(t_{\rm ph}, n\,(t_{\rm ph}))$ depends on the trajectory, which does not exist in quantum mechanics.

What are the *quasiclassical parameters* of a quantum system which characterize the transition to the *classical limit*, or to classical mechanics? Generally, the quantum numbers may play this role, the classical limit corresponding to the large numbers, e.g., $n \to \infty$. Formally, this is equivalent to the vanishing of Planck's constant $\hbar \to 0$. Yet, I prefer to keep $\hbar = 1$ which is more physical.

Inspecting eqs. (3.7) and (3.8), we can see that for the standard map the condition $n \to \infty$ is not sufficient to provide the quasiclassical transition. This is due to a specific perturbation in this model, as the perturbation does not depend on n. It couples $\sim k$ unperturbed states, so k is another (principal) quasiclassical parameter $\left(k \sim \hbar^{-1}\right)$. Since $K = kT$ is the classical parameter independent of $\hbar$, still another quasiclassical parameter is $T \sim \hbar$. Thus, the quasiclassical transition corresponds to $k \to \infty$, $T \to 0$ and $K = \text{ const}$.

3.3. Quasienergy eigenstates

One method of analysis in quantum dynamics is somehow to find out the *eigenvalues* and *eigenfunctions* of all the commuting operators. For the time evolution problem, the most important "eigenquantities" are related to energy.

Let us, again, begin with the quantized standard map (3.9). The unperturbed system ($k = 0$) is conservative and has, generally, the following set of energy eigenfunctions φ_n and eigenvalues E_n (see eq. (3.4)),

$$\sqrt{2\pi}\varphi_n = \mathrm{e}^{-\mathrm{i}E_n t + \mathrm{i}nx}, \quad E_n = (n+\nu)^2/2. \tag{3.14}$$

With a time-dependent perturbation, the energy is no longer conserved but, according to Floquet's theorem, the *quasienergy* eigenfunctions can

be introduced, satisfying

$$\varphi_n(x, t+T) = \varphi_n(x,t)\,\mathrm{e}^{-\mathrm{i}\varepsilon_n T} = \hat{U}_{Tk}\varphi_n(x,t). \tag{3.15}$$

The quantity ε_n is called the *quasienergy*. In a map, the dynamical state is determined only at integer multiples of T, hence t can be dropped in (3.15), to obtain the equation for ε and φ namely,

$$\varphi = \mathrm{e}^{\mathrm{i}\varepsilon T}\,\hat{U}_{Tk}\varphi \quad \text{or} \quad \varphi(l) = \mathrm{e}^{\mathrm{i}\varepsilon T}\,U_{lm}\varphi(m). \tag{3.16}$$

The latter expression is given in the momentum representation, with the matrix U_{lm} from eq. (3.9).

The standard way of solving eq. (3.16) involves the diagonalization of the matrix U_{lm} which generally is possible only numerically, of course. For the standard map, the infinite matrix U_{lm} can be truncated to a fairly high accuracy, as was mentioned above, assuming $|l-m| \leqslant N \sim k$. Then, eq. (3.16) relates $2N+1$ successive values of $\varphi(l)$. Expressing $\varphi(l)$ for the largest l as a function of the $2N$ preceding $\varphi(m)$ we arrive at a $2N$-dimensional *transfer map* which describes a certain abstract dynamical system of N freedoms with the quantum number of unperturbed state l as a "time". This is another way to analyze the quasienergy eigenstates that we are going to use [27].

Problem. Prove that the transfer matrix is canonical (symplectic).

3.4. Quantum resonance

The quantized standard map, as well as the classical one, is periodic in n. This leads to a peculiar phenomenon – the quantum resonance – discovered in ref. [26] and studied thoroughly in ref. [28]. The resonance is related to the dynamics of quantum phases, which are determined (mod 2π) like their changes by the rotation operator (3.7). Since n are integers, the parameter T, which enters this operator only, is determined (mod 4π). In other words, only the fractional part of $T/4\pi$ (mod 1) is essential for the dynamics. Moreover, there is a symmetry with respect to $T = 2\pi$ (see eq. (5.1) below).

Now, suppose $T = 4\pi$. Then, all the quantum phases remain unchanged, and the evolution operator over (discrete) time $\tau = [t/T]$ becomes

$$\hat{U}_\tau = \hat{U}_{Tk}^{\tau} = \mathrm{e}^{-\mathrm{i}\tau k\cos x}. \tag{3.17}$$

Hence a series of τ kicks is equivalent to a single kick with parameter τk, and it couples $\sim \tau k$ unperturbed states. Roughly speaking, the average

momentum $\langle|n|\rangle \sim k\tau$, and the (unperturbed) energy is given by $E = \langle n^2\rangle/2 \sim k^2\tau^2$. More accurately,

$$E = \frac{1}{2}\oint \mathrm{d}x \left|\frac{\partial\psi}{\partial x}\right|^2 = E_0 + \frac{k^2\tau^2}{2}\oint \mathrm{d}x\,|\psi_0|^2 \sin^2 x$$
$$+ k\tau \oint \mathrm{d}x \sin x\ \mathrm{Re}\left(\mathrm{i}\psi_0\,\frac{\partial\bar{\psi}_0}{\partial x}\right) \to \left(\frac{k\tau}{2}\right)^2, \tag{3.18}$$

where the subscript zero denotes the initial state, and the last expression is for $\psi_0 = \mathrm{const.}$ (the ground state). This is the main quantum resonance at $T/4\pi = 0 \pmod 1$. Formally, it also includes the classical limit but the actual transition to this limit is singular.

Problem. Show that, for $T = 2\pi$, the quantum motion is strictly periodic.

As was shown in ref. [28], the resonance occurs at any rational $T/4\pi = p/q$. Except for $q = 2 \quad (T = 2\pi)$, the growth of the energy is proportional to τ^2 as $\tau \to \infty$,

$$E \to r(q)\tau^2, \tag{3.19}$$

but the rate $r(q)$ sharply drops with q. We shall estimate this dependence in section 6. The resonant perturbation is of period q in n (see eq. (3.7)). Hence, any eigenstate satisfies Floquet's condition

$$\varphi(n+q) = \varphi(n)\,\mathrm{e}^{\mathrm{i}qy}, \tag{3.20}$$

and is an unbounded quasiperiodic function of n. There is a striking similarity with eq. (3.12) for the eigenfunction in a spatially periodic potential up to a Fourier transform from a coordinate to momentum or vice versa. For this reason, we may term the quantity y in eq. (3.20) the *quasicoordinate*. It is defined (mod $2\pi/q$). The Fourier transform of $\varphi(n)$, taking account of eq. (3.20), gives the eigenfunction $\varphi(x)$ as a series of equally spaced δ-functions at the points $x_j = y + 2\pi j/q$. The resonant quasienergy spectrum is continuous with q bands $\varepsilon_m(y)$, $m = 1, \ldots, q$. The bands' width is related to the energy growth rate $r(q)$ in eq. (3.19) (see eq. (6.22)).

The above-mentioned analogy between the quantum resonance in the kicked rotator and the Bloch extended states of a particle in a periodic potential is not restricted, of course, to the standard map which describes both. Actually, there is a very broad and deep similarity between quantum

spatial and temporal behaviour, that is between our time-dependent problem and the solid-state physics. In particular, for the standard map such an analogy was apparently first discussed in ref. [29]. We shall come back to this problem in section 7.

Quantum mechanical resonances are not a generic phenomena but are a peculiarity of the standard map. Yet, we may use this peculiarity to construct one more model of some general interest. To this end, we fix the quasicoordinate $y = 0$. Then the quasienergy spectrum becomes discrete and consists of a finite number q of the levels while all q remaining eigenfunctions $\varphi_l(n)$, $l = 1, \ldots, q$ are of period q. If, moreover, we retain just one period ($n = 1, \ldots, q$), the eigenfunctions $\varphi_l(x)$ become smooth, and even analytical, and are represented by q Fourier terms. Obviously, we arrive in this way at the quantized standard map on a torus whose classical counter-part was described in section 2. The number of classical periods in n over the torus $l = qT/2\pi = 2p$ must be even. This map models a closed finite energy surface of a conservative system. We shall use this model in section 8.

4. Quantum stability: perturbative, or extreme, localization

4.1. Resonant perturbation

As was stressed in section 2, in nonlinear dynamics one should first look for resonances. For linear oscillations, this is a matter of the system's parameters, while nonlinearity always provides some resonances that depend on the initial conditions. In the quantized standard map (3.9) there are both linear (quantum) resonances at the parameter values $T = 4\pi p/q$ (p, q integers) and nonlinear (classical) resonances for the initial conditions at $P = (2\pi/T)(p/q)$ and any T.

What does nonlinearity mean in quantum mechanics which, after all, is described by a linear equation (Schrödinger's equation)? First of all, such an ambiguity is also present in classical mechanics, where the always linear Liouville equation for a distribution function is completely equivalent to Newton's equations for the trajectories. So, formally it depends on the representation of dynamics. Yet, from the physical point of view, the most important property of nonlinearity is the dependence of frequencies on initial conditions (the actions). In quantum language, this means that (quasi) energy levels are not equidistant. But this implies, in turn, that the exact resonance may not (and generally will not) occur at all, a typical

detuning being

$$\delta_{mn} \approx \delta\omega(n) \approx \frac{\mathrm{d}\omega(n)}{\mathrm{d}n}\,(n - n_r) \sim \frac{\mathrm{d}\omega(n)}{\mathrm{d}n}. \tag{4.1}$$

Here $\omega(n)$ is the classical frequency, and n_r is a noninteger resonant value of integer action n [$\omega(n_r) = \Omega$ the perturbation frequency].

The perturbation causes some transitions for any detuning, but if $\delta_{mn} \neq 0$ the transitions are suppressed for a sufficiently weak perturbation. How weak? The answer is provided by standard perturbation theory with small parameter

$$\mu = \frac{|V_{mn}|}{|\delta_{mn}|} \sim 1, \tag{4.2}$$

where V_{mn} is the perturbation matrix element. The condition $\mu \sim 1$ determines the *border of quantum stability*: no matter what happens in the classical limit, the quantum state remains close to the unperturbed one. In the case of classically chaotic motion, this important conclusion was drawn first in ref. [30], and we call eq. (4.2) *Shuryak's border*.

In the case of the standard map (2.13), nonvanishing matrix elements are $V_{n,n\pm1} = k/2T$ and detuning at a classical resonance is $\delta_{mn} \sim 1$ as $\omega(n) = n$. Hence, there is quantum stability when $k \lesssim T$. Notice that perturbation theory is certainly inapplicable at $k \gtrsim 1$ since the kick operator (3.8) couples $\sim k > 1$ states, which is obviously a nonperturbative result. This is because for $k \gtrsim 1$, the perturbation parameter $\mu \sim k/T \gtrsim 1$ because $|T| \leqslant 2\pi$.

Another simple meaning of quantum stability at resonance is inferred from eq. (2.11),

$$\mu \sim \frac{k}{T} \sim (\Delta n)_{\mathrm{r}}^2 \sim 1. \tag{4.3}$$

Hence, the quantum system does not "feel" the classical resonance unless it comprises many levels. Thus, quantum motion is more stable than classical motion, and the origin of this stability is in the discreteness of energy spectrum. Notice that the structure of classical motion near nonlinear resonances is qualitatively different from the unperturbed structure even in the case of arbitrarily weak perturbation.

Quantum stability when $\mu \ll 1$ is also called *perturbative localization*, first, because perturbation theory is applicable, and second, because the change of the unperturbed state is small. In other words, nothing happens in the quantum system if $\mu \ll 1$.

If $T \to 0$, the perturbation must be very weak to provide the localization. This is because at resonance the transition continues over many kicks until the detuning is developed.

When $\mu \sim k/T = K/T^2$ and $|T| \leqslant 2\pi$ the quantum stability at resonance ($\mu \ll 1$) is only possible for $K \ll 1$, i.e., for regular classical motion. What happens if $\mu \gg 1$ but $K \ll 1$? The unperturbed eigenstates inside the resonance would completely alter, of course, due to strong coupling. However, another set of eigenfunctions can be introduced corresponding to the motion of a pendulum (2.10), not the rotator. The other resonances (see eq. (2.13)) would perturb the pendulum which results, in classical mechanics, in the formation of a narrow chaotic layer around the resonance separatrix [13]. Such a layer exists no matter how weak the perturbation is, because the pendulum frequency

$$\omega(\tilde{n}) \approx \frac{\pi\omega_0}{\ln(32\omega_0/\pi\tilde{n})}, \tag{4.4}$$

vanishes at the separatrix ($\tilde{n} \to 0$) while nonlinearity grows indefinitely. Here $\tilde{n} = n - n_s$ is the distance from the separatrix in the action n, and $\omega_0 = (k/T)^{1/2} = k/\sqrt{K}$ is the frequency of small oscillations near the resonance center.

In quantum mechanics $\tilde{n} \gtrsim 1$, and the minimal frequency (level spacing) becomes

$$\omega_{\min} \approx \omega(1) \approx \frac{\pi k}{\sqrt{K}\ln\left(\dfrac{32k}{\pi\sqrt{K}}\right)} \gtrsim \omega_s. \tag{4.5}$$

The latter inequality is a sufficient condition for the quantum suppression of chaotic motion in a separatrix layer with classical frequency ω_s at the layer's border. Using the estimate for ω_s in ref. [13],

$$\omega_s \approx \frac{k}{\pi + \dfrac{\sqrt{K}}{\pi}\ln\left(\dfrac{K^{3/2}}{2\pi^4}\right)} \approx \frac{k}{\pi} \quad K \ll 1, \tag{4.6}$$

we obtain for the border of quantum stability in the chaotic layer,

$$k \sim \frac{K^2}{64\pi^3}\exp\left(\pi^2/\sqrt{K}\right), \tag{4.7}$$

which is fairly large for $K \ll 1$, when chaotic layers are narrow. Such estimates were first derived in ref. [30].

4.2. Nonresonant perturbation and chaos

Nonresonant perturbation comprises two completely different cases. One (less interesting) case corresponds to classically regular motion ($K \ll 1$) and to the initial condition away from all primary resonances $n_r = 2\pi r/T$ (r integer). The matrix element $V_{n,n\pm1} = k/2T$ remains the same but the detuning increases up to $\delta \sim T^{-1}$, whence the perturbation parameter

$$\mu \sim k \sim 1, \tag{4.8}$$

the latter estimate being the border of quantum stability, or of perturbative localization. The border does not depend on T because transitions by different kicks are not correlated (not in phase) unlike the resonant perturbation.

The second case of nonresonant perturbation is much more interesting and important. It corresponds to a classically chaotic system with $K \gg 1$. Obviously, the perturbation is nonresonant in the sense that at any n several overlapping resonances are operative, and successive kicks are completely decorrelated. Hence, the estimate (4.8) holds, which is also obvious directly from the kick operator (3.8). Thus, even wild chaos in the classical limit becomes completely quiet in the quantum region.

Suppose that the kicked rotator initially occupies a single level, say, $n = 0$. Then, for $k \ll 1$, one kick produces the distribution

$$|\psi(n)| = J_n(k) \approx \frac{(k/2)^n}{n!}, \tag{4.9}$$

which is steeper than exponential. However, asymptotically as $t \to \infty$, the distribution approaches the exponential steady state, [31]

$$|\psi(n)| \sim \exp\left(-|n|/l_s\right), \tag{4.10}$$

where we introduced the *localization length* l_s, the subscript s indicating the steady state. Eq. (4.9) suggests that,

$$l_s \sim \frac{\alpha}{\ln(\kappa/k)}, \quad k \ll \kappa, \tag{4.11}$$

for suitable numerical factors α and κ, which is confirmed by numerical experiments on a model equivalent to our basic model with $\alpha \approx 1.1$ and $\kappa \approx 3.4$ [31]. In concluding this section, I would like to mention that the perturbative localization is now well known (by one name or another), and

it is extensively used in many problems of quantum dynamics. For us it is very important, however, that sufficiently far in the quasiclassical region, towards the classical limit, the perturbative localization never holds. In the standard map, the absence of localization is related to increasing of $k \sim \hbar^{-1}$. This is a generic result because the energy level density is infinite in the classical limit (cf. eq. (4.2)).

5. Dynamically stable quantum diffusion

5.1. The correspondence principle and quantum diffusion

Consider a classically chaotic quantum system, e.g., the standard map with $K \gg 1$, and suppose that we are above the quantum stability border ($\mu \gg 1$). What would the quantum dynamics be like? The correspondence principle suggests that there must be some resemblance to the classical dynamics: the closer the resemblance, the bigger are the quasiclassical parameters of the quantum system ($k \to \infty$). In particular, there must be diffusion in n as described in section 2. Indeed, this was confirmed in refs. [26,17]. The latter results are presented in fig. 8 by crosses. As expected, the quantum diffusion rate closely follows the classical one (circles) including some deviations from a simple theory (solid line). Moreover, the distribution function has a Gaussian shape, again in accordance with classical theory (fig. 11). It is interesting to note that the distribution function $f(n,t) = |\psi(n,t)|^2$ is obtained for a single quantum system from the solution of Schrödinger's equation $\psi(n,t)$. In classical mechanics, $f(n,t)$ corresponds to an ensemble of many trajectories. So, the quantum state characterizes, in a sense, many systems but not arbitrarily many. As a result, there are quite large fluctuations in f which can be reduced in numerical experiments by averaging over some short intervals of either time or n, or both. We shall come back to this interesting question later.

The quasiclassical parameter $k = 40$ is reasonably large for the data in fig. 8. This is not the case for the second parameter $1/T = k/K$, which falls to $1/T = 2$ for the largest value $K = 20$ in fig. 8. Nevertheless the diffusion proceeds at a nearly classical rate. Further numerical experiments revealed that the diffusion persists at any T, and that the diffusion rate is approximately described by the same classical theory but with a renormalized classical parameter [32] (see fig. 12)

$$K \to K_{\mathrm{q}} = 2k \cdot \sin(T/2). \tag{5.1}$$

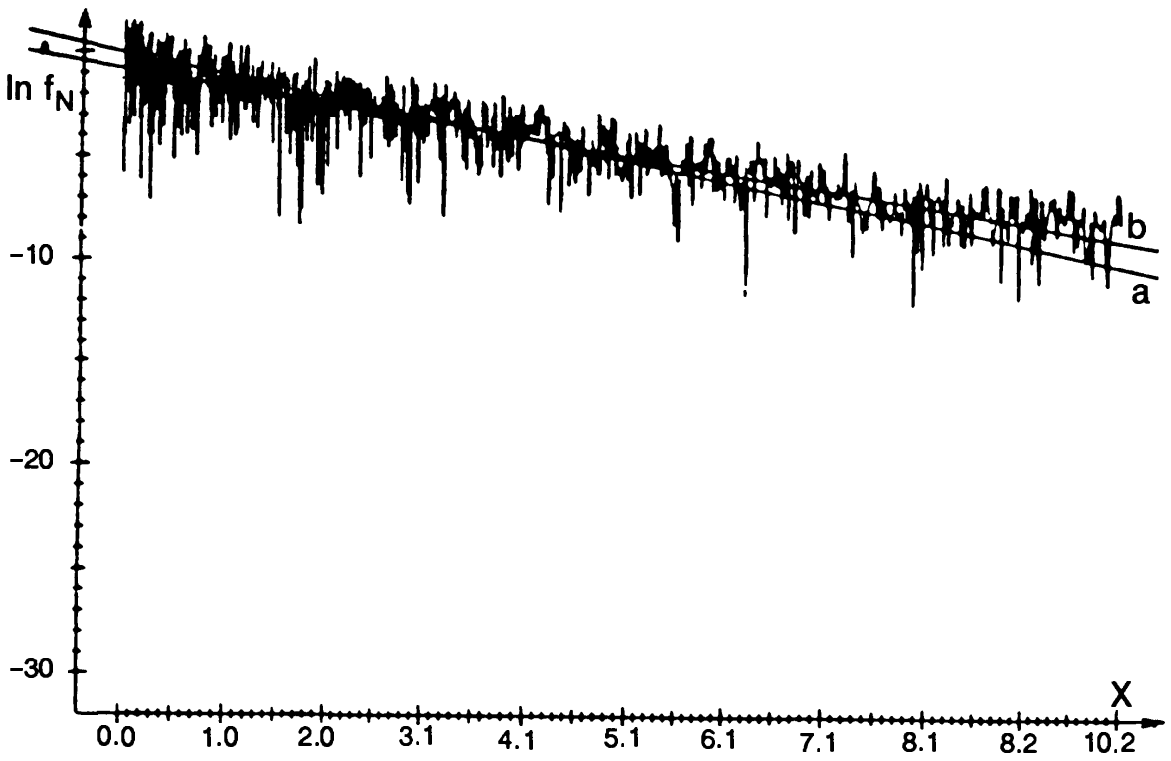

Fig. 11. The normalized distribution function $f_N = f(n,t)\sqrt{2\pi t D_n}$ versus $X = n^2/2tD_n$. The expected Gaussian distribution (2.26) corresponds to the straight line $\ln f_N = -X$.

Thus, the correspondence principle holds even in such an unusual process as the quantum diffusion. This is a very satisfactory result. But is there any difference between the classical description and the corresponding quantum description? There is, and it is a great one!

5.2. Relaxation time scale and quantum steady state

In the classical standard map, the diffusion proceeds indefinitely, the mean energy grows linearly in time (see eq. (2.21), $P = n$),

$$E = \frac{\langle n^2 \rangle}{2} = \frac{D_n t}{2}, \tag{5.2}$$

and the distribution function remains Gaussian (2.26). The time dependence of energy in the quantized standard map is shown in fig. 13. Unlike the classical case (the straight line), quantum diffusion slows down after some time (relatively short in the scale of fig. 13), and eventually completely stops on the average. The upper curve seems to grow slightly but a much longer computation (up to 5×10^4 iterations) in ref. [33] demonstrates that the residual diffusion rate, if there is any, $D_{\rm res}/D_n \lesssim 2 \times 10^{-5}$ (see fig. 17 below). Whatever the final theoretical conclusion is reached about $D_{\rm res}$,

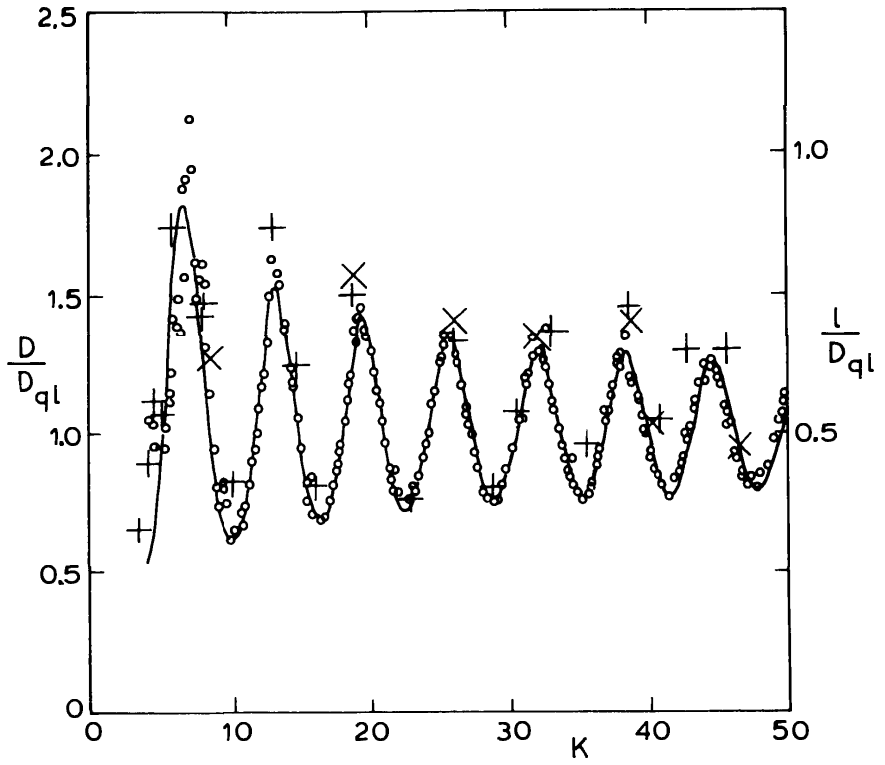

Fig. 12. The quantum diffusion rate and localization length of quasi-energy eigenfunctions in the standard map versus the renormalized parameter $K = 2k \cdot \sin(T/2)$; the circles and the curve are as in fig. 8, $D_{q\ell} = D_0 = k^2/2$; $T \in (0, \pi)(+)$, and $T \in (\pi, 2\pi)(\times)$ (after ref. [32]).

this clear empirical fact, that there is a very strong quantum suppression of classical chaos (diffusion), is of primary importance for quantum dynamics. We shall discuss this in detail in section 6.

The distribution function also changes from an initially Gaussian one spreading in time to, finally, one that is exponential and time-independent (on average),

$$f_s(n) \approx \frac{1}{l_s} \exp\left(-\frac{2|n|}{l_s}\right) \tag{5.3}$$

(for the initial value $n = 0$). The latter is the very specific, quantum, steady state with no analogue in the classical limit, where the diffusion would never stop. On the contrary, in quantum mechanics the relaxation takes place as if the phase space were finite (cf. classical relaxation on a torus, eq. (2.27)).

The steady state (5.3) is a sort of localization (cf. eq. (4.10)) with localization length l_s. But this is not perturbative localization, as both l_s and $k \gg 1$ for the data in fig. 13 (cf. eq. (4.8)). Numerical experiments show that roughly $l_s \sim k^2$ (see section 6). We shall call this new phenomenon the *diffusion localization*, that is the localization of classical-like diffusion. The

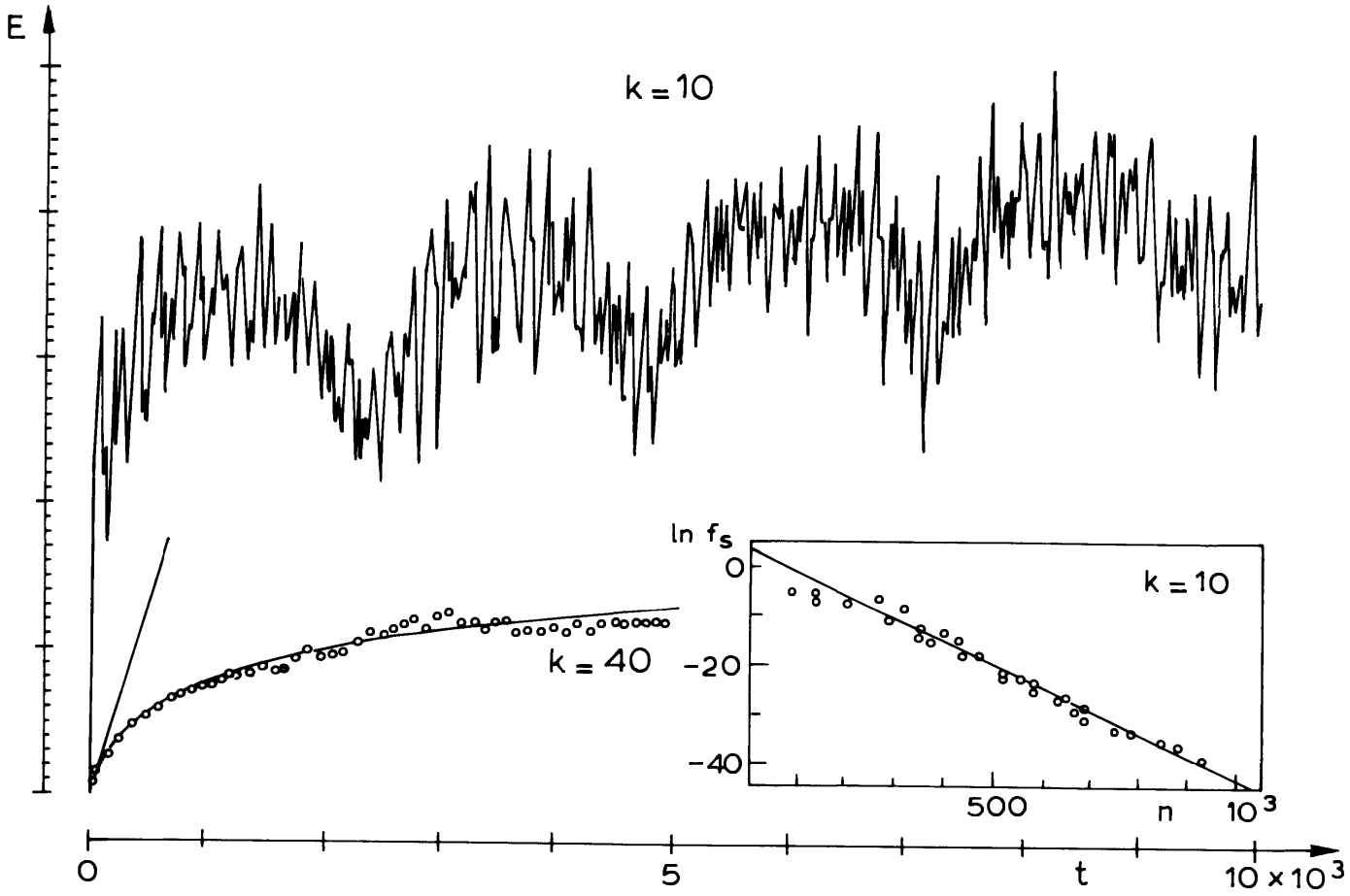

Fig. 13. Time dependence of the average energy $E = \langle n^2 \rangle / 2$ in the quantized standard map [34]; t is the number of map iterations; the straight line shows classical diffusion. Insert: the distribution function $f_s(n) = |\psi(n,t)|^2$ for $t = 10^3$ (full circles) and $t = 10^4$ (open circles); the straight line shows $f_s(n) \sim \exp(-|n|/21)$. The initial state in each case is $n = 0$.

time required for localization, or the relaxation time t_R to the quantum steady state is related to l_s by $D_n t_R \sim l_s^2$, whence,

$$\tau_R \equiv \frac{t_R}{T} \sim \frac{l_s^2}{TD_n} \sim k^2 \sim l_s, \tag{5.4}$$

where τ is the number of the map's iterations, and where $D_n \sim k^2/T$ (see eq. (2.21)). We shall call the quantity t_R the *relaxation time scale* of quantum motion.

These estimates explain how the correspondence principle works in quantum diffusion. The point is that both scales τ_R and l_s grow indefinitely with the quasiclassical parameter k.

The quantum steady state (5.3) is not a quantum stationary state because the energy is indefinite in the former. Hence, the steady state is a stationary oscillation, notably in energy, as can be clearly seen in fig. 13

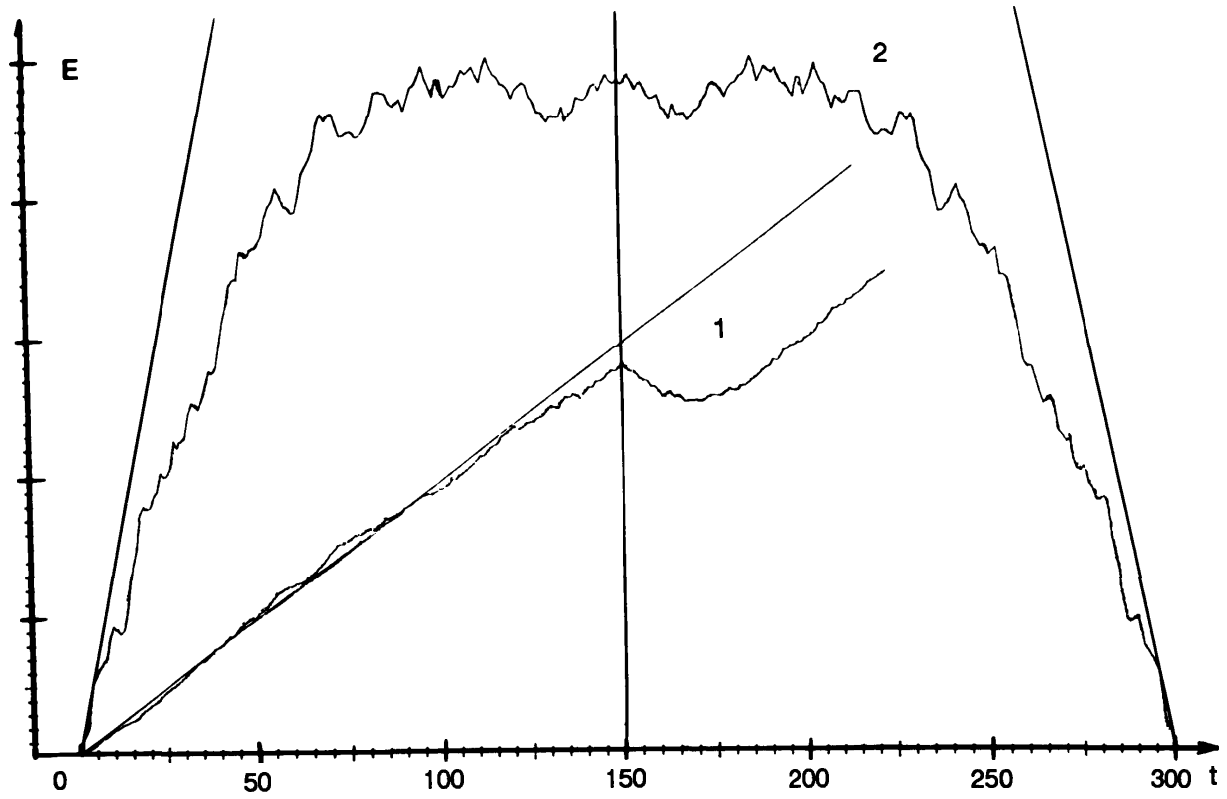

Fig. 14. Time reversal at $t = 150$ in (1) classical chaos and (2) quantum chaos for the standard map with $k = 20$, $T = 1/4$. The straight lines show the expected classical diffusion (in different scales). The accuracy of the quantum recurrence in E at $t = 300$ is better than 10^{-10} (!) (after ref. [35]).

(the upper curve). The oscillation amplitude decreases with an increase in k. Energy fluctuations look rather irregular but not completely chaotic, which is indeed the case, as we shall see in section 6.

5.3. Motion stability in quantum diffusion

Even though quantum diffusion on the relaxation time scale is surprisingly close to classical diffusion, the two turn out to be qualitatively different. In classical mechanics the origin of chaos, in particular of diffusion, is in the strong (exponential) local instability of motion. We spent a lot of time trying to find any sign of quantum motion instability by means of numerical experiments, and we finally failed. The crucial experiment due to Shepelyansky is as follows [35].

Both the classical and quantum standard map are time-reversible (with respect to the instant exactly half-way between two kicks, see eq. (3.10)). Yet, when there is exponential instability, the reversed trajectory will not come back to the initial point, due to unavoidable numerical errors (fig. 14, lower curve). The time (or velocity) is reversed here at $t = 150$, and the energy decreases, but only for a very short time (~ 30 kicks), and then the

diffusion continues at the same rate (backwards in time, one may say).

In the quantum case (fig. 14, upper curve), the impact of velocity reversal ($\psi \to \psi^*$, complex conjugation) is totally different: a sort of "antidiffusion" occurs in the system, back to the initial state. Notice that if the computation were continued beyond $t = 300$, the "normal" diffusion would resume, and the quantum steady state would be eventually reached as well. The moral is that quantum dynamics, even when it is diffusive, lacks any noticeable dynamical instability whatsoever.

In fig. 15 another, even more striking, confirmation of this conclusion is presented [35] (see also ref. [36]). The initial Gaussian distribution (one of upper curves) is diffusing and takes a rather irregular shape at the time of velocity reversal (lower curve which looks quite random). Yet, quantum antidiffusion brings it back, exactly to the initial state (another upper curve shifted upwards in order to distinguish it from the initial one).

Problem (unsolved). Devise a Gedanken experiment to observe the time (velocity) reversal.

Thus, quantum diffusion is a very peculiar phenomenon, even on the relaxation time scale. Formally, it is close to classical diffusion, yet, unlike the latter, it is dynamically stable. What about the correspondence principle, which also implies that there is instability of the motion in the quasiclassical transition? The instability does indeed exist! It was first discovered and explained in ref. [37] (see also ref. [38]). The quantum instability is related to the spreading of initially narrow wave packets. In the quasiclassical approximation, the ψ-function follows the beam of classical trajectories (Ehrenfest's theorem), which exponentially diverge in the case of classical chaos. In the classical limit this process lasts forever: there is no limitation to the scale in classical phase space because it is continuous. In contrast, the quantum phase space is discrete, the bin size being of the order of Planck's constant $\hbar$. Hence, the initial wave packet cannot be arbitrarily small, and the spreading time is finite. Moreover, it grows very slowly (logarithmically) with the quasiclassical parameters.

In the standard map, for example, the optimal shape of a wave packet (the coherent state) is found from the uncertainty relation $\Delta n \Delta x \sim 1$, and the second eq. (2.3) $\Delta x \sim T\Delta n$; it follows that $\Delta x \sim T^{1/2}$, and that the total spreading time, which we call *Ehrenfest's time scale*, is given by,

$$\frac{t_{\mathrm{E}}}{T} \sim \frac{|\ln T|}{T\Lambda} \approx \frac{|\ln T|}{\ln (K/2)}, \tag{5.5}$$

where Λ is the classical Lyapunov exponent (cf. eq. (2.25)). The time t_{E} is very short but, nevertheless, it was recently observed in ref. [39]. According

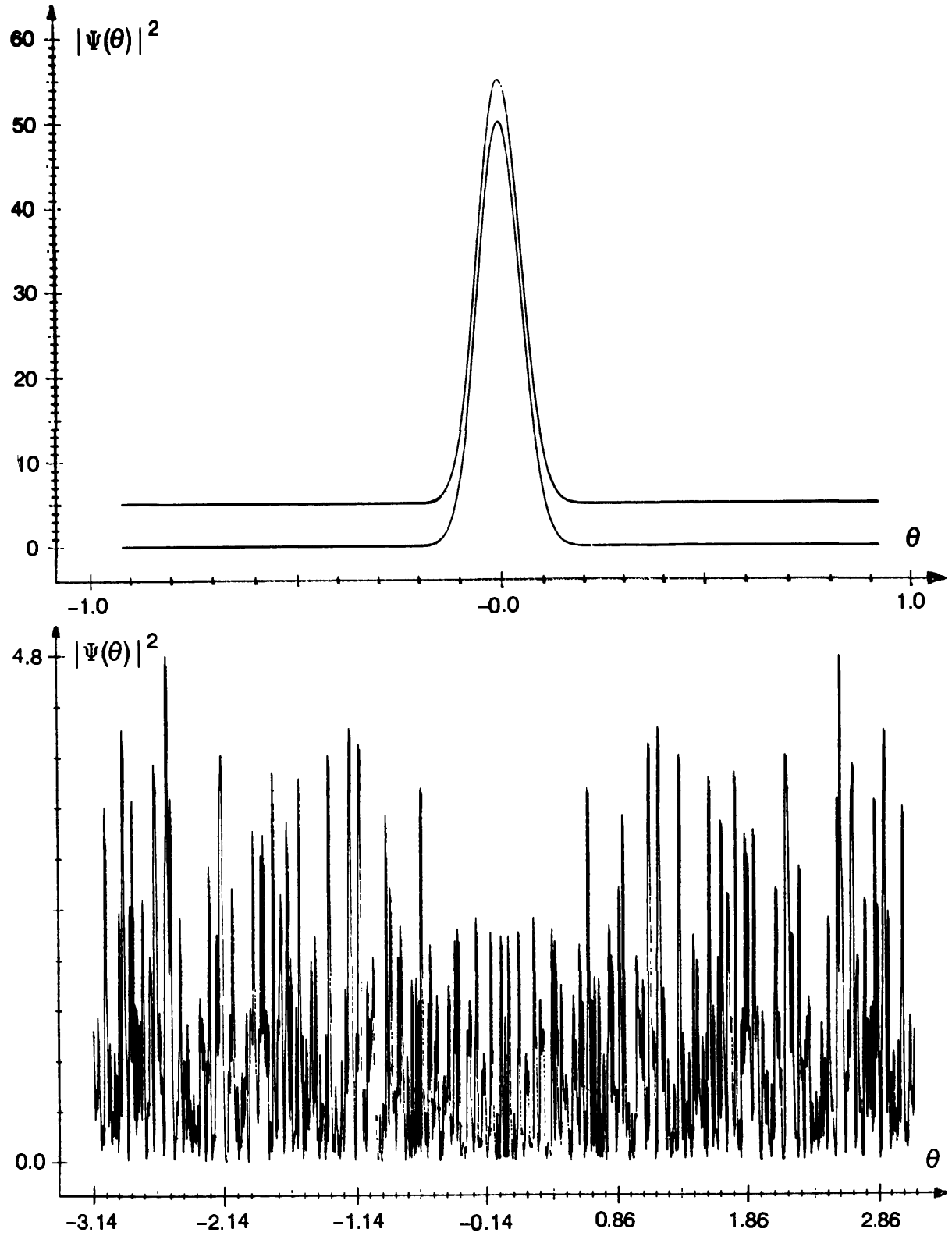

Fig. 15. Time reversal as in fig. 14: the probability distribution, initial (at $t = 0$) and upon recurrence ($t = 300$) (upper part), as well as at time reversal ($t = 150$) (lower part).

to Ehrenfest's theorem, a narrow wave packet follows a classical trajectory and, in this sense, it is as random as specified in the classical limit, only

on a rather short time scale t_E. However, this scale grows indefinitely as $T \to 0$, again in accordance with the correspondence principle.

5.4. An example of true chaos in quantum mechanics

Apart from a short Ehrenfest time scale, quantum dynamics is stable, and, hence, quantum chaos, whatever it is like, cannot be true chaos as it is in the classical limit. We call it *pseudochaos*. In the next section, we shall see that the quantum stability is explained by the discreteness of the energy (and frequency) spectrum of any quantum system bounded in phase space, that is in both coordinates and momenta.

A simple example is the standard map on a torus where the spectrum is obviously discrete and even has a finite number of energy levels. For the map on an infinite cylinder, this is already not the case. Indeed, for rational $T/4\pi$ (and even for some irrational ones, see ref. [40]) the spectrum of the motion becomes continuous as was discussed in section 3. Yet, the continuous spectrum in this case results not in chaos but in regular motion, namely the quantum resonance. The question arises if true chaos is ever possible in quantum mechanics. Yes it is, but under very peculiar conditions, as I shall illustrate using the following simple example, borrowed from ref. [36].

Consider a classical dynamical system on an N-dimensional torus with angle variables θ_i,

$$\dot{\theta}_i = g_i(\theta_k), \quad i,k = 1, \ldots, N. \tag{5.6}$$

In such a system, chaos is possible for $N \geqslant 3$. One particular example due to Arnold is (see ref. [41]),

$$\begin{aligned} \dot{\theta}_1 &= \cos\theta_2 + \sin\theta_3, \\ \dot{\theta}_2 &= \cos\theta_3 + \sin\theta_1, \\ \dot{\theta}_3 &= \cos\theta_1 + \sin\theta_2. \end{aligned} \tag{5.7}$$

This implies that the linearized equations

$$\dot{\xi}_i = \xi_k \left.\frac{\partial g_i}{\partial \theta_k}\right|_{\theta_k = \theta_k^0(t)}, \tag{5.8}$$

where $\theta_k^0(t)$ is the reference trajectory, are exponentially unstable,

$$\xi_i \sim e^{\Lambda t}. \tag{5.9}$$

As was mentioned in section 1, the combined dynamics of the original (5.6) and linearized (5.8) systems can be described by the conserved Hamiltonian (cf. eq. (1.4))

$$H(n_k, \theta_k) = n_k g_k(\theta_i), \tag{5.10}$$

which implies the equations for conjugate momenta (cf. eq. (5.8))

$$\dot{n}_i = -n_k \frac{\partial g_k}{\partial \theta_i}. \tag{5.11}$$

If the main system (5.6) is time-reversible, as is the case for Arnold's example (5.7) ($t \to -t$ is equivalent to $\theta_i \to \theta_i + \pi$), the combined system (5.10) is completely equivalent to the pair (5.6) and (5.8). Another way to see this is by observing that eq. (5.7) conserves the volume $\mathrm{d}\Gamma = \mathrm{d}\theta_1\, \mathrm{d}\theta_2\, \mathrm{d}\theta_3$ because,

$$\dot{\Gamma} = \int \mathrm{d}\Gamma \operatorname{div} \dot{\theta}, \quad \operatorname{div} \dot{\theta} = \frac{\partial \dot{\theta}_i}{\partial \theta_i} \equiv 0. \tag{5.12}$$

On the other hand,

$$\operatorname{div} \dot{\theta} = \sum_{k=1}^{N} \Lambda_k.$$

One of the Lyapunov exponents (along the reference trajectory) is always zero. Hence, in example (5.7), the remaining two satisfy, in view of eq. (5.12): $\Lambda_2 + \Lambda_3 = 0$, or $\Lambda_2 = -\Lambda_3$, thus providing the time-reversible behaviour. I should mention that the sum of all the *positive* Lyapunov exponents

$$h = \sum \Lambda_+ \geqslant 0, \quad \Lambda_+ \geqslant 0, \tag{5.13}$$

constitutes a fundamental characteristic in the modern theory of dynamical systems, the so-called *metric*, or *Kolmogorov–Sinai entropy*.

Coming back to our example, consider now a quantum system with the Hamiltonian operator

$$\hat{H} = \tfrac{1}{2}(g_k \hat{n}_k + \hat{n}_k g_k), \quad \hat{n}_k = -\mathrm{i}\frac{\partial}{\partial \theta_k}, \tag{5.14}$$

which is a quantized version of the classical combined system (5.10). The operator $\hat{n}$ is constructed from the periodicity in θ (cf. eq. (3.3)), and

symmetrization is needed for $\hat{H}$ to be Hermitian. Introducing the quantum probability density $f(\theta,t) = |\psi(\theta,t)|^2$, and using Schrödinger's equation, we arrive at the relation

$$\frac{\partial f}{\partial t} + \frac{\partial}{\partial \theta_k}(f g_k) = 0, \tag{5.15}$$

which exactly coincides with the continuity equation for the classical system (5.6). Hence, the quantum probability would evolve identically to the classical one, including chaotic motion.

This simple example clearly demonstrates how extraordinary the truly chaotic quantum dynamics has to be. Besides unbounded motion in momenta, the momenta must grow exponentially fast. This is necessary because the fine-grained (exact) density $f(\theta,t)$ does not become homogeneous in chaotic motion, as I have already discussed in section 2. Instead, it is getting more and more "scarred" by the mechanism of local motion instability. This results in the exponential growth of the density's wave numbers (Fourier harmonics), and, in quantum mechanics, of momenta.

Problem (unsolved). Devise a Gedanken experiment to observe true quantum chaos.

True chaos is also possible in a semiclassical system, only a part of which is quantal while the rest obeys classical mechanics. One example is the interaction of a quantum atom with a classical electric field, the latter being a dynamical variable of the system (see, for example, ref. [42]).

A very important class of semiclassical processes is the quantum measurement since in the Copenhagen interpretation the measurement device is classical by definition. Moreover, any quantum measurement appears to be always chaotic as it has to be highly unstable to achieve a large macroscopic effect via a very weak microscopic interaction with a quantum system. We shall return to consider further this interesting and important problem.

6. Quantum stability: diffusion localization

6.1. Localization principle for quantum chaos

In the previous section, we have seen that the quantum diffusion in the standard map is always localized, no matter how large the classical parameter k. Why? What is the localization mechanism? In this section, we

shall consider a theory of diffusion localization which was first proposed in ref. [38] and subsequently developed in many papers (see, e.g., refs. [11,43]), especially in the work related to the problem of the diffusive photoelectric effect in hydrogen, to be discussed in section 9. Alternative explanations will be reviewed in the next section.

Consider first the principal idea of our theory. To begin with, we shall relate the localization phenomenon to the discreteness of the (quasi) energy spectrum. The main question here is whether the quantum spectrum is always discrete. For a conservative system with bounded energy surfaces, the affirmative answer is a rigorous mathematical result. In what follows, the most important characteristic of the discrete spectrum is the *mean level density*

$$\varrho = \left\langle \frac{\mathrm{d}n}{\mathrm{d}E} \right\rangle . \tag{6.1}$$

In the unperturbed standard map, the rotator for example, $\varrho = 1/n = (2E)^{-1/2}$ depends on E (and n), and is the inverse classical frequency.

However, in a time-dependent system, even as simple as the standard map, the above question presents a very difficult and delicate mathematical problem, which is still unsolved. We know that the spectrum becomes continuous in a quantum resonance at rational values of $T/4\pi$. Even more important, it does so at very special irrational $T/4\pi$ as well [40]. The Lebesgue measure of these irrationals is zero, yet it is not clear at the moment whether this is a fundamental or technical restriction. So, we have to assume the hypothesis that for a typical irrational $T/4\pi$, the quasienergy spectrum in the standard map is purely discrete. From the physical viewpoint, it is well confirmed by the results of numerical experiments presented in section 5.

Even with this hypothesis, we face another difficulty: the total density of all the quasienergy levels is infinite as quasienergy is defined (mod $2\pi/T$). To cope with this obstacle, we shall further refine the definition of ϱ. Namely, we include in ϱ only the *operative eigenstates* which are actually present effectively in the initial quantum state to evolve.

Obviously, the discrete spectrum cannot produce aperiodic diffusive evolution. How, then, can we explain why the initial quantum diffusion is fairly close, as we have seen, to classical diffusion which has a continuous spectrum? Here, the central point of our theory is directly related to the fundamental quantum law, the uncertainty principle. The latter asserts that in a finite time interval t (in our case from the switching-on of the perturbation or from the birth of a quantum initial state left after the measurement), any energy E is defined only within $\Delta E \sim 1/t$.

If $\Delta E \gtrsim 1/\varrho$ the formally (asymptotically) discrete spectrum is physically continuous, that is it acts as a continuous one while,

$$t \lesssim \varrho \sim t_{\mathrm{R}}. \tag{6.2}$$

If so, the relaxation time scale t_{R}, introduced in the previous section, is simply of the order of the density of the operative quasienergy levels.

This is a fairly simple result, and the next problem is the calculation of ϱ. For the standard map, it can be done as follows. During the time interval $t_{\mathrm{R}} \sim \varrho$, classical diffusion couples $(\Delta n)_{\mathrm{R}} \sim (D_n t_{\mathrm{R}})^{1/2}$ unperturbed states whatever initial $\psi(0)$ was, provided it comprised not too many states: $(\Delta n)_0 \ll (\Delta n)_{\mathrm{R}}$. It is sufficient to consider the case when only one unperturbed state is initially occupied. To explain the diffusion over $(\Delta n)_{\mathrm{R}}$ states in terms of eigenfunctions, we conclude that each state is coupled, in turn, to roughly the same number $(\Delta n)_R$ of eigenfunctions. Hence, we obtain the operative quasienergy level density $\varrho \sim (\Delta n)_{\mathrm{R}}/(2\pi/T) \sim T(\Delta n)_{\mathrm{R}}$ (we shall drop numerical factors in these crude estimates). Using eq. (6.2), we have,

$$t_{\mathrm{R}} \sim T\,(D_n t_{\mathrm{R}})^{1/2}\,. \tag{6.3}$$

Notice that for $t \lesssim t_{\mathrm{R}}$, the left-hand side is less than the right one. This is just the condition for classical-like diffusion to continue because the guaranteed number of operative eigenfunctions provides a still longer time for the currently continuous spectrum.

From equation (6.3), we obtain our main estimate,

$$\tau_{\mathrm{R}} \equiv \frac{t_{\mathrm{R}}}{T} \sim T D_n \equiv D, \tag{6.4}$$

where we have rescaled t and D_n to transform this important relation into the simplest form ($\tau = t/T$ is a dimensionless time).

Further, the maximal diffusion spread $(\Delta n)_{\mathrm{R}} \sim (D_n t_{\mathrm{R}})^{1/2} = (D\tau_{\mathrm{R}})^{1/2} \sim D$ is of the order of the localization length l_{s}. Hence, we have another important estimate,

$$\tau_{\mathrm{R}} \sim D \sim l_{\mathrm{s}}. \tag{6.5}$$

Finally, we can also estimate the energy of the quantum steady state,

$$E_{\mathrm{s}} \sim l_{\mathrm{s}}^2 \sim D^2. \tag{6.6}$$

These results are very remarkable as eqs. (6.5) and (6.6) relate essentially quantal characteristics of motion (τ_R, l_s, E_s) to the classical quantity D.

The best check of a theory is its ability to predict a new phenomenon. This was indeed done in reference [38]! Consider the time-dependent perturbation parameter $k(\tau) = k_0\tau^\alpha$. Then $(\Delta n)^2_R \sim D_0\tau^{2\alpha+1}$ where $D_0 \sim k_0^2$, and we obtain, instead of eq. (6.4),

$$\tau_R \sim D_0{}^{1/(1-2\alpha)}. \tag{6.7}$$

For $\alpha = \frac{1}{2}$, the relaxation time scale becomes infinite, provided that $D_0 > 1$, or $k_0 \gtrsim 1$, i.e., that no perturbative localization occurs. Then, there is no quantum steady state at all, and the diffusion is permanent, as it is in the classical limit. We shall call that regime the *delocalization* of quantum diffusion. It persists for $\alpha > \frac{1}{2}$ as well. In the latter case, the left-hand side of eq. (6.3) is less than the right-hand side for any $\tau > 1$ ($\tau < D_0^{1/2}\tau^{\alpha+1/2}$), again, provided $D_0 > 1$. So, there is no solution for τ_R and the diffusion does not stop. All this has been confirmed in numerical experiments [38].

The delocalization condition $D_0 > 1$ is similar but generally not identical to Shuryak's condition $k_0 > 1$ (see eq. (4.8)). For delocalization, both must be satisfied.

Further, even in the interval $0 < \alpha < \frac{1}{2}$, the diffusion cannot stop completely as for $\alpha = 0$. This is because the quasienergy spectrum is certainly continuous due to the aperiodic variation of $k(\tau)$. As $\tau \to \infty$, the latter perturbation becomes adiabatic because $\dot{k}/k = \alpha/\tau \to 0$. In particular, it implies a slow increase in energy: $E_s \sim k^4 \sim D_0^2\tau^{4\alpha}$. This rate reaches the classical one $E \sim D_0\tau^{2\alpha+1}$ just at the critical value $\alpha = \frac{1}{2}$. Another interesting case corresponds to $k(\tau) = \exp(\gamma\tau)$. The width of the Fourier spectrum of this perturbation is $\Delta \sim |\gamma|$. It implies that the width of quasienergy levels is the same: $T\Delta\varepsilon \sim |\gamma|$ (see eq. (3.15)). If $|\gamma|\tau_R \sim |\gamma|\varrho/T \gtrsim 1$, or,

$$|\gamma|D \gtrsim 1, \tag{6.8}$$

the "thick levels" overlap, and the spectrum remains continuous at any τ. Hence, the diffusion would be classical forever. As condition (6.8) does not depend on the sign of γ, the same classical behaviour holds for decreasing k until the border of quantum stability $k \sim 1$ is reached.

A more interesting example of the latter behaviour is a decaying system, one whose total probability gradually falls: $|\psi| \sim \exp(-\gamma\tau)$. Under the condition (6.8), the mean energy of the remaining part would grow indefinitely: $E \sim D\tau$.

Now consider another version of the standard map with a perturbation $k(n) = k_0|n|^\alpha$ which depends on momentum n, rather than explicitly on time. This model is simpler to analyze because the perturbation is time-periodic and the spectrum can be purely discrete.

Problem. Show that a symmetric solution to diffusion equation (2.23) with $D(n) = D_0|n|^{2\alpha}$ satisfies $\langle |n|^{2(1-\alpha)} \rangle = (1-\alpha)D_0\tau$.

Using the latter result and the estimate $\tau_R \sim (\Delta n)_R \sim n_R$, we arrive at the same relation (6.7) as we obtained for time-dependent $k(\tau)$ [17]. The difference between the two cases is in asymptotic behaviour: the quantum steady state for $k(n)$ (an allegedly discrete spectrum), and the residual diffusion for $k(\tau)$ (certainly a continuous spectrum). The critical $\alpha = \frac{1}{2}$ for $k(n)$ has been recently confirmed in ref. [44] by a very sophisticated calculation.

As a final check of our localization principle, let us consider multi-dimensional diffusion, homogeneous but not necessarily isotropic [32]. Let $D_1, \ldots, D_N$ be principal diffusion rates. Then, relation (6.3) takes the form

$$\tau_R^2 \sim \Pi \tau_R^N, \quad \Pi = D_1 \cdots D_N. \tag{6.9}$$

If the product $\Pi > 1$, this equation has no solution for any $\tau_R > 1$ and $N \geqslant 3$, which implies delocalization. Formally, the same holds for $N = 2$, when eq. (6.9) does not depend on τ_R. However, in the latter case our simple method fails because it is rather too crude. A more refined theory for a similar problem reveals that localization persists for $N = 2$, but the localization length becomes extremely long: $\ln l_s \sim (D_1 D_2)^{1/2}$ (see ref. [35]). This shows the limitations of our simple approach.

With regard to the condition $\Pi > 1$ above, one should bear in mind that for delocalization to occur, quantum transitions in all freedoms must be possible. In the simplest case the latter requires $k_m \gtrsim 1$ $(m = 1, \ldots, N)$ where $D_m \sim k_m^2$, as it is in the standard map. Then, the crucial condition is $k_{\min} \gtrsim 1$ for minimal k_m.

Instead of a "real" many-dimensional system, we may consider, for example, the standard map with a quasiperiodic perturbation [35]: $k(\tau) = k_0 + k_1 \cos \omega_1 \tau + \cdots + k_{N-1} \cos \omega_{N-1} \tau$ of $N-1$ incommensurate frequencies. Qualitatively, the behaviour is similar to the former case.

From the analysis, one may conclude that the diffusion localization is restricted essentially to one-dimensional systems. Yet, this is not always the case. The point is that in eq. (6.9) we tacitly assumed that the time-scales

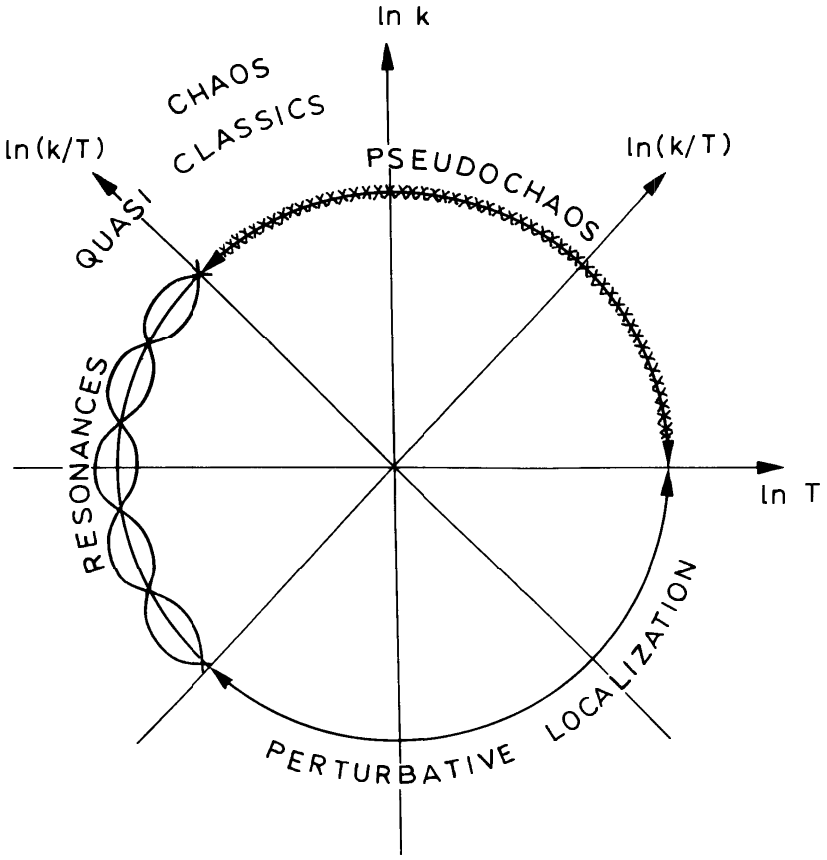

Fig. 16. Outline of various regimes in quantum dynamics as exemplified by the standard map: k is the quantum perturbation parameter; K the classical stability (resonance overlap) parameter; in general, $T = K/k$.

of the motion in all freedoms are comparable, and hence that there are efficient transitions between all freedoms of the many-dimensional system. If this is not the case, the localization may persist. A trivial example is N completely decoupled freedoms. A more interesting situation will be considered in section 9 for the photoelectric effect in hydrogen.

Finally, in this qualitative part of the section, observe on fig. 16 the outline of various regimes in quantum dynamics using the standard map as a representative example.

6.2. A sketch of the quantum steady state

To improve on our rough order-of-magnitude estimates for diffusion localization we need, first of all, precise definitions for localization parameters $\tau_R, l_s, \bar{E}_s$. The latter is trivial to define,

$$\bar{E}_s = \overline{\langle n^2/2 \rangle}\,, \tag{6.10}$$

where the bar denotes time-averaging in the steady state. Localization length l_s is defined via the exponential distribution (5.3), which is approximately confirmed by numerical experiments (see also below). The most

difficult parameter to define is the relaxation scale τ_R, in view of the fact that there is a broad transition region of unknown shape (see lower curve in fig. 13). We shall postpone this definition until section 8.

Using the definition (5.3) for l_s and the estimate (6.5), we have found from numerical experiments [17] that

$$\langle l_s/D\rangle = 1.04 \pm 0.03, \quad l_s \approx D, \tag{6.11}$$

where the errors here and below are only statistical. This would imply that the average energy is $\bar{E}_s \approx \frac{1}{4}D^2$. However, the numerical result is different [36],

$$\left\langle 2\bar{E}_s/D^2\right\rangle = 0.92 \pm 0.04, \quad \bar{E}_s \approx D/2\ . \tag{6.12}$$

We will discuss this discrepancy later. Now I would like to mention that both l_s and $\bar{E}_s$ are sensitive to the arithmetical properties of the parameter T, which do not enter the simple estimates above. This is demonstrated in fig. 17, taken from ref. [33]. The relative difference in T for the two curves is about 2 per cent. Both $T/4\pi$ values are close to the rational number $p/q = 1/25$, but one (lower curve)

$$\frac{T}{4\pi} = \cfrac{1}{25 + \cfrac{1}{1+\cdots}} \equiv (25, 1, 1, \ldots),$$

is a typical irrational with

$$\left|\frac{T}{4\pi} - \frac{p}{q}\right| \approx 10^{-3} \sim \frac{1}{q^2},$$

while the other is much closer (by a factor of 60) to a quantum resonance, which substantially affects the energy growth. This particular example gives an idea of the accuracy of the above relations for the quantum steady state. The real accuracy is, of course, much worse than the statistical one given above.

A characteristic feature of the quantum steady state is its appreciable fluctuations, which are clearly seen in fig. 13. Their amplitude decreases with increasing k. Roughly,

$$\frac{\Delta E_s}{E_s} \sim \frac{1}{\sqrt{l_s}} \approx \frac{1}{\sqrt{D}} \sim \frac{1}{k}. \tag{6.13}$$

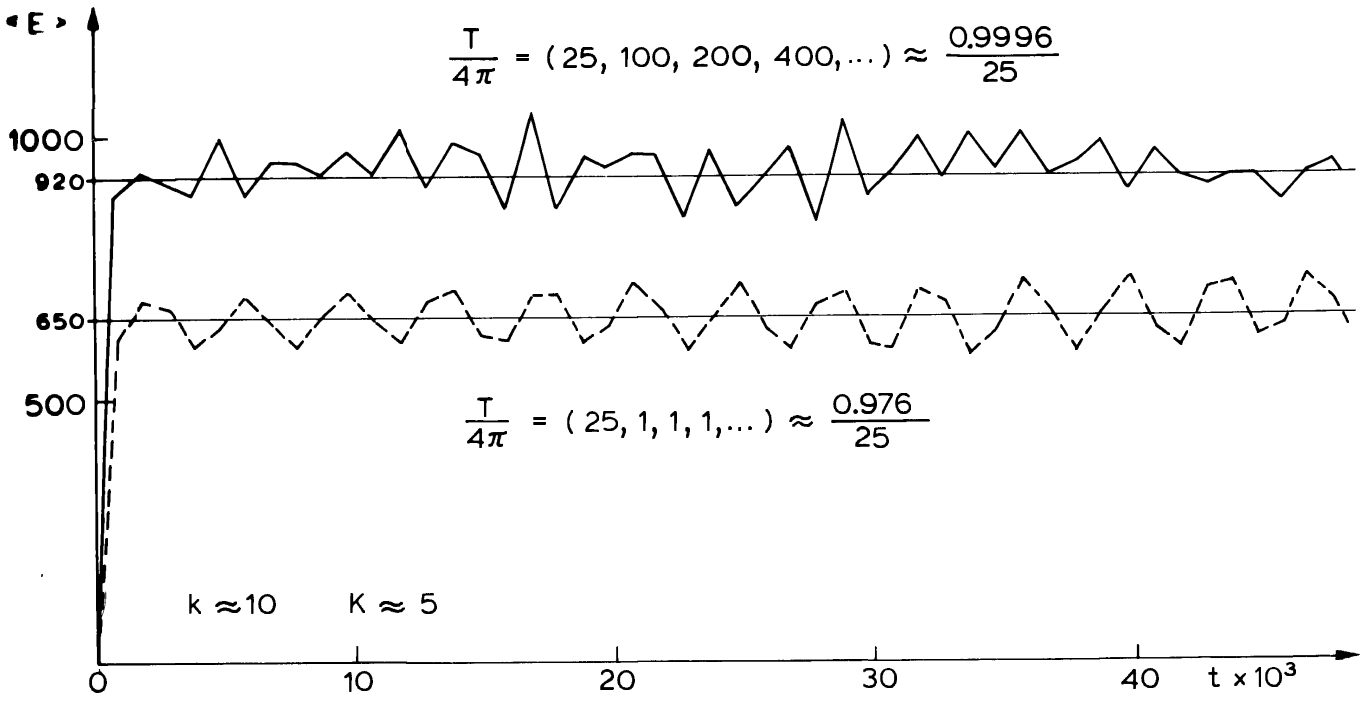

Fig. 17. Quantum steady state in the standard map [33]: $k = 10$; $K \approx 5$; T values are given as continued fractions; t is the number of iterations; the corresponding values of $l_s \approx 40$ and 53. Compare this with the much better time resolution in fig. 13 (upper curve).

This allows a very simple physical interpretation, namely, the quantum steady state of a *single* system represents a small *ensemble* of $\sim l_s$ statistically independent "particles". These particles are not random, of course, because the stationary oscillations in the quantum steady state are quasiperiodic. A regular component of quantum stationary fluctuations is clearly seen in fig. 13 and, especially, in fig. 17 (lower curve).

The dips in E_s corresponds to Poincaré's recurrences, which do not quite reach the initial state $E = 0$. To be sure, they will reach it eventually, but it would take an enormous time, far greater than the relaxation time, τ_R. So, the energy (frequency) level density ϱ (see eq. (6.1)) determines the relaxation scale, not the Poincaré recurrence time; this seems to be widely misunderstood. Notice that Poincaré recurrences occur in a truly chaotic oscillation with a continuous spectrum as well, but in a more irregular manner than for quasiperiodic motion.

An interesting, common feature of deep recurrences is their symmetry, on average, with respect to the minimal E_s (see fig. 13). This means that the recurrence, which is simply a big fluctuation, is developing according to the "antidiffusion" law. This profound statistical property was discovered and rigorously proved in 1936 by Kolmogorov [46].

In a different interpretation of the standard map as the wave-particle interaction, there is a diffusion in x in addition to that in n, as far as

classical mechanics is concerned (section 2). In the case of the quantized standard map, the whole spectrum becomes continuous (eq. (3.14)). However, it does not influence the n-dynamics because the quasimomentum ν is conserved. What about the x-dynamics?

First of all, the steady state in n does not depend on ν on average, yet the fluctuations do, in view of the different phase relations (see eq. (3.14)). Since the quasienergy spectrum $(\varepsilon_n + \Delta(\nu))$ is continuous, the motion in x is unbounded, and the diffusion proceeds as in the classical limit for a given distribution in n. The latter is completely different from the classical one, in that the former is asymptotically localized and time-independent with $\langle n^2 \rangle = 2\bar{E}_s$. Hence, $\langle \Delta x \rangle \sim \langle n \rangle t = T\langle n \rangle \tau$ (generally $\langle n \rangle \neq 0$), and $\langle (\Delta x)^2 \rangle \sim \langle n^2 \rangle t^2 = 2\bar{E}_s T^2 \tau^2$.

Problem. Derive the distribution function $f(x, t)$.

A different qualitative explanation may be given by noting that the eigenfunctions are all unbounded (quasiperiodic) in x (see eq. (3.12)). It is similar to the quantum resonance, also discussed in section 3. In both cases the motion is unbounded but the evolution is different. Why?

Problem. Derive the motion law in x in the case of a quantum resonance in n.

6.3. Quasienergy eigenfunctions

The diffusion localization and formation of the quantum steady state implies localized eigenfunctions. The standard technique for computing them involves the diagonalization of the evolution matrix (3.9); this is very time consuming. The largest feasible interval is $\Delta n \sim 10^3$. On the other hand, if we are interested only in the asymptotic behaviour of the localized eigenfunctions, i.e., in their tails, a much faster technique is available, namely, the transfer matrix discussed in section 3. It was used first for the problem under consideration in ref. [27]. The asymptotic behaviour of the eigenfunctions is determined by the minimal Lyapunov's exponent of the "dynamical system" (3.16). Calculating the smallest exponent is more difficult than the calculation of the largest one in studies of classical motion instability. Still, the former is fairly fast, and it allows us to follow an eigenfunction over $\Delta n \sim 10^5$ and more.

Is there any relation between the local instability in the transfer matrix and the corresponding motion instability in the classical limit? There seems to be none. First, the rate of the local instability is determined by

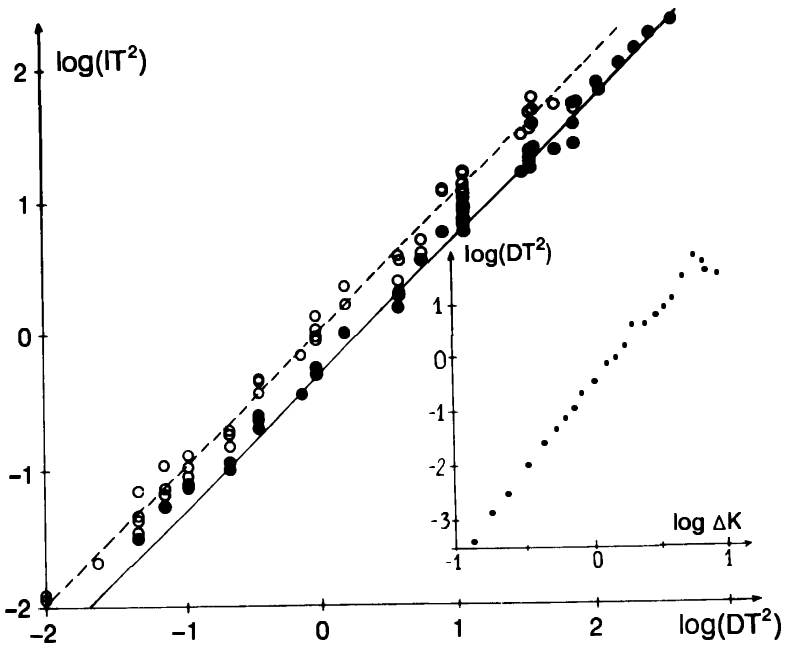

Fig. 18. Relation between the scaled localization length and the diffusion rate in the standard map [17]: open circles denote the steady state; full circles denote the eigenfunctions. Insert: scaled diffusion rate versus classical parameter K down to $K_c \approx 0.97$; $\Delta K = K - K_c$. The logarithm is decimal.

the classical diffusion, not by classical instability. Second, the quantum localization persists even if the classical motion is perfectly stable and regular (e.g., for $k \ll 1$).

The first surprising result, in the standard map, was that the asymptotic localization length for eigenfunctions $l \neq l_s$ differs from that for the steady state (fig. 18). In spite of the large fluctuations, the mean difference is clearly seen and it amounts to a factor of 2 [17],

$$\langle l/D \rangle = 0.57 \pm 0.02, \quad l \approx D/2. \tag{6.14}$$

This is further confirmed in fig. 12 (right-hand scale).

What could be the cause of this strange discrepancy? At first glance, it looks like a contradiction. Indeed, if we assume that the eigenfunctions are purely exponential,

$$\varphi_m(n) = \frac{1}{l} \, \mathrm{e}^{-|m-n|/l}, \tag{6.15}$$

and that $n = 0$ is the initial state, the time-averaged steady state is given by

$$\bar{f}_s(n) = \overline{|\psi(n,\tau)|^2} = \sum_m |\varphi_m(0)\varphi_m(n)|^2$$
$$\approx \frac{(1+X)\,e^{-X}}{2l}, \quad X = \frac{2|n|}{l} > 0. \tag{6.16}$$

Apart from a relatively small deviation from the exponential dependence, to be discussed later, the localization length is the same: $l_s = l$. But, empirically, $l_s \approx 2l$ (!). What is wrong?

At long last, we have found that the origin of this apparent contradiction is in the very large spatial fluctuations of $\varphi_m(n)$. Instead of a smooth exponential (6.15), they are described as something like

$$\varphi_m(n) \sim \exp(-|m-n|/l + \xi_{mn}), \tag{6.17}$$

with some random ξ_{mn}, and $\langle \xi_{mn} \rangle = 0$ by definition.

Large fluctuations in quantum chaos are quite comprehensible and are immediately seen in any numerical data (see, e.g., fig. 13). However, we have been very surprised to discover in numerical experiments that ξ_{mn} are not only large and highly irregular but that they grow diffusively with n,

$$\left\langle (\Delta\xi_{mn})^2 \right\rangle = D_\xi |\Delta n|, \quad D_\xi \approx 1/l. \tag{6.18}$$

Now, the length l is defined via $\langle n^{-1} \ln|\varphi_0(n)| \rangle = l$, while the steady state is related to a different average $\langle |\varphi|^2 \rangle$. Our first idea was to renormalize l by averaging (6.17) over ξ, assuming a Gaussian distribution, which was more or less confirmed by numerical experiments [17]. The result

$$\langle |\varphi_0(n)| \rangle \sim e^{-|n|/l_1}, \quad \frac{1}{l_1} = \begin{cases} \dfrac{1}{l} - \dfrac{D_\xi}{2}, & lD_\xi \leqslant 1, \\ \dfrac{1}{2D_\xi l^2}, & lD_\xi \geqslant 1, \end{cases} \tag{6.19}$$

appeared to be very satisfactory because in combination with the numerical evidence $lD_\xi \approx 1$, we obtained $l_1 \approx 2l \approx l_s$, just as required. Yet, the problem is that eq. (6.16) suggests that we should use the averaged $|\varphi|^2$ rather than $|\varphi|$. Then, the result

$$\left\langle |\varphi_0(n)|^2 \right\rangle \sim e^{-2|n|/l_2}, \quad \frac{1}{l_2} = \begin{cases} \dfrac{1}{l} - D_\xi, & lD_\xi \leqslant \frac{1}{2}, \\ \dfrac{1}{4D_\xi l^2}, & lD_\xi \geqslant \frac{1}{2}, \end{cases} \tag{6.20}$$

is different ($l_2 = 4l$), and contradicts with numerical experiments ($l_s \approx 2l$), unless $lD_\xi = \frac{1}{2}$, which would contradict another numerical experiment ($lD_\xi \approx 1$). The origin of these inconsistencies is not yet clear. A suspicious point is the truncation of the Gaussian distribution at $\xi = n/l$, leading to the second expression in eqs. (6.19) and (6.20). Such a procedure is, perhaps, too crude and needs to be refined. Anyway, we have failed to achieve a quantitative explanation for the empirical relation $l_s \approx 2l$.

The exponential localization is related to the periodicity in n of the standard map. At least, some homogeneity seems to be required. Generally, the diffusion localization is of a different shape, for example, in our basic model. A sufficiently large inhomogeneity may even result in delocalization, as in the above example of the standard map with the variable $k(n)$. We shall come back to this problem later.

Now, a few words about the deviation of the steady-state distribution (6.16) from the exponential form. It is hardly observable on the background of large fluctuations discussed above. Yet, this "slight" deviation doubles the mean energy $\bar{E}_s$ (eq. (6.12)) in agreement with the numerical results. But E_s fluctuates as well (see, e.g., an example in fig. 17), so that the realistic accuracy is actually within a factor of 2. Another source of discrepancy is in the shape of both the eigenfunctions and the steady state near their maxima, which is most important for E_s, and which is very difficult to measure, again due to large fluctuations. A different approach to this problem will be discussed in section 8.

An interesting problem is to find the rate of energy growth at a high-harmonic quantum resonance $T/4\pi = p/q$; $q \gg 1$ (section 3). On the one hand, the modulus of the eigenfunction has period q (eq. (3.20)), but on the other hand, it must be "localized" during each period if $l \ll q$, because during a sufficiently short time the fine structure of the spectrum is irrelevant owing to the uncertainty principle, and the motion is insensitive to a small change in $T/4\pi$, shifting it from a rational to a typical irrational value. This implies that the overlapping of different eigenfunctions and the corresponding rate of transitions over a period q will be exponentially small in the parameter $q/l \gg 1$. Hence, we can assume for the rate (see eq. (3.19)),

$$r(q) = E/\tau^2 \approx (k/2)^2 \, \mathrm{e}^{-q/2\pi l}, \tag{6.21}$$

where $(k/2)^2 \approx r(1)$ (see eq. (3.18)), and the empirical factor in the exponent has been derived from numerical data in ref. [33] and proved to be very close to 2π.

The band-width $(\Delta\varepsilon)_b$ of the quantum resonance spectrum can be estimated as the inverse of the characteristic time τ_b at which the reso-

nant growth of energy (6.21) is of the order of the steady-state energy $E_s = D^2/2 = 2l^2 \sim k^4$, whence,

$$T(\Delta\varepsilon)_b \sim \frac{1}{\tau_b} \sim \frac{e^{-q/4\pi l}}{\sqrt{l}} \sim \frac{\sqrt{r}}{l}. \tag{6.22}$$

For $\tau_b \gg \tau_R \sim l$, a temporary steady state persists at resonances with $q \gtrsim 2\pi l \ln l$. This is close to, but not identical with, the estimate in ref. [76].

6.4. Addendum: the impact of noise and of measurement

If external noise is present, the problem is no longer purely dynamical, and hence is not really part of the subject that I am discussing. However, I will briefly mention the effect of noise, in order to complete the picture.

The effect was studied in ref. [47] by modifying the standard map (3.11): $k\cos x \to k\cos x + \tilde{k}g(x)$, where g is some random function, and $\tilde{k} \ll k$, $k \gg 1$. Two principal conclusions have been drawn by the authors: (i) any, arbitrarily weak, noise breaks up the localization and produces some diffusion with rate D_N where

$$\frac{D_N}{D} \sim \begin{cases} D\tilde{D}, & D\tilde{D} \lesssim 1, \\ 1, & D\tilde{D} \gtrsim 1, \end{cases} \tag{6.23}$$

and $\tilde{D} \sim \tilde{k}^2$ is the rate under noise only; (ii) for $D\tilde{D} \gtrsim 1$, the noise restores classical diffusion. The latter conclusion is especially important in quasi-classical transitions when $D \sim k^2 \to \infty$ and, hence, when the critical noise level $\tilde{D}_c \sim k^{-2}$ goes to zero.

The interesting question of whether noise could restore the classical exponential instability of motion, remains open.

Generally, successive measurements also restore classical diffusion but this is not weak noise at all, owing to the collapse of the wave. To the best of my knowledge, this problem has not yet been thoroughly analyzed (for brief remarks, see ref. [48]). First, we need to control the measurement-induced diffusion rate

$$D_m \sim \frac{(\Delta n)_m^2}{\tau_m} \ll D, \tag{6.24}$$

where τ_m is the measurement period (in the number of map's iterations), and $(\Delta n)_m^2$ is the momentum dispersion per measurement.

To maintain classical diffusion, the measurement period must be $\tau_m \lesssim \tau_R \sim D \sim \varrho$. Hence, any such measurement would produce transitions

between quasienergy eigenstates. It is not easy to estimate the corresponding dispersion $(\Delta n)^2_{\rm m}$. A plausible guess would be $(\Delta n)^2_\tau \sim l_{\rm s} \approx D$. Then, the minimal value $D_\tau \sim (\Delta n)^2_\tau/\tau_{\rm m} \sim l_{\rm s}/\tau_{\rm m} \ll D$ is for $\tau_{\rm m} \gg 1$. And, of course, $D_\tau/D \sim l_{\rm s}/\tau_m \; k^{-2} \to 0$ as $k \to \infty$ (the classical limit).

Suppose now that we measure x, and do it in the optimal way, that is to accuracy $\Delta x \sim T^{1/2}$ (see eq. (5.5) and the associated text). Then $(\Delta n)^2_x \sim 1/T$, which is much smaller than $(\Delta n)^2_\tau$, so that $D_x/D_\tau \sim (\Delta n)^2_x/(\Delta n)^2_\tau \sim 1/Tl_{\rm s} \sim 1/Kk \to 0$ as $k \to \infty$.

Principally, it is also possible to "keep" a narrow quantum packet on a classical trajectory by appropriate successive measurements of a sufficiently short period $\tau_{\rm m} \lesssim \tau_{\rm E} \sim |\ln T|/\ln K \sim (\ln k)/\ln K$ (see eq. (5.5)). In this case, the minimal $D_\tau/D \sim \ln K/\ln k \to 0$ when $k \to \infty$.

7. Diffusion localization: alternative explanations

7.1. Quantum corrections in the quasiclassical region

The phenomenon of quantum diffusion and its localization has recently attracted much attention, especially after it was applied to an apparently simple and well-known process of photoionization in hydrogen. Confirmed in many numerical experiments, and recently also in a few laboratory experiments, the phenomenon stimulated many attempts to understand it from different points of view. In this section, I shall briefly review various approaches known to date, each of which, if true, sheds some new light on this interesting problem, and facilitates a more complete and deep understanding of the underlying physics.

Quantum stability, discovered in ref. [30] and also called perturbative localization (section 4), is well-known by now and widely used. However, it is not our main topic. Quantum stability is certainly sufficient but not, in general, necessary for diffusion localization.

Another early approach involved calculating the quantum corrections to the classical behaviour which is quite natural in the quasiclassical region where one would expect a sort of dynamical chaos if it occurs in the classical limit. The first calculations [37] revealed a fast exponential growth of the quantum corrections to various average quantities, like the energy E in the standard map, for example. This fast growth, related to the spreading of wave packets, restricts the applicability of perturbation theory to a very short time scale $t_{\rm E}$ (see eq. (5.5)).

To cope with this difficulty in ref. [38], the quantum corrections were calculated to the ψ-function itself, rather than to the averages, using Maslov's

asymptotic expansion. Surprisingly, the exponential terms completely disappeared from the final expression even though they were explicitly present in the initial expansion. Apparently, this is explained by isolating the most unstable part in the zeroth approximation, $\psi^0 \sim \exp(\mathrm{i}S/\hbar)$, which is directly related to classical dynamics with action S. In any event, this method allowed us to follow quantum corrections up to the relaxation time scale t_{R} (eq. (6.5)), and to obtain the first estimate for this scale.

Still another approach was related to the behaviour of quantum time correlations, which determine the diffusion rate [35,49]. Correlations rapidly decay, as in the classical limit, on the short Ehrenfest time scale t_{E} but the further decrease (if any) is very slow. However, the residual correlations are very small, of the order of k^{-1}, so that they can affect the quantum dynamics (diffusion) only on a much longer time scale, presumably t_{R}. However, these quantitative estimates are very uncertain, mainly, due to a crude estimate for t_{E}.

7.2. Anderson's localization mechanism

An interesting analogy with the well-known Anderson localization of quantum motion in a static, spatially random potential was discovered in ref. [29], and further developed in ref. [32]. The idea was to compare the stationary Schrödinger equation (3.16) in the momentum representation for the standard map, for example, with that in the coordinate representation in a disordered one-dimensional lattice. The former can be represented as

$$\varphi_n \mathrm{e}^{-\mathrm{i}\chi_n} - \sum_{r\neq 0}(-\mathrm{i})^r J_r(k)\varphi_{n-r} = J_0(k)\varphi_n, \tag{7.1}$$

where $\chi_n = T\left(\varepsilon - n^2/2\right)$, and ε is the quasienergy, while the latter (Lloyd's model) is usually taken in the form,

$$u_n E_n + \sum_{r\neq 0} W_r u_{n+r} = E u_n. \tag{7.2}$$

Here n is the integer spatial coordinate along the lattice, E the energy, the vector W_r describes the translation operator, that is the motion along the lattice, and E_n represents the potential energy at the nth site of the lattice. In Anderson's theory, the values of E_n are assumed to be random with the statistical properties homogeneous along the lattice. In particular, in Lloyd's model $E_n = \tan(\chi_n/2)$ where the random χ_n are uniformly distributed in the interval $(0, \pi)$. Then, the distribution in E_n is

$$f(E_n) = \frac{1/\pi}{1 + E_n^2}, \tag{7.3}$$

and does not depend on n, while all the eigenfunctions are exponentially localized.

There is a transformation that relates both Schrödinger's equations, (7.1) and (7.2), with $\chi_n = T\left(\varepsilon - n^2/2\right)$. It is essentially a Fourier transformation. If the χ_n were random, the Anderson theory could be applied to the standard map to prove the existence of localization. This was the original logic in ref. [29]. But the χ_n in eq. (7.1) are certainly not random, they are only ergodic. Hence, the supposed explanation of diffusion localization via Anderson's mechanism fails. Moreover, the logic may be reversed: because there is a direct connection between eqs. (7.1) and (7.2), on the one hand, and as the diffusion localization is firmly established, if only from numerical experiments, on the other, quantum localization in the solid-state problem does not require a random potential but only an irregular one. How irregular? It seems that only a periodic potential completely excludes localization, and provides, instead, the extended Bloch eigenstates. In the standard map, it corresponds to the quantum resonance.

Some researchers argue (see e.g., ref. [36]) that diffusion localization is a dynamical version of the statistical Anderson's localization. True, in the standard map (7.1) there are no random parameters, whereas in Anderson's model (7.2) the E_n are assumed to be random. On the other hand, the perturbation in both models is regular, and dynamical chaos in the classical standard map is itself the delocalization factor. To counteract the diffusion and to provide localization, one needs to avoid quantum resonances which may or may not help, depending on the diffusion.

The analogy between dynamical and solid-state problems proves, as usual, to be fruitful since it allows various ideas, methods and concepts in the fields to be shared. In particular, the method of the transfer matrix borrowed from solid-state physics is very helpful in dynamical problems, as we have seen. On the other hand, in addition to the non-random Anderson localization which we have discussed, there is another interesting conjecture: in a nonhomogeneous irregular lattice, it is possible that there exist some delocalized states that are quite different from the homogeneous Bloch states. This would correspond to delocalization in the standard map with the variable $k(n)$ considered in section 6.

7.3. Two-level statistical approximation

In ref. [51], an extremely simple approximation was proposed, taking into account only two (!) unperturbed states directly coupled by a time-dependent perturbation. It seems very strange, but this method appears to work!

As this is certainly a very local description, the standard map is the appropriate model. Consider two unperturbed states, n and $n+1$, coupled via the matrix element $V_{n,n+1} = k/2T$ (section 4). Leaving only one frequency in the Hamiltonian (2.13), which is of course another approximation, we arrive at Rabi's elementary theory of the two-level system. Assuming that the system is initially in state n, the time-averaged probability for another state $n+1$ is

$$\bar{P}_{n+1} = \frac{V^2/2}{V^2 + (\Delta/2)^2} = \frac{k^2/2}{k^2 + (T\Delta)^2}, \tag{7.4}$$

where $\Delta = E_{n+1} - E_n - 2\pi m/T$ is the detuning (m fixed). So far, there is nothing new in eq. (7.4). But the next main step in ref. [51] is the following: instead of solving the very complicated problem of many back-and-forth transitions among unperturbed states, the authors average eq. (7.4) in D, assuming that its distribution in the interval $(0, \pi/T)$ is uniform. Actually, they considered a particular case of a hydrogen atom in a microwave field (sections 2 and 9), but here I shall simply rephrase their arguments for the more general situation of the standard map. The result of the averaging is

$$P \equiv \langle \bar{P}_{n+1} \rangle = (k/2\pi) \arctan(\pi/k). \tag{7.5}$$

Finally, if the localization in the steady state is exponential (5.3), then,

$$\frac{P}{1-P} \approx \exp(-2/l_s). \tag{7.6}$$

In particular, in the two limiting cases, the localization length is given by

$$l_s \approx \begin{cases} 3k^2/\pi^2, & k \gg \pi, \\ \dfrac{2}{\ln(4/k)}, & k \ll \pi. \end{cases} \tag{7.7}$$

The upper expression is close but not identical to the result of diffusion localization $l_s \approx D \sim k^2$ (cf. fig. 12). The lower expression may be compared to eq. (4.11). Again, they differ by a factor of 2. This is no surprise as the two-level approximation is too crude, of course.

The averaging process that we have used makes this theory conceptually similar to Anderson's. As illustrated in fig. 19, it provides a reasonable description of quantum localization in the overall range of k. Curiously, in ref. [51] the relation $P = \exp(-2/l_s)$ was used by mistake (lower solid curve in fig. 19) with no agreement in the region of diffusion localization

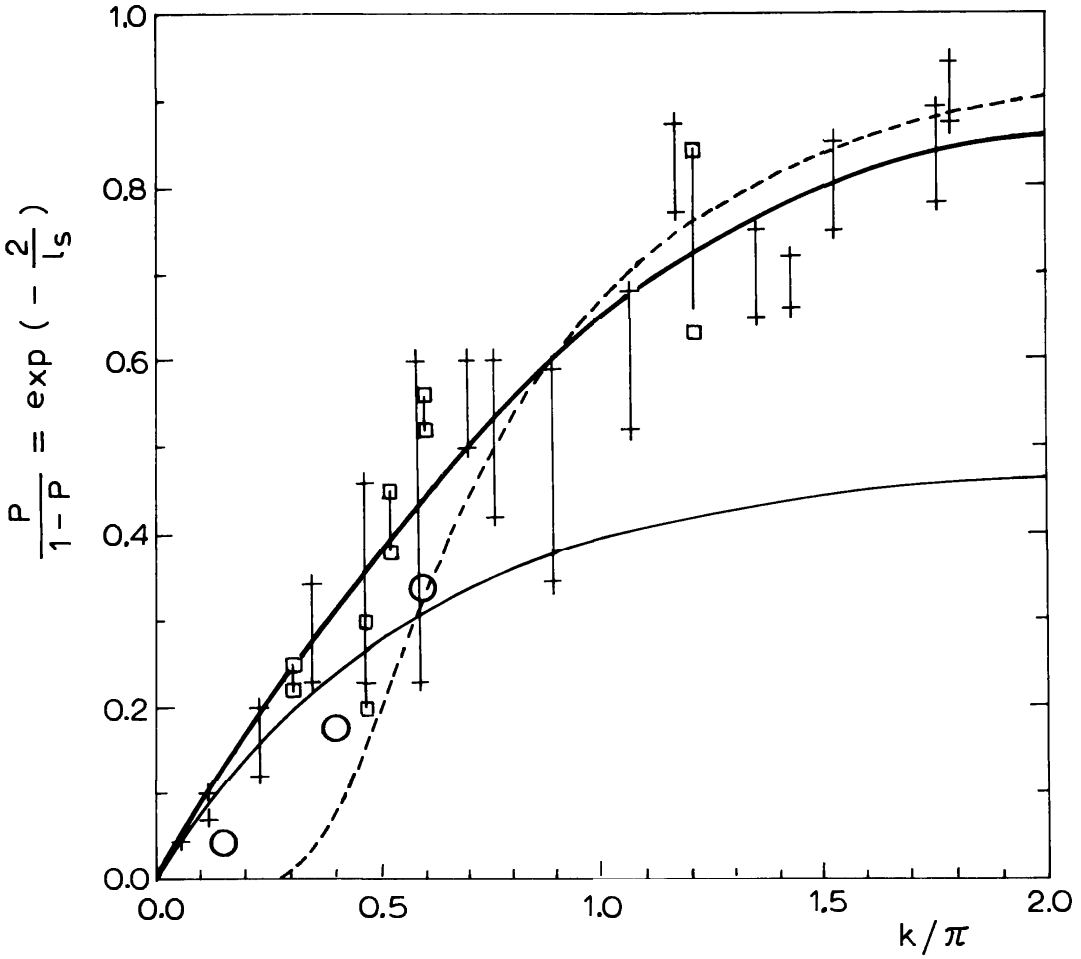

Fig. 19. Two-level approximation for momentum localization in the standard map: crosses and squares are numerical results presented in ref. [51], while numerical data from ref. [31] are shown by open circles; the lower solid curve is P (eq. (7.5)) [51] and the upper one is $P/(1-P)$; the broken line represents the average diffusion localization length $l_s \approx k^2/2$.

($k \gtrsim 1$). With the correct equation (7.6), the approximation works much better!

The main quantum resonance with extended Bloch eigenfunctions is also included into the two-level approximation, corresponding to the only detuning factor in this case, $\Delta = 0$. Notice, however, that the second parameter T does not enter this approximation at all, and this is the principal weakness of the method.

7.4. Localization and cantori

In the classical standard map when $K < K_c \approx 1$, the motion in n is strictly bounded by continuous invariant (KAM) curves $n(x)$ with some irrational

rotation numbers (frequencies),

$$r \equiv \frac{\bar{\omega}}{2\pi} = \frac{1}{2\pi} \lim_{m\to\infty} \frac{x_m - x_0}{m}. \tag{7.8}$$

Any KAM curve acts as an absolute barrier for a trajectory. It is not very obvious for the map with its "jumps" in the phase space but we can always imagine some equivalent continuous system in the extended phase space. Above the critical $K_c(r)$, which depends in a very complicated way on r, the KAM curve is destroyed and transformed into the so-called *cantorus*, a nowhere dense set of points along some line $n(x)$ [18]. Loosely speaking, the cantorus is a curve that everywhere contains holes. This is a part of the critical structure briefly considered in section 2. Cantori are called also partial barriers as they allow some trajectories to pass through. In quantum mechanics, the cantorus may become an absolute barrier for the motion if its biggest hole is less than an elementary cell of the quantum phase space. Apparently, this was the main idea used in refs. [53,54] to explain localization phenomena. Indeed, one conclusion of this work was the existence of the well-known Shuryak border (4.8). The work also indicated a substantial modification of diffusion localization by the critical structure but only near the classical chaos border where $\Delta K = K - K_c \approx K - 1 \to 0$. This had already been established in ref. [17], although it was missed in ref. [54].

According to ref. [17] the crucial parameter is the ratio of the localization length l_s to the map's period $2\pi/T$ in n, or,

$$l_s T \approx 0.3k(\Delta K)^3 \lesssim 1, \tag{7.9}$$

where $K \approx 1$ is assumed. The latter inequality is the condition for a new type of localization, which we called the *inhomogeneous localization* (fig. 20). The steady-state distribution $\bar{f}(n)$ reveals here the resonance structure of the standard map with plateaus corresponding to $n_m \approx 2\pi m/T$. The mean localization length $\bar{l}_s \approx 7$ (fig. 20), which is close to $k = 10$ and represents a one-kick effect of the perturbation. Using the results of ref. [17], a more general relation can be derived,

$$\bar{l}_s^2 \approx \bar{l}_s l_s + k^2/3, \tag{7.10}$$

where the diffusion localization length l_s is given by eq. (6.11), and the numerical factor is adjusted from the data in fig. 20. Whence

$$\bar{l}_s \approx \frac{l_s}{2} + \sqrt{\frac{l_s^2}{4} + \frac{k^2}{3}} \to \begin{cases} l_s, & l_s \gg k, \\ k/\sqrt{3}, & l_s \ll k, \end{cases} \tag{7.11}$$

where $k \gg 1$ is assumed to be large.

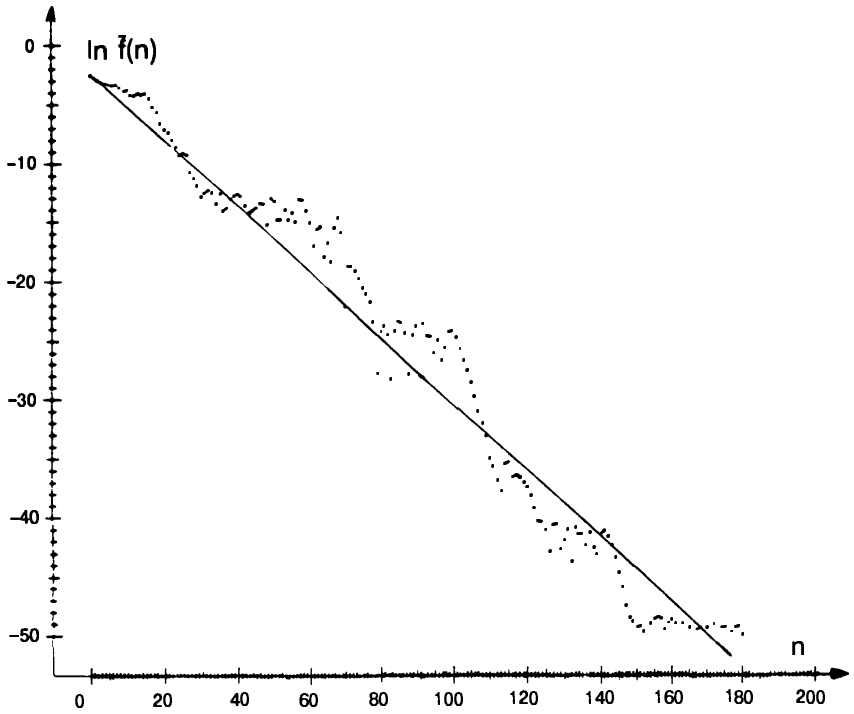

Fig. 20. Inhomogeneous localization in the standard map near the classical chaos border [17]; $K = 1.5$; $\Delta K \approx 0.53$; $k = 10$; $T = 0.15$; $l_s \approx 2.0$; $\bar{l}_s \approx 7$; $l_s T \approx 0.3$; $\bar{l}_s/k \approx 0.7$; the straight line: $\ln \bar{f} = 2n/\bar{l}_s$.

We should also point out that the change in the localization shape under the border (7.9) results in a periodical variation of the steady state distribution function superimposed on the average exponential dependence with the modified length (7.10).

In ref. [54], the relation

$$K_b \approx e^{(1.3T)^{1/3}}, \tag{7.12}$$

was derived which is similar to our eq. (7.9) for $\Delta K = K_b - K_c \ll 1$ (with a numerical factor of ≈ 0.7 instead of our 0.3). But K_b is interpreted in ref. [54] as the border for quantum penetration through cantori. Actually, as we have seen, the localization exists at both sides of this border, although with a different shape and length.

7.5. Classical model for quantum dynamics

In our early attempts to understand the mechanism of quantum localization, we studied a very simple modification of the classical standard map (2.3), namely [38],

$$\bar{n} = n + [k \sin x], \qquad \bar{x} = x + T\bar{n}, \tag{7.13}$$

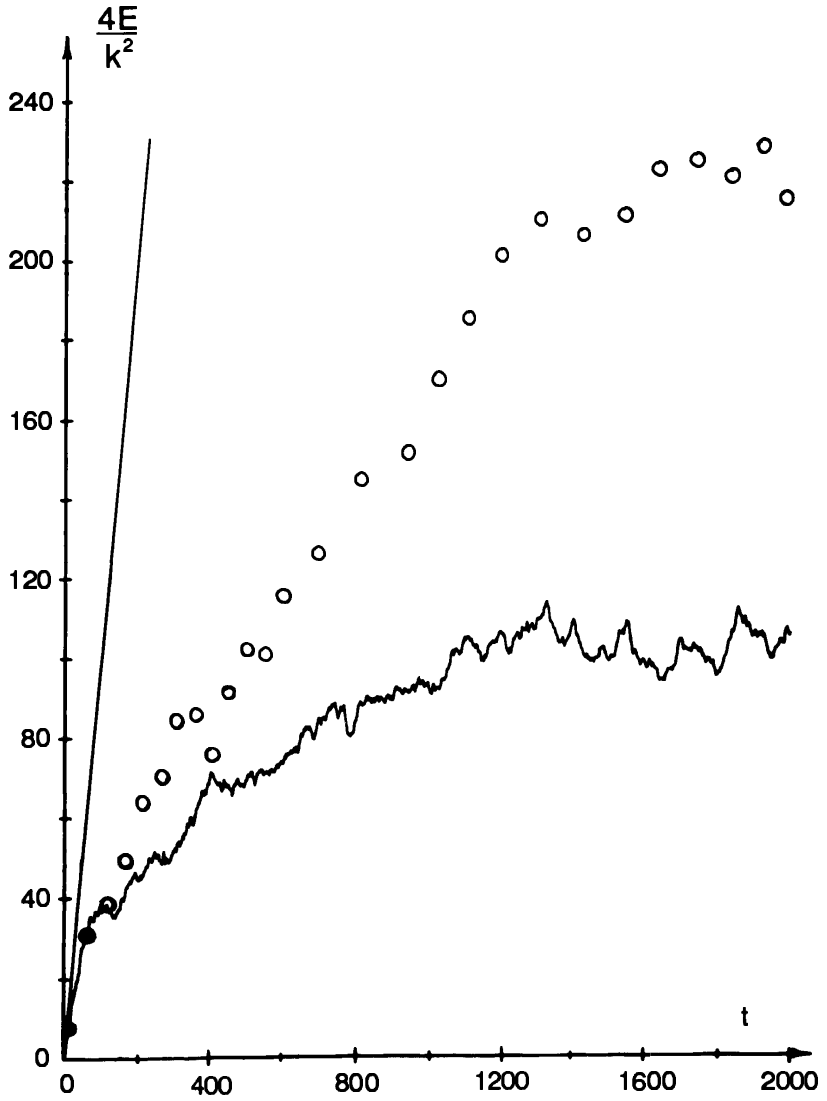

Fig. 21. "Quantum localization" in the classical discrete map (7.13) [38]: the straight line represents classical diffusion; the wiggly curve shows quantum localization, and circles are for the discrete model; t is the number of iterations; $k = 20$; $K = 5$.

where the brackets denote the integer part. The main idea was to introduce a quantization of action by some means into the classical mechanics. Of course, this quantization is not equivalent to a complete quantum mechanical description. However, numerical experiments demonstrated a surprising qualitative similarity between the semidiscrete classical model (7.13) and the quantized standard map (fig. 21). The agreement between the two models is only within an order of magnitude, but one hardly could expect any better.

Besides the localization, the classical model accounts also for the quantum stability border $k \sim 1$ (nonresonant and chaotic cases, see section 4) but not for $k \sim T \ll 1$ (resonant case). The model also accounts for the quantum resonance, but with the wrong resonant values $T/2\pi = p/q$ (see

section 3).

An attempt to improve the discrete model was made in ref. [55] by adding a very complicated term to the first eq. (7.13); this is more complicated to compute than the exact quantum map. Nevertheless, this unusual approach may help in a qualitative analysis of quantum dynamics. In particular, it demonstrates that the discretization of phase space alone drastically changes the dynamics.

Another interesting application of the model (7.13) is to numerical experiments in classical dynamics [38]. The point is that any quantity stored in a digital computer is discrete, or "quantized" . Such a numerical quantization is even more severe than in quantum mechanics where only actions (and not coordinates) are quantized. The principal result here is that there is no true chaos in numerical experiments but only pseudochaos, as in quantum mechanics. Asymptotically, as $t \to \infty$, all trajectories in the computer become periodic. This important fact was known long ago from the theory and practice of so-called computer pseudorandom number generators, which are widely used in various numerical simulations (e.g., the Monte-Carlo method, see also ref. [56]).

Problem. Estimate periods of motion for the standard map in discretized calculations done using a digital computer.

A novel effect of discretization that has been discovered is that even partial discretization (of one or two variables in the map (7.13)) may cause a crucial change in the dynamics.

8. Statistical properties of chaotic eigenstates

8.1. Quantum ergodicity and level "repulsion"

The statistical properties I am going to discuss in this section are not the fundamental ones inevitably related to quantum measurement and to the very interpretation of quantum mechanics. On the contrary, we shall restrict ourselves, as before, to the properties of the ψ-function, which represents the quantum system.

In the case of the discrete (quasi)energy spectrum, asymptotically (as $t \to \infty$), almost-periodic quantum evolution loses any resemblance to classical chaos, and turns into its opposite, the regular motion of a completely integrable system. Only spatial chaos remains embedded in the eigenfunctions, and also in the distribution of (quasi)energy levels. This is the topic

of this section. We shall mainly discuss the level statistics, which have now been studied very thoroughly, and only briefly the so-called chaotic eigenfunctions whose investigation is only beginning.

Consider first the concept of *integrability* in quantum mechanics. The origin of the confusion involved in analyzing this problem is that there are two concepts that are completely different, and, I would say opposite. One is related to the Hilbert space of the ψ-functions considered as the phase space (dynamical space) in quantum mechanics. In this space, the integrability is equivalent to the discreteness of the spectrum and to the very existence of eigenfunctions (see, e.g., nice reviews [57,58]). In this sense, all bounded quantum systems are integrable, independent of their classical behaviour. Notice that in classical mechanics the situation is completely different – the Liouville equation may have no eigenfunctions at all, and this just corresponds to chaotic motion.

To a physicist, the above concept of quantum integrability is too formal and certainly insufficient if only because it has no classical counterpart, even in the classical limit. In physics, we need to use the conventional phase space in action-angle variables, for example. In this sense, besides the ψ-function, the so-called *Wigner function* $W(n, x)$ is very convenient. It is a particular type of density matrix, being the quantum counterpart of the classical phase density $f(n, x)$ (see the review [61]).

The second (physical) concept of quantum integrability is directly related to the classical limit. In the latter case, the (conservative) system of N freedoms is called completely integrable if there are N motion integrals (usually actions), so that any trajectory is confined to an N-dimensional torus in phase space. The opposite case – *ergodic motion* – corresponds to the case in which only one integral, the energy, exists and in which the trajectories cover uniformly the whole energy surface. In a similar way, an integrable quantum system possesses N commuting operators (again, usually actions), and the eigenstates all have fixed actions. The corresponding Wigner eigenfunctions are localized around "thick" tori in ordinary phase space. In the opposite case of ergodic eigenstates, there are no quantities with definite values except the energy. The Wigner eigenfunctions uniformly fill up the energy shell of a finite width corresponding to the energy surface in the classical limit.

Turning to our simple models, we choose the standard map on a torus with a finite number of states (sections 2 and 3), to illustrate the quantum statistical properties in question. In this model, a string of q momentum states around the torus, comprising $qT/2\pi$ classical periods (resonances) simulates an energy shell of a conservative quantum system. We shall consider the quasiclassical region with $q \to \infty$, $T \to 0$, and $qT = \text{const}$.

If the perturbation is weak ($k \lesssim T$, perturbative localization), the system is integrable because $n \approx$ const. is a motion integral independent of the quasienergy ε_n. Notice that for $k = 0$ the model becomes conservative, which implies that it is always integrable because it has one freedom.

A version of Wigner's function for the standard map, both on cylinder and torus, is given by the expression

$$W(n,x) = \frac{1}{2\pi} \oint \mathrm{d}y \; \psi(x)\psi^*(x-y)\,\mathrm{e}^{-\mathrm{i}ny}$$
$$= \frac{1}{2\pi} \sum_m \psi(n+m)\psi^*(n)\,\mathrm{e}^{-\mathrm{i}nx}\,. \tag{8.1}$$

It has the following obvious properties of normalization,

$$\oint \mathrm{d}x\, W(n,x) = |\psi(n)|^2,$$
$$\sum_n W(n,x) = |\psi(x)|^2, \tag{8.2}$$
$$\oint \mathrm{d}x \sum_n W(n,x) = 1.$$

Problem. Calculate the upper bound for $|W(n,x)|$.

This less obvious property is directly related to discreteness of the quantum phase space in which each elementary cell has a finite volume of ~ 1.

Generally, the quantum phase density W is neither positive nor even real. If, for example, $\psi(0) = \psi(1) = 1/\sqrt{2}$, the two nonzero components of the density are,

$$4\pi W(0,x) = 1 + \mathrm{e}^{\mathrm{i}x}, \qquad 4\pi W(1,x) = 1 + \mathrm{e}^{-\mathrm{i}x},$$

thus,

$$|W(0,x)|^2 = |W(1,x)|^2 = \frac{1 + \cos x}{8\pi^2},$$

and

$$W(0,x) + W(1,x) = \frac{1 + \cos x}{2\pi} = |\psi(x)|^2\,.$$

In the quasiclassical region, W oscillates at a diminishing spatial scale around the classical phase density.

There are many statistical properties of the energy levels. We shall consider only the most popular one, namely, the distribution of the spacings $\Delta\varepsilon$ between neighbouring levels normalized to the average (local) level density ϱ of eq. (6.1): $s = \Delta\varepsilon.\varrho$; $\langle s\rangle \equiv 1$.

In a one-dimensional conservative system, the spacing is equal to the classical frequency of the motion, so that the statistical distribution is an inappropriate concept. However, the situation drastically changes in higher dimensions or in any time-dependent system. In the standard map, for example, the unperturbed quasi-energies $\omega_n \equiv T\varepsilon_n/2\pi = Tn^2/4\pi \pmod 1$ are distributed very irregularly for irrational values of $T/4\pi$. We rescaled here ε_n to the unit interval. Moreover, the spacing distribution was shown to be Poissonian (see ref. [64])

$$p(s) = \mathrm{e}^{-s}, \tag{8.3}$$

as if ω_n were random and independent. Of course, they are not, but the origin of the ω_n irregularity is in the random arithmetical structure of a typical irrational factor $T/4\pi$. Instead, one can model the level distribution in many-dimensional integrable systems using a random sequence of (quasi)energies. This would be a simple example of Random Matrix Theory (RMT), which analyzes statistical properties of various matrix ensembles supposed to represent "typical" quantum systems (see, e.g., review [59]). In its approach to the problem, RMT is reminiscent of Anderson's theory of localization (section 7).

In conservative systems, the level statistics was experimentally observed long ago. A particular distribution (8.3) was derived in ref. [60]. The study of quasienergy level statistics in time-dependent systems was begun by Izrailev [62], using the standard map on a torus. The distribution he observed was close to Poissonian (8.3). This distribution was rigorously proved for the Anderson localization in a random potential [63]. Yet, for the apparently very simple nonrandom set $\omega_n = T(n+\nu)^2/4\pi \pmod 1$, the rigorous proof of eq. (8.3) has been given by Sinai only recently, following the results of numerical experiments [64]. Some details of the statistical properties, and the proof, require that the irrational quasimomentum should be non-zero, $\nu \neq 0$, but eq. (8.3) holds approximately for $\nu = 0$ as well.

Coming back to our standard map on a torus, we should mention that here the parameter $T/4\pi = p/q$ is rational. Yet, for sufficiently large $q \to \infty$ (in the quasiclassical region), and for $n \ll q$, the distribution (8.3) approximately holds as well under perturbative localization, that is when $k \to 0$. For a resonant perturbation, the Poisson distribution persists also for $k \gtrsim T$

but $K \lesssim 1$ (i.e., in the interval $T < k < 1/T$). In this case, the perturbative localization breaks down but the system remains integrable with a new set of resonance eigenfunctions, and two incommensurate frequencies. One frequency is that of phase oscillations at resonance $\left(\sim \sqrt{k/T}\right)$ and the other is a frequency of perturbation $(2\pi/T)$ (see section 4).

With all these results, one might think that in the chaotic region ($K \gtrsim 1$ and $k \gtrsim 1$) of irregular quantum phases, a random-like distribution (8.3) would hold as well. However, this is generally not the case!

True, in the standard map on a cylinder, the Poisson distribution does indeed hold as well as for the corresponding solid-state Lloyd model (7.2). However, on a torus it does not, in general [62]. Here, a new parameter becomes of importance, namely,

$$\lambda = l/q, \tag{8.4}$$

which we shall call the *ergodicity parameter*. The standard map on a torus is intended to model an energy shell of a conservative system. Ergodicity implies that any initial distribution function will relax to the *microcanonical distribution*, which homogeneously fills up the energy shell. In quantum mechanics, this would imply that the eigenstates themselves or, rather their Wigner functions, must be also microcanonical, which is only possible when $\lambda \gg 1$. We shall call such functions *ergodic*. In this case, the spacing distribution drastically changes from Poissonian to

$$p(s) = As^{\beta}\, \mathrm{e}^{-Bs^2}, \tag{8.5}$$

where A and B are normalizing constants, to be determined from the conditions $\int p\,\mathrm{d}s = 1$ and $\langle s \rangle = 1$, and where $\beta \neq 0$ is the *level repulsion parameter*. Contrary to our expectation, the successive quasienergy values of chaotic eigenstates are correlated, and in this sense are "less random" compared with the Poisson distribution. Neighbouring levels avoid each other, or "repel", hence the term for the parameter β. Notice that there is repulsion at both small and large spacings (cf. eqs. (8.3) and (8.5)).

The phenomenon of energy level repulsion has been known since the beginning of quantum mechanics [65]. The distribution (8.5) with $\beta = 1$ was surmised by Wigner [66], using an early version of RMT, to explain experimental data for the level statistics of heavy nuclei.

A further important development in RMT was due to Dyson (see ref. [59]), who considered three values of $\beta = 1$, 2 and 4, depending on the system's symmetry. Equation (8.5) is now called the *Wigner–Dyson distribution*. The principal underlying philosophy of RMT is that a random

matrix from a certain statistical ensemble represents a "typical" complex quantum system of the corresponding class. This is, by the way, in accord with the modern understanding of randomness. RMT represents a typical statistical approach to the problem. Recently, it was complemented by a dynamical picture related to the phenomena of classical and quantum chaos. This was first done in numerical experiments by Bohigas and Giannoni [67] using simple Sinai billiard models.

Coming back to our model, I should emphasize again that the Wigner–Dyson distribution holds only for ergodic eigenstates, that is under the condition $\lambda \gg 1$ (8.4). For this reason, it was called the *limiting distribution* [62]. What is the mechanism of the level repulsion? An interesting insight into this problem is given by a dynamical analogy due to Dyson [68]. One may consider the dependence of (quasi)energy on some perturbation parameter, say k for the standard map, as the motion in abstract "time" k. Suppose that the perturbation is proportional to k. Then, the exact "equations of motion" can be derived using standard perturbation theory for the infinitesimal variation $\mathrm{d}k$,

$$\frac{\mathrm{d}^2\varepsilon_n}{\mathrm{d}k^2} = 2\sum_{m\neq n}\frac{|V_{mn}|^2}{\varepsilon_n - \varepsilon_m} \equiv F_n, \tag{8.6}$$

where ε_n are "instantaneous" quasienergies, and V_{mn} are the transfer matrix elements calculated for $k = 1$, and with "instant" eigenfunctions. The right-hand side of eq. (8.6) is the "force" of level interaction which clearly shows the repulsion. I should mention that Percival [69] considered the force F_n as a measure of the quantum instability of the system with respect to variations of its parameters.

Now, the main question we must answer is why the levels do not always repel, so that the Poisson distribution (8.3) is also possible. One reason is trivial: due to some symmetry $V_{mn} \equiv 0$, so that the states m and n are physically decoupled. Then, lines $\varepsilon_m(k)$ and $\varepsilon_n(k)$ cross, and nothing happens. This explanation does not work even in the case of perturbative localization ($k \to 0$), because matrix elements are taken at $k = 1$, to say nothing of the resonance eigenstates for $T \lesssim k \lesssim 1/T$.

A more general (qualitative) answer is apparently the following. The main factor determining the level repulsion is the correlation between the transition strength V_{mn} and the level spacing $\Delta_{nm} = \varepsilon_n - \varepsilon_m$. The latter is a frequency of classical motion (in the quasiclassical region) if $V_{mn} \neq 0$. If the classical motion is regular, as in the above example of separated resonances, the frequencies Δ_{nm} are not small, and the repulsion is weak. However, in the case of chaos, the classical spectrum becomes continuous,

which implies arbitrarily small spacings Δ_{nm} coupled, nonetheless, by a perturbation. Hence, strong level repulsion and the Wigner–Dyson distribution are to be expected. In turn, level repulsion prevents the spacings from being too small. Does it influence the classical continuous spectrum in any way? This is an interesting question that you may like to think about!

To complete the picture of level repulsion, one should not forget the localization. Owing to this phenomena, very close quasienergy levels ($|\varepsilon_n - \varepsilon_m| \to 0$) can occur belonging to well separated localized states, with consequently negligible coupling ($V_{mn} \to 0$). This would modify the limiting distribution (8.15). The ergodicity condition $\lambda \gg 1$ is inferred from precisely this consideration.

8.2. Localization and intermediate statistics

The ergodicity of eigenfunctions obviously depends on the particular dynamics and is not a universal property. In the first work on quantum ergodicity, von Neumann claimed to have proved the opposite [70]: under very weak conditions (which later turned out to be also unnecessary!) he allegedly established the approximate equality of the time and phase averages for any quantum system provided that there are a sufficiently large number of quantum states (cells) within the energy shell. The error was actually an instructive physical confusion (see ref. [57] for an interesting discussion).

The point is that for a system to be ergodic, the two averages must coincide for any physical quantity whose eigenfunction occupies a certain part of the energy shell. Of course, this is not always the case, as von Neumann found immediately. But because he was apparently completely sure that ergodicity must be a universal property, he decided to "cope" with this difficulty by introducing a global average physical quantity. What he missed was the ergodicity of this global quantity itself. Hence, his theorem actually turned out to be only an approximate identity! To the best of my knowledge, the first rigorous result on quantum ergodicity was due to Shnirelman [71] (see also ref. [72]). Formally, it was restricted to billiard systems. For most eigenfunctions to be ergodic, two conditions must be fulfilled: (i) ergodicity in the classical limit, and (ii) large quasiclassical parameters. The latter condition is particularly important, in view of quantum localization. In our model, it corresponds to the condition $\lambda = l/q \sim k^2/q \sim kK/qT \gg 1$, which is satisfied as $k \to \infty$, since K and qT are classical parameters.

Now, our problem is the impact of localization on the quasienergy level

statistics. If $\lambda \gg 1$, we have one limiting statistics, Wigner and Dyson's (8.5), with the parameter $\beta = 1$ in our model. For $\lambda \ll 1$, there is another limiting statistics, Poisson's (8.3), with $\beta = 0$ for small s. It is quite natural to assume that in between ($0 < \lambda \lesssim 1$), the level statistics is an intermediate one corresponding to noninteger β ($0 < \beta < 1$). On purely empirical grounds, that was introduced in ref. [73] in the form,

$$p(s) = As^{\beta} \exp\left[-Bs^{1+\beta}\right], \tag{8.7}$$

where β is a free parameter required to fit experimental data.

A different approach has been adopted by Izrailev [74]. His main idea was to make use of Dyson's nice Coulomb gas model for level repulsion [81]. In RMT, this model has meaning only for the integer values $\beta = 1, 2$ and 4. Izrailev conjectured that Dyson's model actually makes sense at any β, intermediate β values corresponding to localized eigenfunctions. Moreover, he looked for and found the relation between the repulsion parameter β and the localization parameter λ. Finally, he managed to find a simple approximate solution to Dyson's model for any value of β.

The first step in this argument was a new definition of the localization parameter λ. In eq. (8.4), l describes the eigenfunction tail, and it loses its meaning, at least quantitatively, if $\lambda \gtrsim 1$. Izrailev introduced another definition,

$$\tilde{\lambda} = \frac{2}{q}\, \mathrm{e}^{\tilde{H}}, \quad \tilde{H} = -\sum_{n=1}^{q} |\varphi(n)|^2 \ln |\varphi(n)|^2. \tag{8.8}$$

Here $\tilde{H}$ is the standard statistical entropy, and the factor 2 accounts for the Gaussian fluctuations that provide $\tilde{\lambda} = 1$, in the case of ergodic eigenfunctions.

The main result of this theory is the *Izrailev distribution*,

$$p(s) = As^{\beta} \exp\left[-\frac{\pi^2}{16}\beta s^2 - \frac{\pi}{2}\left(B - \frac{\beta}{2}\right) s\right], \tag{8.9}$$

which seems to apply in the entire interval ($0 \leqslant \beta \leqslant 4$). At the first stage, the repulsion parameter β was determined empirically by the relation,

$$\beta = \left\langle \tilde{\lambda} \right\rangle, \tag{8.10}$$

where the averaging applies over all the exact eigenfunctions. Recently, the empirical dependence $\beta(D/q)$ has been found [75,79] (fig. 22). The

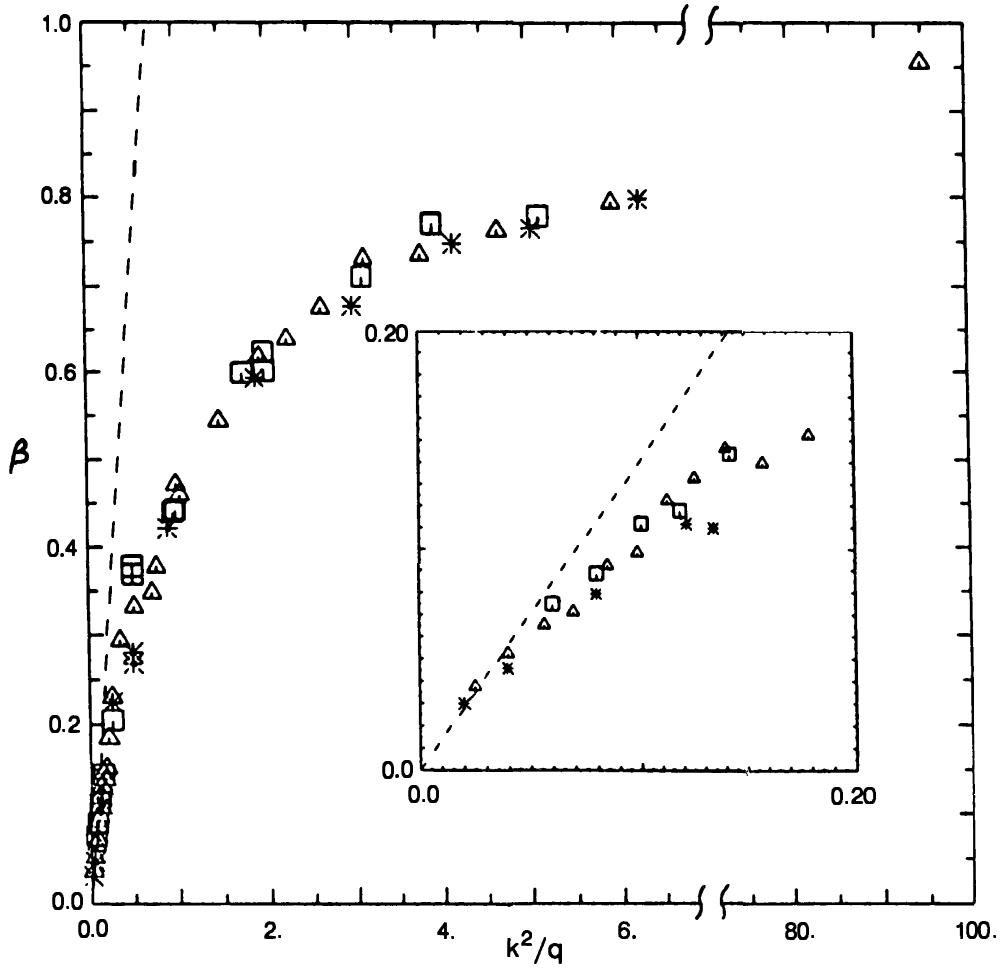

Fig. 22. Intermediate statistics [75]: the level repulsion parameter β versus the localization parameter k^2/q in the standard map on a torus; different symbols correspond to $q = 400$, 600, 800. Notice the change in the scale k^2/q.

argument of this function was actually k^2/q, but I believe that the true dependence must relate to D/q, in accord with the dependence of the original localization parameter λ (eq. (8.4)). One question remains open: which is the better procedure, to average $\tilde{\lambda}$, as in eq. (8.10), or to use the average of $\ln \tilde{\lambda} \sim \tilde{H}$ (eq. (8.8)), as in ref. [79]?

8.3. Level repulsion and diffusion suppression

Level statistics can serve as a criterion for quantum chaos, although the criterion is somewhat ambiguous. For example, the Poisson distribution may indicate either integrability (no chaos) or a strongly localized quantum chaos.

Do the level statistics have any direct effect on the quantum evolution? Yes, some, but it is not a very important effect. The basic spectral parameter is the mean level density (6.1), which determines the relaxation time scale τ_R. The level spacing statistics influences the decrease of dif-

fusion rate for $\tau \gtrsim \tau_R$. The main idea is the following. The diffusion rate is proportional to the mean spectral density of the perturbation. It remains unchanged while $\tau \lesssim \tau_R$, owing to the uncertainty principle (section 6). However, at $\tau > \tau_R$ it decreases as the only eigenstates that continue to contribute are those whose spacing is $s \lesssim \tau_R/\tau$. The relative number of the latter (hence, relative diffusion rate) is given by the spacing distribution $p(s)$,

$$\frac{D(\tau)}{D(0)} \sim \int_0^s p(s')\,ds' \sim s^{\beta+1} \sim \left(\frac{\tau_R}{\tau}\right)^{\beta+1}, \tag{8.11}$$

where $\tau \gg \tau_R$ is assumed, and $D(0)$ is the classical diffusion rate on the relaxation time scale.

If we neglect the level repulsion ($\beta = 0$), the rate $D(\tau) \sim \tau^{-1}$, and the mean energy $E \sim D^2 \ln(\tau/\tau_R)$ formally diverges [34]. However, the above estimates hold only for $\tau/\tau_R \lesssim l_s \sim \sqrt{E_s}$, that is until there are at least a few spacings $\lesssim \tau_R/\tau \sim 1/l_s$. From this, it follows that $E_s \sim D^2 \ln D$. Still, there seems to be a contradiction in the latter estimate for $l_s \sim D\sqrt{\ln D}$, as compared with the previous result presented in section 6 ($l_s \approx D$).

The answer is apparently related to the level repulsion with some $\beta_D \neq 0$ [76]. Remember that the quantum evolution depends on the operative eigenfunctions (section 6), which partially overlap and hence repel. The result is,

$$E = E_s\left[1 - (1 + \tau/\tau_R)^{-\beta_D}\right], \qquad \tau_R = D\beta_D, \quad E_s = D^2/2. \tag{8.12}$$

Preliminary numerical experiments give $\beta_D \approx 0.2$, a fairly low value. One unclear point is that eq. (8.12) holds only if $\ln D \gtrsim 1/\beta_D$, otherwise the finite l_s limitation is decisive, as for $\beta_D = 0$ above.

In any event, the vanishing diffusion rate does not give a complete description of diffusion localization because the distribution function also changes from a Gaussian to an exponential form. This suggests that a different explanation can be given by introducing a *drift* into the classical diffusion equation

$$\frac{\partial f}{\partial t} = \frac{1}{2}\frac{\partial}{\partial n} D \frac{\partial f}{\partial n} + \frac{\partial}{\partial n} R f \equiv -\frac{\partial Q}{\partial n}, \tag{8.13}$$

where the flux Q is given by

$$Q = -\frac{D}{2}\frac{\partial f}{\partial n} - Rf. \tag{8.14}$$

The second term describes an additional flux that is proportional to the phase density f; hence the term drift. Consider the Green function of diffusion equation, that is the solution with an initial single value $n = n_0$. For the steady-state distribution to be exponential, $f_s \sim \exp(-2|n - n_0|/l_s)$, the drift rate must satisfy

$$R = \frac{n - n_0}{|n - n_0|} \cdot \frac{D}{l_s} \approx \pm 1. \tag{8.15}$$

This expression is rather peculiar because the rate depends on the initial conditions. The physical meaning of the drift is the quantum reflection of the ψ-wave back to the initial state. The whole problem requires, of course, further study.

8.4. Spatial fluctuations in eigenfunctions

The spatial structure of chaotic eigenstates is much less known compared with the statistics of energy levels. The main reason seems to be related to the scarcity of experimental data on the eigenstates. This information is much more difficult to obtain than information on energy-level statistics. However, there is no such limitation on data from numerical experiments.

As regards the localized eigenfunctions, we have already discussed this problem in some detail in section 6. Consider now ergodic eigenstates. Their level spacing distribution agrees well with the prediction of statistical RMT. It is quite reasonable to expect a similar agreement for eigenfunctions. For these, Gaussian fluctuations are predicted in the limit of very large matrices of dimension $q \to \infty$,

$$p(\varphi) = \sqrt{\frac{q}{2\pi}}\, e^{-q\varphi^2/2}, \tag{8.16}$$

where the quantity φ is any of the $\varphi(n)$, $\langle\varphi\rangle = 0$, and $\langle\varphi^2\rangle = 1/q$ from normalization.

In RMT, the parameter q is arbitrary, and is subject only to technical limitations in numerical experiments. However, in a real quantum system, q is determined by the size of the energy shell which depends, in turn, on the system's dynamics. Hence, in the dynamical problem, unlike RMT, q is a physical parameter which may not be very large. For example, in complex nuclei, $q \sim 10^6$ is very large indeed. Yet, in complex atoms $q \sim 10$ is rather small, and this should be taken into account [77]. In this respect RMT, which is the local theory, is more applicable to nuclei than to atoms.

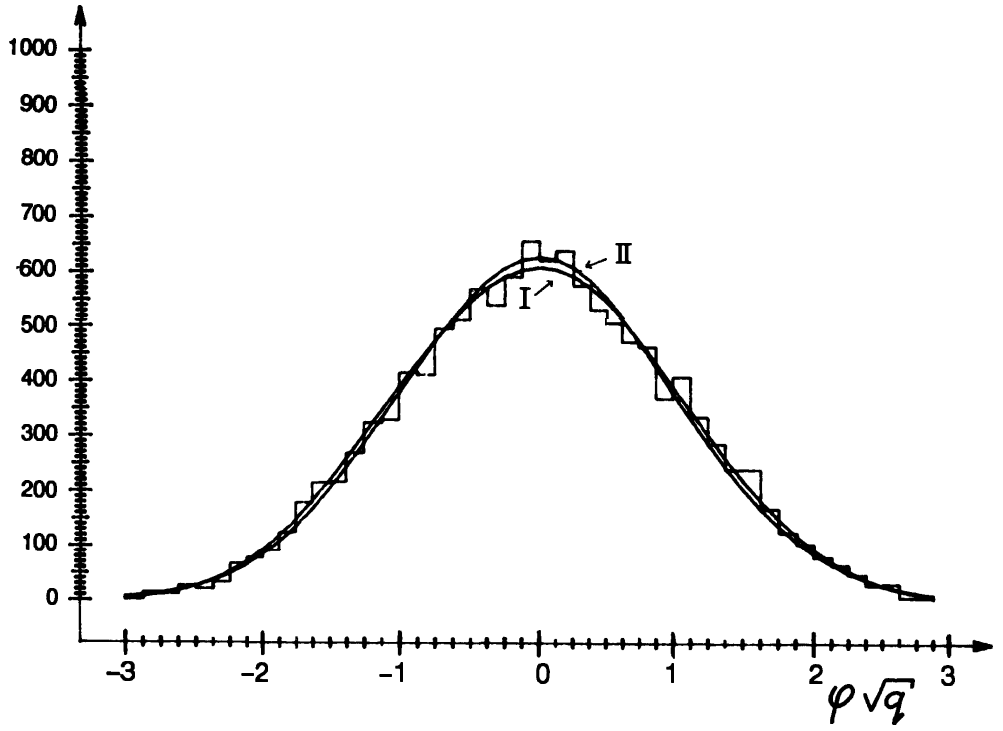

Fig. 23. Histogram (arbitrary units) of fluctuations for ergodic eigenfunctions [78]: $q = 25$; $k = 20$; $K \approx 20$; $l \approx 130$; $\lambda \approx 5$; $\tilde{\lambda} \approx 0.90$; curve I shows the Gaussian fluctuations rejected by a χ^2-criterion ($\chi^2(38) = 98$, confidence level $< 10^{-6}$(!)); curve II shows the microcanonical fluctuations compatible with the numerical data ($\chi^2(38) = 56$, confidence level 0.03).

In particular, if q is small, the fluctuations differ from Gaussian expectations and, according to RMT, they have the form

$$p(\varphi) = \frac{\Gamma(q/2)}{\sqrt{\pi}\,\Gamma[(q-1)/2]}\left(1-\varphi^2\right)^{(q-3)/2}. \tag{8.17}$$

We call these *microcanonical fluctuations*. Figure 23 illustrates the difference. Even for $q = 25$, the difference is fairly small, and can be safely distinguished by χ^2 criterion only.

The detailed structure of the chaotic eigenfunctions is more complicated. In particular, they carry the signs of classical unstable periodic trajectories, which have been discovered by Heller [80] who called them "*scars*". He studied conservative models. In maps, we don't see any scars; we do not understand this. The scars don't contradict Shnirelman's theorem [71], because their integral contribution to $|\varphi|^2$ vanishes in the quasiclassical region.

9. Diffusive photoelectric effect in hydrogen

9.1. Classical ionization in Rydberg atoms

In this section we consider a more physical problem – the photoelectric effect in hydrogen, that is the excitation and ionization of a hydrogen atom in a given monochromatic electric field. What could be simpler? However, this problem, allegedly solved at the dawn of quantum mechanics, has recently attracted the attention of both theoreticians and experimentalists. Why?

The hydrogen atom was studied intensively at the beginning of quantum mechanics, where it played the role of the famous Kepler two-body problem in classical mechanics. In both cases, new fundamental physics emerged from surprisingly simple problems, later to explain a vast range of phenomena. One of the first, in quantum mechanics, was the photoelectric effect. As early as 1905, Einstein explained the surprising existence of a threshold frequency, rather than a threshold intensity, of the ionizing field. Now we know that this threshold is not absolute, and that multi-photon ionization is possible. However, the probability of the latter type of ionization is usually negligible unless the electric field strength is comparable with the atomic field strength. This is why the experimental results of Bayfield and Koch [82] in 1974 presented a surprising puzzle for both experimentalists (who thought they knew all about the photoelectric effect, at least, in hydrogen) as well as for theoreticians (who presumptuously believed that they possessed the complete theory of such simple processes).

The new feature of Bayfield and Koch's experiments was that they studied the ionization not from the ground state of the atom but from a very high energy state corresponding to the principal quantum number $n \approx 66$ (the so-called *Rydberg atom*). Accordingly, they used a low-frequency microwave field ($\omega/2\pi \approx 10$ GHz). However, to ionize the atom, as many as about 80 photons were required! Nevertheless, the ionization was very fast in spite of a rather moderate field strength $\varepsilon \sim 15\,\mathrm{V/cm}$.

In this section, we shall use atomic units $e = m = \hbar = 1$ where e and m are the electron's charge and mass. The frequency unit is $\omega_1/2\pi \approx 0.66 \times 10^{16}\,\mathrm{Hz}$, and the field unit is $\varepsilon_1 \approx 5.14 \times 10^9\,\mathrm{V/cm}$. In the ground state, the atomic units are of the order of the actual values of the physical quantities for the hydrogen atom. In a highly excited state, this is already not the case. To restore the physical meaning of the units, we need to rescale them as follows: $\omega \to \omega_0 = \omega n^3$, $\varepsilon \to \varepsilon_0 = \varepsilon n^4$, etc. It is already a (bad) tradition to denote rescaled quantities by a subscript zero because usually (but not always!) they describe the initial condition (then $n = n_0$).

The rescaled field in Bayfield and Koch's experiments was $\varepsilon_0 \sim 0.06$, quite small. Why, then, did the ionization proceed fairly quickly? The first guess – that there was a *diffusive excitation* (whatever the mechanism might be) – was put forward in ref. [83]. This implies a chain of transitions in both directions, that is absorption as well as re-emission of field quanta, instead of a direct multi-photon transition. One immediate conclusion from this picture is that the total number of quanta involved becomes incredibly big: of the order of $(n_0/2\omega_0)^2 \sim 6000$ (!), instead of $\sim n_0/2\omega_0 \sim 80$ in the direct transition.

The next step, which determined the direction of further studies, was the observation that for a quantum number as high as $n \sim 100$, the classical treatment of the problem seems to be appropriate. In ref. [84], the classical criterion for chaos was derived, and thus the diffusion conjecture was justified. Meanwhile, in ref. [97], numerical experiments on the classical model were reported to be in agreement with laboratory experiments [82], thus confirming the classical description.

The problem seemed to be settled. Following this early trend, we shall consider first the classical theory of excitation of Rydberg atoms [85]. The simplest such theory is the so-called one-dimensional model, which is specified by the Hamiltonian

$$H = \frac{p^2}{2} - \frac{1}{z} + \varepsilon z \cos\omega t = -\frac{1}{2n^2} + \varepsilon z(n,\theta)\cos\omega t, \tag{9.1}$$

where $z > 0$, and n and θ are the action-angle variables. There are two parameters in this model, the field frequency ω and the field strength ε, which are easily expressed in the rescaled form for some initial unperturbed state $n = n_0$. Then the rescaled frequency $\omega_0 = \omega n_0^3$ is the ratio of the field frequency ω to the Kepler frequency $\Omega(n) = \partial H_0/\partial n = 1/n^3$, where $H_0 = -1/2n^2$ is the unperturbed Hamiltonian. Similarly, the rescaled field $\varepsilon_0 = \varepsilon n_0^4$ is the ratio of the external field strength ε to the atomic field $\varepsilon_a \sim n^{-4}$, because the orbit size $z_a \sim n^2$ (energy $|E_0| = 1/2n_0^2 \sim z_a^{-1}$). We may call the rescaled atomic units the "classical atomic units" because the motion of model (9.1) is similar for all n_0 provided that ω_0 and ε_0 are both fixed.

Problem. Transform the Hamiltonian (9.1) to the rescaled variables.

For numerical experiments, we can and did use the Hamiltonian (9.1) in special variables to avoid a singularity at $z = 0$ [43]. The analytical study was performed initially with the same Hamiltonian [85]. Later, a much simpler approach was invented in ref. [86] (see also ref. [87]), namely,

a map over Kepler's period was constructed, as described in section 2 (see eqs. (2.6), (2.8), and (2.9)). We shall rewrite it here using the excitation energy $N_\omega = (E - E_0)/\omega$ (in the number of absorbed quanta) and field phase φ as canonically conjugate variables,

$$\bar{N}_\omega = N_\omega + k \sin \varphi, \qquad \bar{\varphi} = \varphi + 2\pi\omega \left(-2\omega \left(\bar{N}_\omega + \nu\right)\right)^{-3/2} \tag{9.2}$$

where $\nu = E_0/\omega$, and the perturbation parameter is given by the expression

$$k \approx 2.6 \frac{\varepsilon}{\omega^{5/3}} = 2.6 \frac{\varepsilon_0 n_0}{\omega_0^{5/3}}, \tag{9.3}$$

provided that $\omega_0 \gtrsim 1$ (see ref. [11]). The latter inequality defines the region of the so-called "high-frequency" field which is the most interesting region, as we shall see.

In spite of the dependence $k(n_0)$, the classical motion of the model (9.2) is similar of all n_0, which is immediately clear upon rescaling $N_\omega \to N_\omega/n_0 = (1 - E/E_0)/2\omega_0$. In the corresponding standard map, the second parameter is

$$T = 6\pi\omega^2 \left(-2\omega \left(N_\omega + \nu\right)\right)^{-5/2} = 6\pi\omega^2 n_0^5 = 6\pi\omega_0^2/n_0. \tag{9.4}$$

The border of classical global chaos (see section 2) corresponds to $K = kT = K_c \approx 1$, or

$$\varepsilon_0^{cl} \approx \frac{1}{50\omega_0^{1/3}}, \qquad \varepsilon^{cl} \approx \frac{1}{50\omega^{1/3} n^5}. \tag{9.5}$$

Notice the rapid decrease in ε^{cl} with n. For a low-frequency field ($\omega_0 \lesssim 1$), this simple estimate doesn't hold because the parameter k decreases with ω_0 (ref. [11]), which would increase the critical ε_0^{cl},

$$\varepsilon_0^{cl} \approx \frac{1}{50\omega_0^{4/3}}. \tag{9.6}$$

The latter estimate approximately describes experimental data (both laboratory and numerical) [88] down to $\omega_0 \approx 0.25$, when the static field border $\varepsilon_0^s = 0.13$ is reached. The whole classical chaos border curve $\varepsilon_0^{cl}(\omega_0)$ is outlined in fig. 24.

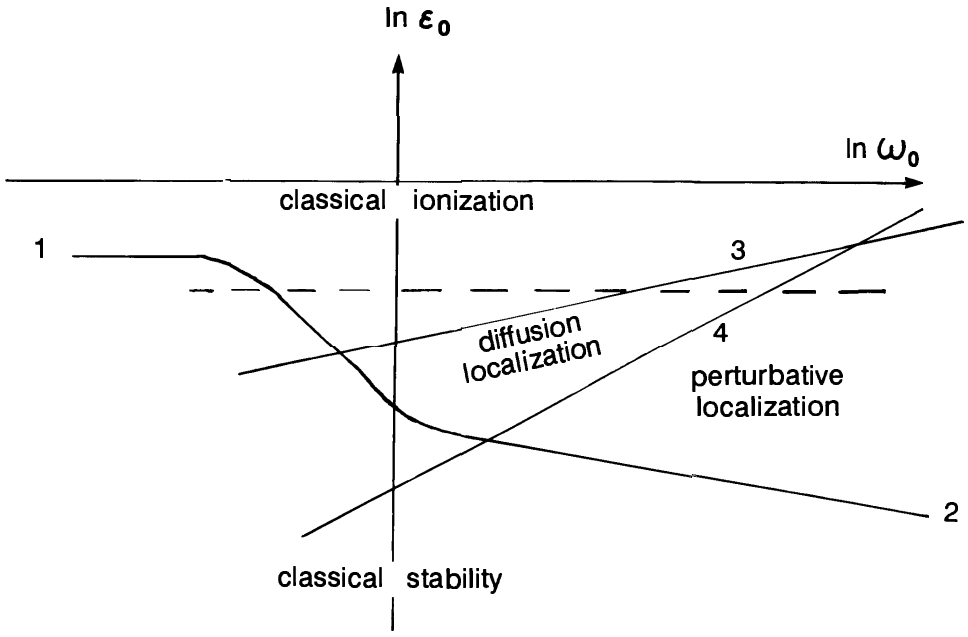

Fig. 24. Various borders related to the diffusive photoelectric effect in Rydberg atoms: (1) the static field border $\varepsilon_0 = 0.13$; (2) the classical chaos border, eqs. (9.5) and (9.6); (3) the quantum delocalization border, eq. (9.17); (4) Shuryak's border, eq. (9.19). The dashed line corresponds to the dependence shown in fig. 27.

Above the chaos border, the diffusion in N_ω proceeds at the mean rate

$$\bar{D} \approx \frac{k^2}{2} \approx 3.3 \frac{\varepsilon_0^2 n_0^2}{\omega_0^{10/3}} = 3.3 \frac{\varepsilon^2}{\omega^{10/3}}. \tag{9.7}$$

We can neglect here the rapid oscillations in D due to the correlation factor $C(K)$ (see eq. (2.22) and fig. 8) because of the strong dependence of T on n_0 (eq. (9.4)), and set $\bar{C}(K) \approx 1$. The mean rate does not depend on n, which is the advantage of using the variables (N_ω, φ). In the unperturbed action-angle variables (n, θ), the rate (per field period)[85],

$$D_n \equiv \frac{\langle (\Delta n)^2 \rangle}{\omega t / 2\pi} \approx 3.3 \frac{\varepsilon^2 n^3}{\omega^{7/3}}, \tag{9.8}$$

strongly depends on n, which complicates the theoretical analysis.

In order to ionize an atom, about $|\nu| = |E_0| / \omega$ photons are required, and the ionization time is

$$\tau_D \sim \frac{\nu^2}{\bar{D}} \sim \frac{\omega_0^{4/3}}{\varepsilon_0^2}, \quad t_D = \tau_D n_0^3, \tag{9.9}$$

(in Kepler's periods, and in physical time t). A peculiar feature of diffusive ionization is that the rate $\gamma_D \sim t_D^{-1}$ is proportional to ε_0^2, as it is for a

direct one-photon transition, where actually as many as $\sim \nu^2 \gg 1$ such transitions occur. On the other hand, diffusive ionization lags compared with immediate direct transitions.

Problem. Estimate the initial growth of the ionization probability.

The diffusion approximation for the excitation is valid if the resonance width $4\sqrt{k/T}$ (see eq. (2.11)) is small compared with the distance $|\nu|$ to the ionization border, or if

$$\frac{16k}{T\nu^2} \approx \frac{9\varepsilon_0}{\omega_0^{5/3}} \approx \frac{3k}{n_0} \approx \frac{K}{5\omega_0^2} \ll 1. \tag{9.10}$$

This is compatible with chaotic ionization ($K \gtrsim 1$) for $\omega_0 \gtrsim \sqrt{K/5}$.

In real laboratory experiments, the ionization threshold, or *cut-off* may be much lower, at some $n = n_c$ [94]. Then, on the right-hand side of inequality (9.10), a small factor $\eta^2 = \left(1 - n_0^2/n_c^2\right)^2$ appears, and the opposite inequality is compatible with $\omega_0 \gtrsim 1$, if $\eta^2 \lesssim K/5$, even for $K \lesssim 1$. In the latter case, a fast, though partial, ionization occurs during one period of the phase oscillation $\tau_r \sim K^{-1/2} \gtrsim 1$.

Still faster ionization (in one Kepler period, but also partial) occurs if $k > \eta|\nu|$, or if

$$\frac{k}{|\nu|} \approx \frac{5\varepsilon_0}{\omega_0^{2/3}} \approx \frac{K}{10\omega_0} \gtrsim \eta. \tag{9.11}$$

The one-dimensional model was challenged in ref. [90], where the motion was theoretically shown to be unstable unless an additional, sufficiently strong, static field was applied. This would deprive the model of any physical significance and convert it into something of only theoretical interest. Fortunately, the one-dimensional model was later rehabilitated in ref. [91], at least in the chaotic region where this instability turned out to be very slow, with the characteristic rise-time $\tau_u \sim (n_0/k)^2$. This time is longer than the ionization time (9.9),

$$\frac{\tau_u}{\tau_D} \sim \frac{n_0^2}{\nu^2} \sim \omega_0^2 \gtrsim 1. \tag{9.12}$$

Hence, the instability is unimportant if the initial state is approximately one-dimensional, when it is also called the *extended state*.

A particularly simple version of the one-dimensional model the Kepler map, (9.2) – faces another difficulty: it describes the motion in a non-uniform time (number of Kepler's periods) with respect to the continuous physical time t. This problem has already been discussed in sections 2 and 3. In numerical experiments with the classical Kepler map, one can record continuous time t for each trajectory, to obtain the distribution function at a given t. In the diffusion approximation, the general answer for a steady-state distribution can be derived from the Fokker–Planck–Kolmogorov (FPK) equation (see, e.g., ref. [6]),

$$\frac{\partial f}{\partial t} = \frac{1}{2}\frac{\partial^2}{\partial J^2} D_J f - \frac{\partial}{\partial J} B_J f, \tag{9.13}$$

where the diffusion rate and the drift in the action variable J are defined as

$$D_J = \frac{\langle (\Delta J)^2 \rangle}{t}, \qquad B_J = \frac{\langle \Delta J \rangle}{t} \ . \tag{9.14}$$

If we change only the time variable ($t \to \bar{t}(t, J)$), both D_J and B_J are multiplied by $\partial t/\partial \bar{t} \equiv \lambda(J)$, which is equivalent to a change of phase density: $f_s(J, \bar{t}) = f_s(J, t)/\lambda(J)$. Unfortunately, this simple rule doesn't hold if $\partial f/\partial t \neq 0$.

9.2. Quantum suppression of diffusive excitation

As I have already mentioned, the first studies of ionization in Rydberg atoms – experimental, theoretical, and numerical – confirmed the simple classical picture. Everybody seemed to be satisfied, except our group. We knew well, from our "exercises" with the standard map, that in any one-dimensional system there must be quantum localization under some conditions. So, we looked carefully for localization in the photoelectric effect, and eventually we found it!

First, we noticed that the classical picture had actually been checked only for low-frequency fields ($\omega_0 \lesssim 1$), where no simple theory exists. For both reasons, we concentrated our efforts on the high-frequency region $\omega_0 \gtrsim 1$.

The technique of numerical experiments with the quantized model (9.1) is straightforward in the discrete part of the spectrum [43]. The continuum can only be partially included using the so-called Sturmian basis. There was a lot of discussion concerning the importance of including the continuum. Our impression is that the inclusion is certainly not crucial, particularly because the "ionization border" corresponds to some finite $n = n_c$, as I have already mentioned.

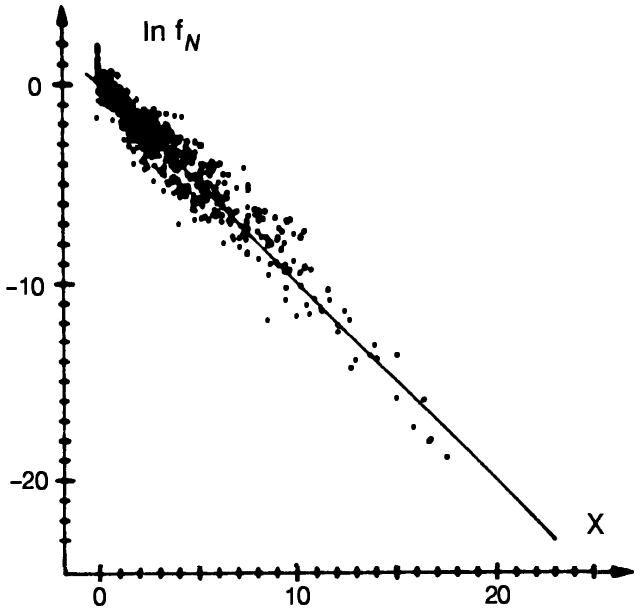

Fig. 25. Dependence of the normalized distribution function $f_N = \bar{f}_N(N_\omega)/\bar{f}(0)$ on $X = 2N_\omega/l_s$ for 41 cases with various ε_0, ω_0 and n_0. The straight line describes $\ln f_N = -X$ (after ref. [86]).

From the theoretical point of view, using the standard map with the parameters (9.3) and (9.4) as a local approximation for the Kepler map (9.2) immediately implies the universal localization of length (see eq. (9.7)) [86]

$$l_s \approx \bar{D} \approx 3.3\frac{\varepsilon^2}{\omega^{10/3}} = 3.3\frac{\varepsilon_0^2 n_0^2}{\omega_0^{10/3}}. \tag{9.15}$$

The difficulty is that the map's parameter T strongly depends on n (9.4), so the local description rapidly changes. On the other hand, the localization length depends only on the parameter $k = \text{const.}$ (eq. (9.15)). Anyway, the numerical experiments in refs. [11,86] confirmed not only the localization but also its length and exponential shape (fig. 25). Two examples of the full distribution function are shown in fig. 26. A chain of one-photon transitions is clearly seen with distribution peaks becoming more and more narrow as n (or E) increases. We shall call each peak a *photonic state*. In the full description $\psi(n)$, the Kepler map's probability $|\psi(N_\omega)|^2$ corresponds to the probability in the interval $N_\omega \pm 1/2$.

Above the last photonic-state peak, the excitation $\psi(n) \to 0$ as $n \to \infty$. Some researchers call it localization in the discrete spectrum. This terminology is possible, but what is important is that this "localization" does not prevent ionization because of the possibility of direct transition from this last peak to the continuum.

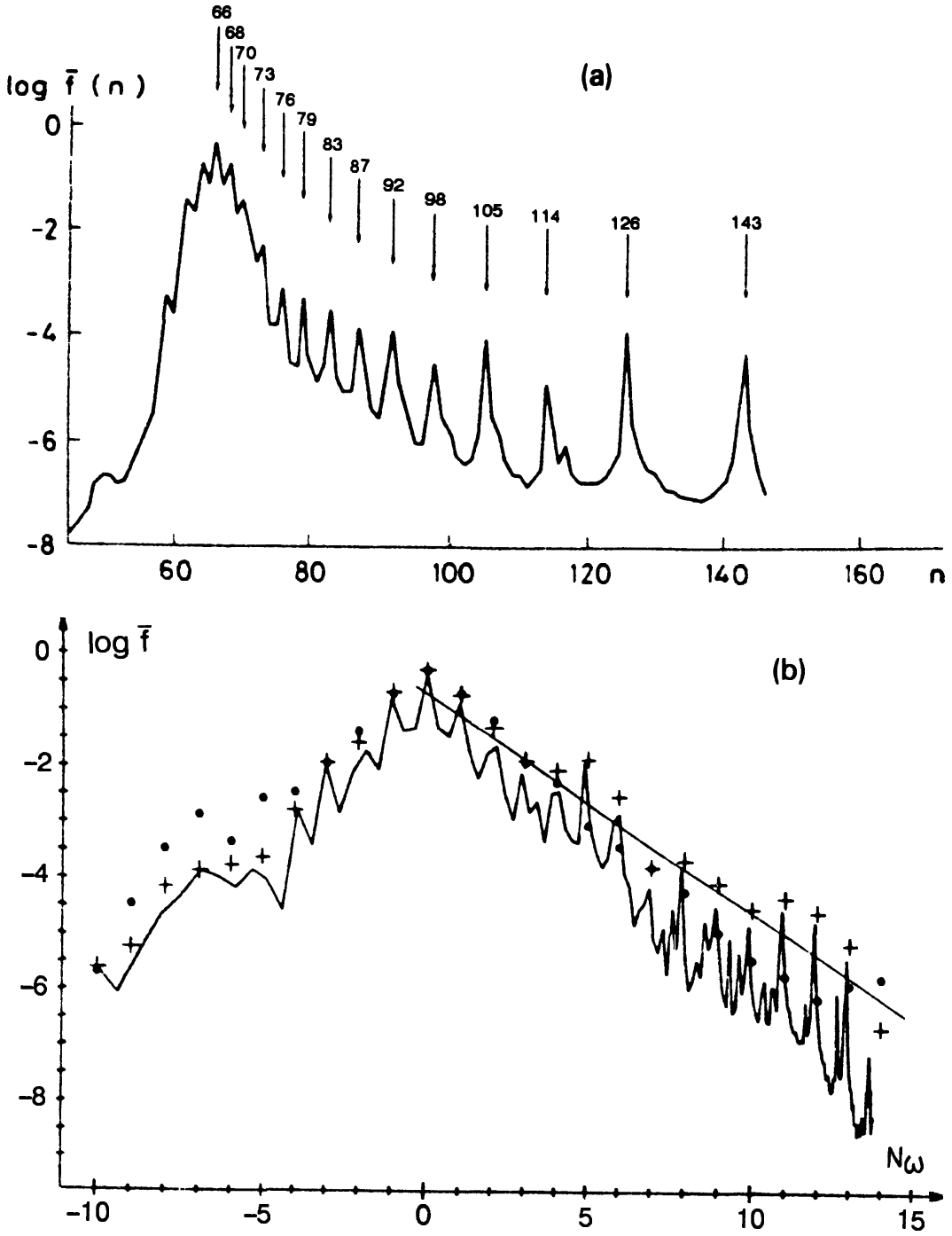

Fig. 26. Examples of steady-state distributions in n (a) [43], and in N_ω (b) [86]; the wiggly curves show the probability distribution for each n (from Schrödinger's equation), while the crosses give the integral probability in the intervals $N_\omega \pm \frac{1}{2}$; the points are for the quantized Kepler map; $k \approx 1.7$; $l_s \approx 1.4$; $T \approx 1.7$ (b). The logarithm is base 10.

The rather wide scattering of points in fig. 25, as well as the difference between the two descriptions in fig. 26b, are apparently related to the following factors. First, we express l_s via the mean diffusion rate $\bar{D}$ (eq. (9.15)), whereas the local rate changes with T (eq. (9.4)). Second, the proper quasiclassical parameters are not n and other unperturbed quantum numbers but, rather, the map's parameters k and $1/T$ (cf. section 3), which

are actually not at all large. The latter point was especially emphasized in ref. [51]. Finally (so far!), the Kepler-map description, being very simple, is incomplete and makes use of non-uniform time as I discussed above.

To estimate the importance of the latter factor we may apply, as a preliminary crude approximation, the classical diffusion equation, which includes the drift (section 8). As I have shown, the steady-state distribution $f_s(t)$ at fixed t is related to $f_s(\tau)$ at fixed τ by,

$$f_s(t) \sim \frac{f_s(\tau)}{\Omega(N_\omega)} \sim f_s(\tau)(1 - N_\omega/|\nu|)^{-3/2}. \tag{9.16}$$

Some increase in the distribution near the continuum ($N_\omega \to |\nu|$) is apparent in fig. 26b ($|\nu| \approx 17$).

Because there is a finite number of photonic states $|\nu| = n_0/2\omega_0$ (which can be as low as $|\nu|\eta$, due to a possible cut-off at $n = n_c$), the ionization rate depends crucially on the ratio $l_s/|\nu|\eta \approx 1$. The latter equality determines a quantum border of fast ionization [11],

$$\varepsilon_0^q \approx \omega_0^{7/6}\sqrt{\frac{\eta}{6.7n_0}}. \tag{9.17}$$

This is not a very sharp border, of course. Ionization occurs at any $l_s/|\nu|\eta$, but its rate exponentially drops with $|\nu|\eta/l_s \gtrsim 1$. If $|\nu|\eta/l_s \lesssim 1$, the ionization is roughly classical. In this case, we often speak of delocalization, hence, the term *delocalization border* for eq. (9.17).

Above this border, the diffusion is roughly classical but it is dynamically stable as it is in the standard map (section 5). In particular, the time (velocity) reversal brings the atom back to the initial state with high accuracy [89]. An interesting peculiarity of "antidiffusion" in atoms is that it comprises not only a discrete spectrum but also a continuum, a sort of coherent recombination.

Estimate (9.17) coincides with our earlier result [43], which was obtained in a continuous model (9.1), but which seemed to indicate a sharp transition from localization to classical diffusion. This distinction is not yet completely clear.

The border (9.17) is also outlined in fig. 24 for some n_0 and η. Unlike the classical chaos border (9.5), the quantum border decreases with $1/n_0$ (for fixed ε_0 and ω_0), in accordance with the correspondence principle. At this point, I should explain that the quasiclassical transition must be performed under given classical conditions, that is for $\varepsilon_0, \omega_0 = \text{const}$. Lifting these conditions may lead to an apparent contradiction with the correspondence

principle. For example, the ratio of the quantum to classical ε_0 border values (see eqs. (9.17) and (9.5)) is,

$$\frac{\varepsilon_0^{\rm q}}{\varepsilon_0^{\rm cl}} \approx 19\,\sqrt{\eta}\frac{\omega_0^{3/2}}{\sqrt{n_0}} = 19\,\sqrt{\eta}\,\omega^{3/2}n_0^4. \tag{9.18}$$

If we were to fix ω (instead of ω_0) the difference between the quantum and classical behaviour would grow with n_0!

The two borders (2 and 3 in fig. 24) cross at $\omega_0^{(23)} \approx 0.14\,(n_0/\eta)^{1/3}$, which exceeds unity for $n_0 \gtrsim 360\eta$. At smaller n_0, eq. (9.6) should be used instead of eq. (9.5), which gives, $\omega_0^{(23)} \approx 0.3\,(n_0/\eta)^{1/5}$.

Finally, the border of quantum stability, or Shuryak's border $k \sim 1$ (section 4), is given by,

$$\varepsilon_0^{\rm Sh} \sim 0.4\omega_0^{5/3}/n_0. \tag{9.19}$$

It grows faster with ω_0 than the delocalization border (9.17) and crosses the latter at

$$\omega_0^{(34)} \sim \eta n_0, \tag{9.20}$$

which is quite large unless η is very small. Shuryak's border crosses the classical chaos border at

$$\omega_0^{(24)} \sim \sqrt{\frac{n_0}{20}}. \tag{9.21}$$

The whole picture in fig. 24, although it lacks many details, looks rather complicated. That's typical of any real problem in this area, even the simplest one!

Another interesting feature of the diffusive photoelectric effect is its remarkably high rate, in spite of the multi-photon character of this process. It is instructive to compare the diffusive photoelectric effect with ordinary one-photon ionization [43]. The maximal rate of the ordinary process at the threshold $\omega_0 = \eta n_0/2$ is,

$$\gamma_{\rm ph}^{\rm max} \approx \frac{3\varepsilon_0^2}{(\eta n_0)^{13/3}}. \tag{9.22}$$

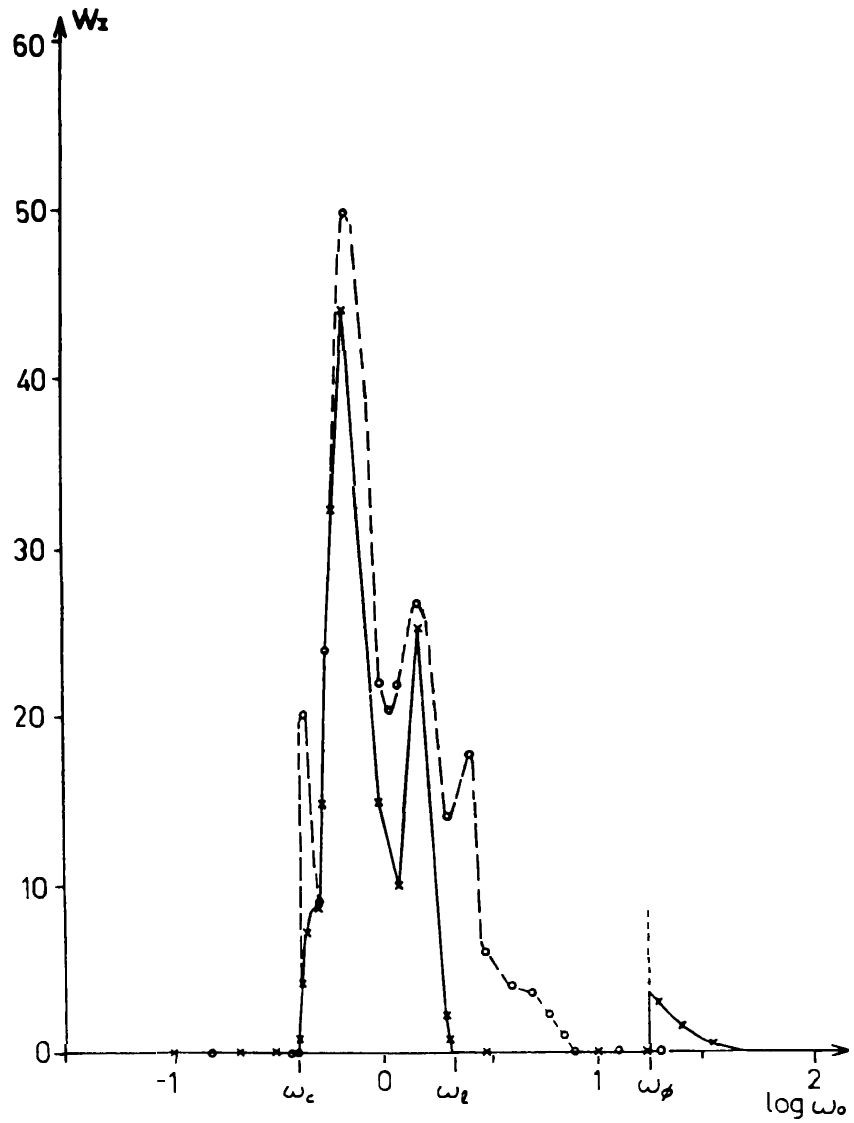

Fig. 27. Ionization probability (per cent) versus the scaled frequency (numerical experiments in ref. [43]): $n_0 = 66$; $\varepsilon_0 = 0.05$; $n_c = 99$; $\eta = 0.56$; the solid line is for Schrödinger's equation; the dashed line describes the classical model; the logarithm is base 10.

On the other hand, diffusive ionization has its maximal rate (see eq. (9.9)) $\gamma_D^{max} \sim \varepsilon_0^2/n_0^3$ at around $\omega_0 \sim 1$, where the critical field strength ε_0 is minimal (see fig. 24). This corresponds approximately to the main classical resonance, $\omega_0 = 1$. However, it does not directly explain the fast excitation because the resonance is nonlinear. Hence, we need to assume the overlap of many resonances, which results in diffusive, rather than monotonic, excitation. The ratio of diffusive to one-photon ionization rates at different (optimal) frequencies is equal to

$$\frac{\gamma_D^{max}}{\gamma_{ph}^{max}} \sim \eta^{13/3} n_0^{4/3}. \tag{9.23}$$

Typically, diffusive ionization is the faster process unless the cut-off param-

eter $\eta = 1 - n_0^2/n_c^2$ is small. This is illustrated in fig. 27, where the dependence of the ionization probability on the scaled frequency is presented for fixed ε_0 and fixed interaction time t_{in}. The dependence corresponds to the dashed line in fig. 24. The ionization occurs only within some window between the classical chaos border $\omega_0 = \omega_c$ on the left and the quantum delocalization border $\omega_0 = \omega_l$ on the right. Classical ionization persists for larger ω_0 as well, although with a decreasing rate (see eq. (9.9)). The small peak on the right corresponds to one-photon ionization.

9.3. Two freedoms in the atom and two frequencies in the field

Now I shall briefly review some results obtained with other models of the photoelectric effect in hydrogen. Consider first a more realistic model involving two freedoms [91]. In the classical case, the one-dimensional motion is unstable, as I've already mentioned, but if the motion is chaotic, which is of primary interest to us, the instability is negligibly weak (the rise time is long). In the quantum case, our first prediction [43] was that there should be a considerable decrease of the value of the localization border, following the general estimates discussed in section 6. However, numerical experiments [91] refuted this prediction: the localization in n did not change, while the motion in n_2 (a parabolic quantum number related to the second freedom) showed no sign of localization. The theory of the diffusive photoelectric effect in the two-freedoms model was presented in ref. [91], using a four-dimensional map that was a generalization of the Kepler map. Notice that in the linearly polarized electric field, the magnetic quantum number is an exact integral of the motion, so that the system can always be reduced to two freedoms.

According to the theory in ref. [91], a monotonic increase in n_2 is explained by the classical instability in this freedom. However, the corresponding spectrum width $\gamma_2 \sim \tau_u^{-1} \sim (k/n_0)^2$ (see above) is too narrow (because the instability is too weak) to overlap the discrete spectrum of the N_ω-motion. Indeed, the density of the latter is $\varrho \sim l_s$, and

$$\varrho\gamma_2 \sim \left(\frac{\varepsilon_0}{\varepsilon_0^q}\right)^4 \frac{\eta^2}{30\omega_0^2} \ll 1, \tag{9.24}$$

is always very small below the one-dimensional delocalization border ε_0^q (9.17). Another qualitative explanation is that slow n_2-motion acts as an adiabatic perturbation, which cannot produce any additional transitions. The origin of this adiabaticity is the Coulomb degeneracy.

Instead of the second freedom, we may add to the one-dimensional model a second incommensurate frequency: $\omega \to \omega_1, \omega_2$, so that the ratio ω_1/ω_2 is

irrational. The quasiperiodic perturbation in the standard map was studied in ref. [35] (see also ref. [92]).

The quasiperiodic photoelectric effect was considered recently by Shepelyansky [93] using the following generalization of the Kepler map,

$$\begin{aligned} &\bar{N}_1 = N_1 + k_1 \sin\varphi_1, \qquad \bar{N}_2 = N_2 + k_2 \sin\varphi_2, \\ &\bar{\varphi}_1 = \varphi_1 + 2\pi\omega_1 \left(-2\bar{E}\right)^{-3/2}, \qquad \bar{\varphi}_2 = \varphi_2 + 2\pi\omega_2 \left(-2\bar{E}\right)^{-3/2}, \\ &\bar{E} = E_0 + \omega_1 \bar{N}_1 + \omega_2 \bar{N}_2. \end{aligned} \tag{9.25}$$

This map describes two chains of transitions coupled via the electron's energy E. For incommensurate frequencies, the photonic states do not overlap, and we have a two-dimensional situation with the delocalization condition $D_1 D_2 \gtrsim 1$, or $k_1 k_2 \gtrsim 2$. As was discussed in section 6, this actually reduces to Shuryak's condition for the minimal value

$$k_{\min} \gtrsim 1. \tag{9.26}$$

Otherwise, the excitation remains essentially one-dimensional.

9.4. First laboratory observations of quantum chaos in hydrogen

We spent a lot of time trying to persuade experimentalists to raise the field frequency to $\omega_0 \gtrsim 1$ and hence to try to observe quantum localization, a characteristic feature of quantum pseudo-chaos. Somehow, we finally succeeded, and the first observations recently emerged [94,95] from two experimental groups led by Koch and by Bayfield, now working separately. In fig. 28, an example of the quantum suppression of the diffusive photoelectric effect is shown [94]. Although it is not large, the deviation of the experimental (quantal!) 10% ionization border from the classical model is clearly seen and it grows with ω_0. The field frequency ω was actually fixed, so the difference between the classical and quantal behaviour increases here with the quantum number n_0. However, there is no contradiction here, as I have explained.

Several rather different explanations of the observed phenomenon were reviewed in section 7. In a recent paper [96], Meiss (but not his co-author MacKay!) insists that their theory [54] provides the best agreement with the experimental data. In my opinion, there is some confusion here because the border curve $\varepsilon_0(\omega_0)$ depends on the ionization level (10%), on the interaction time, on the cut-off parameter η, and possibly on other details of the process. None was included in any of the competing theories. For example, our theory is stated in ref. [96] to give values that are too large

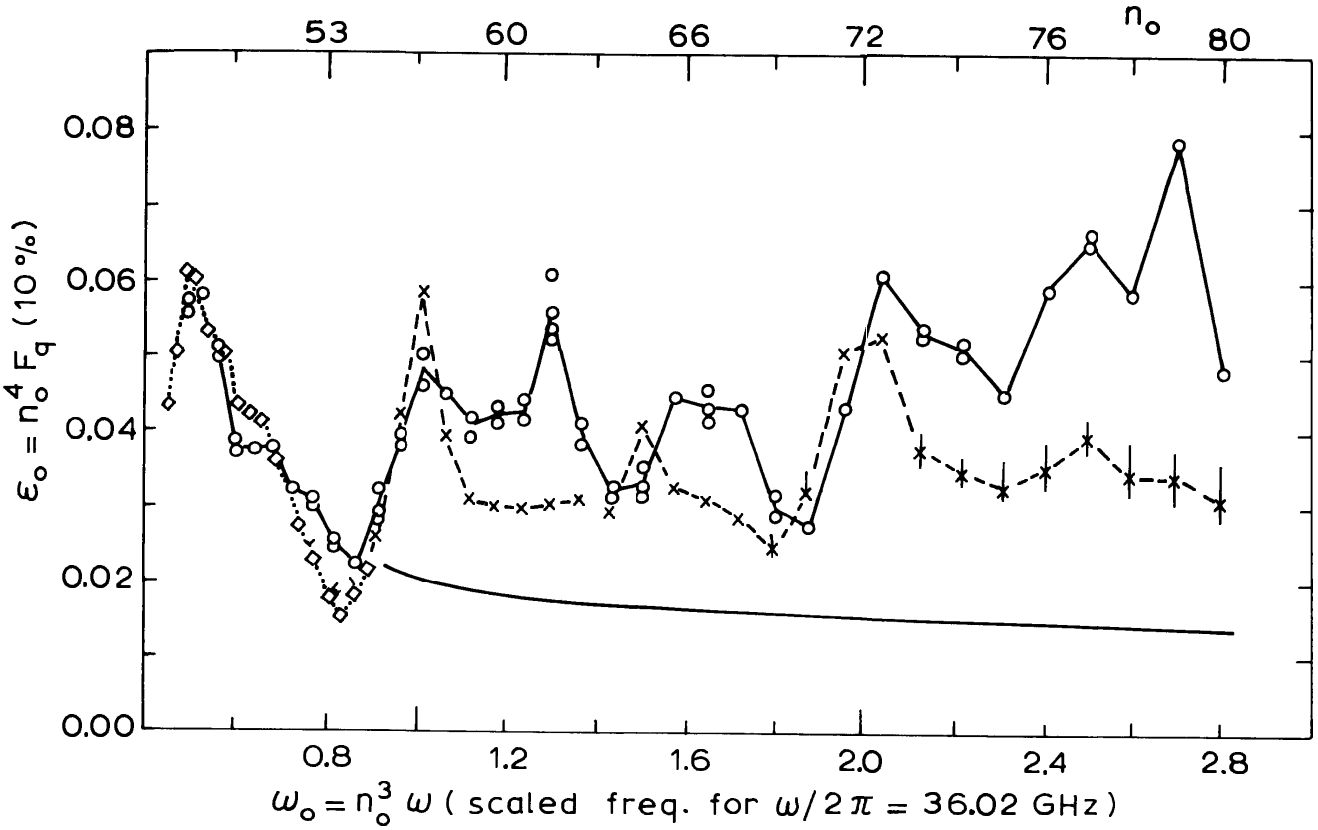

Fig. 28. Ionization threshold ε_0 (10%) versus the scaled frequency ω_0 [94]: cut-off $n_c \approx 90$; the interaction time is about 10^{-8} s (360 field periods); the upper scale indicates the initial value n_0; experimental data are shown by open circles (o) and connected by a solid line; dashed and dotted lines with symbols ×, ◇ and error bars represent numerical simulations with classical models; the lower curve is the classical chaos border $K \approx 1$ (eq. (9.5)).

by a factor of 2. Yet, if a rather small value of $\eta = 1 - n_0^2/n_c^2$ ($n_c \approx 90$) is used (eq. (9.17)) the agreement with experiment becomes excellent for this particular case (fig. 28). But in the second case in ref. [94], with a higher cut-off $n_c \approx 180$, the difference is already about 50% . In theoretical terms, one could hardly expect better agreement. Another important detail in fig. 28 is that the classical ionization border considerably exceeds the chaos border. Why? Apparently, this is because diffusive ionization requires a finite time (eq. (9.9)): $\omega t_D/2\pi \sim \eta^2 \omega_0^{7/3}/\varepsilon_0^2 \sim 300$ field periods. The latter value, close to the interaction time, is given for $\varepsilon_0 = 0.03$, which is roughly constant away from the integer resonances $\omega_0 = 1$ and 2.

In experimental (quantal) data, the classical resonance structure was also observed and emphasized in ref. [94]. This is because the classical stability parameter $K \approx 50\varepsilon_0\omega_0^{1/3} \lesssim 4$ is relatively small for the data in fig. 28, so that for integer resonances at least, there exist domains of stable classical motion that impede ionization.

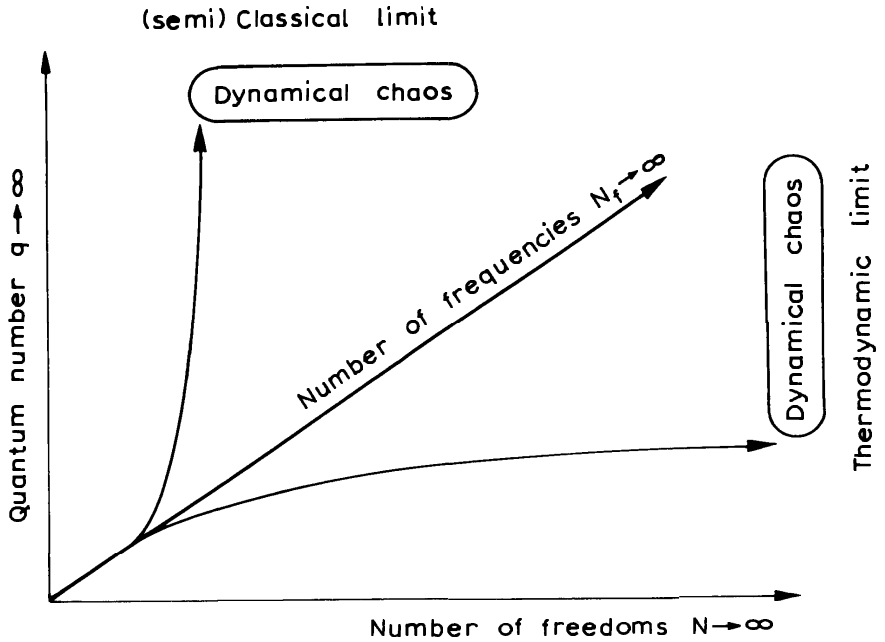

Fig. 29. A sketch of quantum pseudochaos with (semi)-classical and thermodynamic limits, where true dynamical chaos is reached.

10. Conclusion: questions, problems, conjectures ...

The study of quantum chaos is still only beginning. Yet, a lot of work has already been done. The main result? The absence of chaos! In quantum mechanics there is no true chaos, but only pseudochaos – *some* chaos, as much as it is compatible with a discrete spectrum.

From the viewpoint of fundamental physics, true classical chaos is but an illusion – a scientific abstraction, if you like – which exists nowhere but is very useful from a conceptual point of view. Classical chaos is the ideal model, a pattern, to compare with real quantum pseudochaos.

Pseudochaos exists in a "fictitious" classical world as well, where it is a part of the limit opposite to true chaos. The crucial point is what is the set of frequencies determining the time evolution of a dynamical system. This basic idea is illustrated in the simple scheme presented in fig. 29.

There are two ways to increase the number of frequencies and, thus, to achieve a complicated, irregular, and even "pseudorandom" evolution. The first way is to increase the number of freedoms, which obviously leads to chaos! The limit $N \to \infty$ is well known in statistical mechanics and is usually called the *thermodynamic limit*. This is the *traditional* mechanism for obtaining statistical laws in both classical and quantum mechanics, and it has nothing to do with the new ideas on dynamical chaos.

The second way is to increase the values of a quantum number or, rather, to increase some characteristic quasiclassical parameter, say q, for any num-

ber of freedoms, including very small numbers. This is the brand-new quantum pseudochaos, now under mass attack by many researchers. In the classical limit $q \to \infty$, a new quality – dynamical chaos – may or may not be born, depending on the particular dynamics of the system. As I have already mentioned, the semiclassical limit is sufficient for dynamical chaos. I understand the semiclassical limit as the classical limit even in a single freedom.

In the thermodynamic limit, true dynamical chaos is also possible under some conditions related to the dynamics of a system. The crucial point is that infinitely many freedoms have to be operative ("active"), and not just present in the system.

At first glance, it might seem that the thermodynamic limit is more formal than the classical limit to which we are very much more accustomed. On the one hand, the world appears to be quantal, and on the other hand, the fields, which do not enter our simplified theory, each have infinitely many freedoms. In the theory of quantum chaos, the main problem is the finiteness of N and q and (sometimes) of t as well. This problem is much more difficult than the limiting cases.

This is similar to some problems in computer mathematics: continuous differential equations in real (irrational) quantities are much simpler to analyze than difference equations in integers (rationals). In section 7, I mentioned the classical discrete model of quantum dynamics. Unfortunately, the model in its present form is either too complicated or too crude an approximation. The dream of numerical experimentalists is to invent a way of direct quantum simulation, making use not of very complicated and time-consuming partial differential equations but of the very defect of the digital computer – the rounding errors – that is of computer discreteness, or "quantization". That would indeed be a great break-through!

Another global problem is that we actually need chaos to explain the world around us. This was especially emphasized by Ford in relation to the problem of quantum chaos (see, e.g., his popular article in ref. [98]). Obviously, there are universal statistical laws, so that any real dynamical system is always at least partly statistical, in the sense that some noise and dissipation is always present. What is much more fundamental and important is the very structure of the dynamics.

Strange as it may seem, the causality principle in physics, which appears as something opposite to statistical indeterminacy, is actually closely related, I believe, to the same statistical independence from the past. Indeed, the causality principle requires a definite time ordering between a cause and its effect; this is of course confirmed in a wide range of experiments. However, the principle itself stands alone, separated from the rest

of modern physics. My conjecture is that this principle is a subtle corollary of chaos. The reason is that only chaos can decorrelate events and, thus, justify the very conception of a cause which is independent of the past. The problem here is to analyze the noncausal/causal transition in parallel with the order/chaos transition.

This problem already arises in the classical limit. In quantum mechanics, it becomes even more severe as we can no longer avoid the quantum measurement problem. A cause is an event which is realized as the outcome of some measurement. Otherwise, only virtual possibilities would exist, and their number would rapidly increase due to any interaction within the system. A quantum measurement sharply breaks the connections with the past to create a definite initial condition for the future evolution of the system. This is also a typical statistical process. What is its origin? Apparently, in some chaotic interaction with the measurement device. Indeed, the device is, by definition, a classical system, so, it admits chaos. Moreover, the device has to be very unstable to amplify microinteractions, so it is actually inclined to be chaotic. Now, what is the actual role of the observer, so important in the Copenhagen interpretation of quantum mechanics?

I should like to put forward the following conjecture. Before the measurement, the quantum probability is qualitatively different from that in classical mechanics because of the interference of various states in an overall superposition state. So, for a pure state, the quantum probability has nothing to do with incomplete knowledge of the system. On the contrary, it is complete or, at least, the maximum possible. But in the course of any chaotic process, including measurement, the coherence of a pure state is lost, the state becomes a mixture, the interference vanishes, and the quantum probability resumes its usual meaning of incomplete knowledge. At this stage, the role of the observer in quantum mechanics is as natural as it is in classical mechanics: to convert incomplete knowledge into complete knowledge.

True, the mixture appears each time we consider a part of the system after any interaction (not necessarily chaotic) with another part of the system. But in this case the pure quantum state can be recovered by including the rest of the system. A principal distinction of the measurement is that one part of the whole system – the measuring apparatus – is so complicated that it cannot be described in terms of quantum mechanics. In this sense, the collapse of the system's ψ-function after the measurement is, in fact, the result of the absence of any superposition of states in the measuring device. The main problem here is to follow the transition from a purely quantum description to a semiclassical description of the measurement.

Another question, even more unclear, is the following. The chaotic interaction destroys quantum interference. However, to convert the quantum probability into a classical one it is a necessary but still not a sufficient condition. Somehow, the quantum probability must be redistributed between former superimposed states to provide a particular result of the measurement. Precisely this problem has been addressed recently by Percival [23]. In my opinion, a drawback of his approach is that he is trying to solve the problem for a measured quantum system that is relatively simple. I believe that one should, instead, pose this problem for a measuring device that is incomparably more complicated, and where the required redistribution of probabilities is much more likely to be found.

On the other hand, Percival's approach leads to a very interesting and delicate question if the wave collapse in any form is normally possible without a special measurement, the corresponding device, and the observer. The Copenhagen interpretation, rejecting that possibility, is perfectly suitable for the conventional man-made experiment with its routine "preparation" of the system and recording of the results. However, there is a different class of problems, those involving a natural free evolution. Of course, you may imagine an observer who is spying on the system, but in quantum mechanics this is not the same, because the measurement interaction cannot be neglected. If the natural evolution is of a statistical nature, then there seem to be no serious problems. However, in the case of a dynamical process related, for example, to the formation of new chemical or biological structures, the situation needs to be carefully analyzed. There is implicit confirmation of possible difficulties here in an old paper due to Wigner [99], who "proved" that quantum mechanics is incompatible with the reproduction of structures. Even though the proof seems to be erroneous, I believe that the problem remains.

Again the quantum chaos, which destroys interference, may help, but only partially. The mechanism for probability redistribution is needed!

The main purpose of these chaotic concluding remarks is to remind you again that many questions in this exciting field of research are still open and that many problems remain to be solved. Try your hand, and good luck!

Acknowledgements

I should like to express my sincere gratitude to the organizers of the Institute, Professor M.-J. Giannoni and Professor A. Voros, for kindly inviting my Siberian colleagues and myself to the Institute. Special thanks are

due to Dr. Graham Farmelo who carefully read the manuscript and made important suggestions and improvements.

References

[1] V.M. Alekseev and M.V. Yakobson, Phys. Rep. 75 (1981) 287.
[2] G. Chaitin, Adv. Appl. Math. 8 (1987) 119.
[3] F. Galton, Natural Inheritance (London, 1889).
[4] V. Arnold and A. Avez, Ergodic Problems of Classical Mechanics (Benjamin, 1968).
[5] I. Cornfeld, S. Fomin and Ya. Sinai, Ergodic Theory (Springer, 1982).
[6] A. Lichtenberg and M. Lieberman, Regular and Stochastic Motion (Springer, 1983).
[7] T. Bountis, B. Dorizzi, B. Grammaticos and A. Ramani, Physica A128 (1984) 268; S. Kowalevskaya, Acta. Math. 14 (1890) 81.
[8] M. Born, Z. Phys. 153 (1958) 372.
[9] T. Petrosky, Phys. Lett. A117 (1986) 328.
[10] B.V. Chirikov and V.V. Vecheslavov, Astron. Astrophys. 221 (1989) 146.
[11] G. Casati, I. Guarneri and D.L. Shepelyansky, IEEE Journ. Quantum Electronics 24 (1988) 1420.
[12] J. Greene, J. Math. Phys. 20 (1979) 1183.
[13] B.V. Chirikov, Phys. Rep. 52 (1979) 263.
[14] D. Umberger and J. Doyne Farmer, Phys. Rev. Lett. 55 (1985) 661.
[15] A. Rechester and R. White, Phys. Rev. Lett. 44 (1980) 1586; A. Rechester, M. Rosenbluth and R. White, Phys. Rev. A23 (1981) 2664.
[16] B.V. Chirikov, Reviews of Plasma Physics, Vol.13, ed., B.B. Kadomtsev (Consultants Bureau, New York, 1987) 1.
[17] B.V. Chirikov, D.L. Shepelyansky, Radiofizika 29 (1986) 1041.
[18] R. MacKay, J. Meiss and I. Percival, Physica D13 (1984) 55.
[19] C. Karney, Physica D 8 (1983) 360.
[20] B.V. Chirikov and D.L. Shepelyansky, Physica D 13 (1984) 395.
[21] C. Karney, A. Rechester and R. White, Physica D 4 (1982) 425.
[22] P. Davies and J. Brown, The ghost in the atom (Cambridge University Press, 1986).
[23] I. Percival, Diffusion of Quantum States (Queen Mary and Westfield College, Univ. London, 1989) preprints QMC-DYN 89/3 and 4.
[24] K. Lee, Physica D 35 (1989) 186.
[25] J. Leopold and R. Jensen, J. Phys. B22 (1989) 417.
[26] G. Casati, B.V. Chirikov, J. Ford and F.M. Izraelev, in: Stochastic Behavior in Classical and Quantum Hamiltonian Systems, Como, 1977, eds., G. Casati and J. Ford, Lecture Notes in Physics 93 (1979) 334 (Springer, 1979).
[27] D.L. Shepelyansky, Phys. Rev. Lett. 56 (1986) 677; R. Blümel, S. Fishman, M. Griniasti and U. Smilansky, in: Quantum Chaos and Statistical Nuclear Physics, Cuernavaca, 1986, eds., T.H. Seligman and H. Nishioka, Lecture Notes in Physics 263 (1986) 212 (Springer, 1986).
[28] F.M. Izrailev and D.L. Shepelyansky, Teor. Mat. Fiz. 43 (1980) 417.
[29] S. Fishman, D. Grempel and R. Prange, Phys. Rev. A29 (1984) 1639.

[30] E.V. Shuryak, Zh. Eksp. Teor. Fiz. 71 (1976) 2039 (Sov. Phys. JETP 44 (1976) 1070).
[31] G. Casati, I. Guarneri and D.L. Shepelyansky, Physica A 163 (1990) 205.
[32] D.L. Shepelyansky, Physica D 28 (1987) 103.
[33] G. Casati, J. Ford, I. Guarneri and F. Vivaldi, Phys. Rev. A34 (1986) 1413.
[34] B.V. Chirikov, Usp. Fiz. Nauk 139 (1983) 360.
[35] D.L. Shepelyansky, Physica D 8 (1983) 208.
[36] D.V. Chirikov, F.M. Izrailev and D.L. Shepelyansky, Physica D 33 (1988) 77.
[37] G.P. Berman and G.M. Zaslavsky, Physica A91 (1978) 450; G.M. Zaslavsky, Phys. Rep. 80 (1981) 157.
[38] B.V. Chirikov, F.M. Izrailev and D.L. Shepelyansky, Sov. Sci. Rev. C2 (1981) 209.
[39] M. Toda and K. Ikeda, Phys. Lett. A124 (1987) 165.
[40] G. Casati and I. Guarneri, Comm. Math. Phys. 95 (1984) 121.
[41] M. Hénon, C.R. Acad. Sci. Sér. A 262 (1966) 312.
[42] D.L. Shepelyansky, Phys. Rev. Lett. 57 (1986) 1815.
[43] G. Casati, B.V. Chirikov, I. Guarneri and D.L. Shepelyansky, Phys. Rep. 154 (1987) 77.
[44] V.M. Akulin and A.M. Dykhne, Zh. Eksp. Teor. Fiz. 94 (1988) 366 (Sov. Phys. JETP 67 (1988) 856).
[46] A.N. Kolmogorov, Math. Ann. 112 (1936) 155; 113 (1937) 766.
[47] E. Ott, T. Antonsen Jr. and J. Hanson, Phys. Rev. Lett. 53 (1984) 2187.
[48] B.V. Chirikov, Quantum limitations of classical dynamics in quasiclassical region, Proc. Int. Conf. Classical Dynamics in Atomic and Molecular Physics, Brioni, Yugoslavia, 1988 (World Scientific, 1989) p. 307.
[49] G.P. Berman and G.M. Zaslavsky, Physica A 111 (1982) 17.
[50] G.M. Zaslavsky, Chaos in Dynamical Systems (Harwood, New York, 1985).
[51] R. Jensen, S. Susskind and M. Sanders, Phys. Rev. Lett. 62 (1989) 1476.
[53] R. Brown and R. Wyatt, Phys. Rev. Lett. 57 (1986) 1; T. Geisel, G. Radons and J. Rubner, ibid, p. 2883.
[54] R. MacKay and J. Meiss, Phys. Rev. A37 (1988) 4702.
[55] G. Berman and A.R. Kolovsky, Physica D 17 (1985) 183.
[56] F. Rannou, Astron. Astrophys. 31 (1974) 289; C. Beck, Physica D 25 (1987) 173.
[57] P. Pechukas, J. Phys. Chem. 88 (1984) 4823.
[58] B. Eckhardt, Phys. Rep. 163 (1988) 205.
[59] T.A. Brody, J. Flores, J.B. French, P.A. Mello, A. Pandey and S.S.M. Wong, Rev. Mod. Phys. 53 (1981) 385.
[60] M. Berry and M. Tabor, Proc. R. Soc. London A356 (1977) 375.
[61] V.I. Tatarsky, Usp. Fiz. Nauk 139 (1983) 587 (Sov. Phys. Usp. 26 (1983) 311).
[62] F.M. Izrailev, Phys. Rev. Lett. 56 (1986) 541.
[63] S.A. Molchanov, Comm. Math. Phys. 78 (1981) 429.
[64] G. Casati, I. Guarneri and F.M. Izrailev, Phys. Lett. A124 (1987) 263.
[65] J. von Neumann and E. Wigner, Phys. Z. 30 (1929) 467.
[66] E. Wigner, SIAM Rev. 9 (1967) 1.
[67] O. Bohigas and M.-J. Giannoni, in: Mathematical and Computational Methods in Nuclear Physics, Granada, 1983, eds., J.S. Dehesa et al., Lecture Notes in Physics 209 (1984) 1 (Springer, 1984).
[68] F. Dyson, J. Math. Phys. 3 (1962) 1190.

[69] I. Percival, J. Phys. B6 (1973) L229.
[70] J. von Neumann, Z. Phys. 57 (1929) 30.
[71] A.I. Shnirelman, Usp. Mat. Nauk 29/6 (1974) 181.
[72] A. Voros, in: Stochastic Behavior in Classical and Quantum Hamiltonian Systems, Como, 1977, eds., G. Casati and J. Ford, Lecture Notes in Physics 93 (1979) 326 (Springer, 1979); M. Berry, J. Phys. A10 (1977) 2083.
[73] T. Brody, Lett. Nuovo Cimento 12 (1973) 482.
[74] F.M. Izrailev, Phys. Lett. A134 (1988) 13; J. Phys. A22 (1989) 865.
[75] G. Casati, I. Guarneri, F.M. Izrailev and R. Scharf, Phys. Rev. Lett. 64 (1990) 5.
[76] G.P. Berman and F.M. Izrailev, On the Dynamics of Correlation Functions and Diffusion Limitation in the Region of Quantum Chaos (Kirensky Institute of Physics, Krasnoyarsk, 1988) preprint 497.
[77] B.V. Chirikov, Phys. Lett. A108 (1985) 68.
[78] F.M. Izrailev, Phys. Lett. A125 (1987) 250.
[79] R. Scharf, J. Phys. A22 (1989) 4223.
[80] E. Heller, Phys. Rev. Lett. 53 (1984) 1515.
[81] F. Dyson, J. Math. Phys. 3 (1962) 140.
[82] J. Bayfield and P. Koch, Phys. Rev. Lett. 33 (1974) 258.
[83] N.B. Delone, B.A. Zon and V.P. Krainov, Zh. Eksp. Teor. Fiz. 75 (1978) 445 (Sov. Phys. JETP 48 (1978) 223).
[84] B.I. Meerson, E.A. Oks and P.V. Sasorov, Pisma Zh. Eksp. Teor. Fiz. 29 (1979) 79 (JETP Lett. 29 (1979) 72).
[85] N.B. Delone, B.P. Krainov and D.L. Shepelyansky, Usp. Fiz. Nauk 140 (1983) 335 (Sov. Phys. Usp. 26 (1983) 551); R. Jensen, Phys. Rev. A30 (1984) 386.
[86] G. Casati, I. Guarneri and D.L. Shepelyansky, Phys. Rev. A36 (1987) 3501.
[87] V. Gontis and B. Kaulakys, J. Phys. B20 (1987) 5051.
[88] K. van Leeuwen et al., Phys. Rev. Lett. 55 (1985) 2231.
[89] G. Casati, B.V. Chirikov, I. Guarneri and D.L. Shepelyansky, Phys. Rev. Lett. 56 (1986) 2437.
[90] J. Leopold and D. Richards, J. Phys. B19 (1986) 1125.
[91] G. Casati, B.V. Chirikov, I. Guarneri and D.L. Shepelyansky, Phys. Rev. Lett. 59 (1987) 2927.
[92] P. Milonni, J. Ackerhalt and M. Goggin, Phys. Rev. A35 (1987) 1714.
[93] D.L. Shepelyansky, Thesis (Institute of Nuclear Physics, Novosibirsk, 1988).
[94] E.J. Galvez, B.E. Sauer, L. Moorman, P.M. Koch, D. Richards, Phys. Rev. Lett. 61 (1988) 2011.
[95] J. Bayfield and D. Sokol, Phys. Rev. Lett. 61 (1988) 2007; J. Bayfield, G. Casati, I. Guarneri and D. Sokol, Phys. Rev. Lett. 63 (1989) 364.
[96] J. Meiss, Phys. Rev. Lett. 62 (1989) 1576.
[97] J. Leopold and I. Percival, Phys. Rev. Lett. 41 (1978) 944; J. Phys. B12 (1979) 79.
[98] J. Ford, Physics Today 36/4 (1983) 40.
[99] E. Wigner, in: The Logic of Personal Knowledge (London, 1961).